

ISSN 1881-7831 Online ISSN 1881-784X

DD & T

Drug Discoveries & Therapeutics

Volume 13, Number 4
August 2019



www.ddtjournal.com

DD & T

Drug Discoveries & Therapeutics



ISSN: 1881-7831
Online ISSN: 1881-784X
CODEN: DDTRBX
Issues/Year: 6
Language: English
Publisher: IACMHR Co., Ltd.

Drug Discoveries & Therapeutics is one of a series of peer-reviewed journals of the International Research and Cooperation Association for Bio & Socio-Sciences Advancement (IRCA-BSSA) Group and is published bimonthly by the International Advancement Center for Medicine & Health Research Co., Ltd. (IACMHR Co., Ltd.) and supported by the IRCA-BSSA and Shandong University China-Japan Cooperation Center for Drug Discovery & Screening (SDU-DDSC).

Drug Discoveries & Therapeutics publishes contributions in all fields of pharmaceutical and therapeutic research such as medicinal chemistry, pharmacology, pharmaceutical analysis, pharmaceuticals, pharmaceutical administration, and experimental and clinical studies of effects, mechanisms, or uses of various treatments. Studies in drug-related fields such as biology, biochemistry, physiology, microbiology, and immunology are also within the scope of this journal.

Drug Discoveries & Therapeutics publishes Original Articles, Brief Reports, Reviews, Policy Forum articles, Case Reports, News, and Letters on all aspects of the field of pharmaceutical research. All contributions should seek to promote international collaboration in pharmaceutical science.

Editorial Board

Editor-in-Chief:

Kazuhisa SEKIMIZU
Teikyo University, Tokyo, Japan

Co-Editors-in-Chief:

Xishan HAO
Tianjin Medical University, Tianjin, China
Munehiro NAKATA
Tokai University, Hiratsuka, Japan

Chief Director & Executive Editor:

Wei TANG
National Center for Global Health and Medicine, Tokyo, Japan

Senior Editors:

Guanhua DU
Chinese Academy of Medical Science and Peking Union Medical College, Beijing, China
Xiao-Kang LI
National Research Institute for Child Health and Development, Tokyo, Japan
Masahiro MURAKAMI
Osaka Ohtani University, Osaka, Japan
Yutaka ORIHARA
The University of Tokyo, Tokyo, Japan
Tomofumi SANTA
The University of Tokyo, Tokyo, Japan
Hongbin SUN
China Pharmaceutical University, Nanjing, China

Fengshan WANG
Shandong University, Ji'nan, China

Managing Editor:

Hiroshi HAMAMOTO
Teikyo University, Tokyo, Japan

Web Editor:

Yu CHEN
The University of Tokyo, Tokyo, Japan

Proofreaders:

Curtis BENTLEY
Roswell, GA, USA
Thomas R. LEBON
Los Angeles, CA, USA

Editorial and Head Office:

Pearl City Koishikawa 603,
2-4-5 Kasuga, Bunkyo-ku,
Tokyo 112-0003, Japan
Tel.: +81-3-5840-9697
Fax: +81-3-5840-9698
E-mail: office@ddtjournal.com

Drug Discoveries & Therapeutics

Editorial and Head Office

Pearl City Koishikawa 603, 2-4-5 Kasuga, Bunkyo-ku,
Tokyo 112-0003, Japan

Tel: +81-3-5840-9697, Fax: +81-3-5840-9698
E-mail: office@ddtjournal.com
URL: www.ddtjournal.com

Editorial Board Members

Alex ALMASAN <i>(Cleveland, OH)</i>	Rodney J. Y. HO <i>(Seattle, WA)</i>	Ken-ichi MAFUNE <i>(Tokyo)</i>	Quanxing WANG <i>(Shanghai)</i>
John K. BUOLAMWINI <i>(Memphis, TN)</i>	Hsing-Pang HSIEH <i>(Zhunan, Miaoli)</i>	Sridhar MANI <i>(Bronx, NY)</i>	Stephen G. WARD <i>(Bath)</i>
Jianping CAO <i>(Shanghai)</i>	Yongzhou HU <i>(Hangzhou, Zhejiang)</i>	Tohru MIZUSHIMA <i>(Tokyo)</i>	Yuhong XU <i>(Shanghai)</i>
Shousong CAO <i>(Buffalo, NY)</i>	Yu HUANG <i>(Hong Kong)</i>	Abdulla M. MOLOKHIA <i>(Alexandria)</i>	Bing YAN <i>(Ji'nan, Shandong)</i>
Jang-Yang CHANG <i>(Tainan)</i>	Amrit B. KARMARKAR <i>(Karad, Maharashtra)</i>	Yoshinobu NAKANISHI <i>(Kanazawa, Ishikawa)</i>	Chunyan YAN <i>(Guangzhou Guangdong)</i>
Fen-Er CHEN <i>(Shanghai)</i>	Toshiaki KATADA <i>(Tokyo)</i>	Siriporn OKONOGI <i>(Chiang Mai)</i>	Xiao-Long YANG <i>(Chongqing)</i>
Zhe-Sheng CHEN <i>(Queens, NY)</i>	Gagan KAUSHAL <i>(Philadelphia, PA)</i>	Weisan PAN <i>(Shenyang, Liaoning)</i>	Yun YEN <i>(Duarte, CA)</i>
Zilin CHEN <i>(Wuhan, Hubei)</i>	Ibrahim S. KHATTAB <i>(Kuwait)</i>	Chan Hum PARK <i>(Eumseong)</i>	Yasuko YOKOTA <i>(Tokyo)</i>
Xiaolan CUI <i>(Beijing)</i>	Shiroh KISHIOKA <i>(Wakayama, Wakayama)</i>	Rakesh P. PATEL <i>(Mehsana, Gujarat)</i>	Takako YOKOZAWA <i>(Toyama, Toyama)</i>
Shaofeng DUAN <i>(Lawrence, KS)</i>	Robert Kam-Ming KO <i>(Hong Kong)</i>	Shivanand P. PUTHLI <i>(Mumbai, Maharashtra)</i>	Rongmin YU <i>(Guangzhou, Guangdong)</i>
Mohamed F. EL-MILIGI <i>(6th of October City)</i>	Nobuyuki KOBAYASHI <i>(Nagasaki, Nagasaki)</i>	Shafiqur RAHMAN <i>(Brookings, SD)</i>	Guangxi ZHAI <i>(Ji'nan, Shandong)</i>
Hao FANG <i>(Ji'nan, Shandong)</i>	Norihiko KOKUDO <i>(Tokyo, Japan)</i>	Adel SAKR <i>(Cairo)</i>	Liangren ZHANG <i>(Beijing)</i>
Marcus L. FORREST <i>(Lawrence, KS)</i>	Toshiro KONISHI <i>(Tokyo)</i>	Gary K. SCHWARTZ <i>(New York, NY)</i>	Lining ZHANG <i>(Ji'nan, Shandong)</i>
Takeshi FUKUSHIMA <i>(Funabashi, Chiba)</i>	Chun-Guang LI <i>(Melbourne)</i>	Yuemao SHEN <i>(Ji'nan, Shandong)</i>	Na ZHANG <i>(Ji'nan, Shandong)</i>
Harald HAMACHER <i>(Tübingen, Baden-Württemberg)</i>	Minyong LI <i>(Ji'nan, Shandong)</i>	Brahma N. SINGH <i>(New York, NY)</i>	Ruiwen ZHANG <i>(Houston, TX)</i>
Kenji HAMASE <i>(Fukuoka, Fukuoka)</i>	Xun LI <i>(Ji'nan, Shandong)</i>	Tianqiang SONG <i>(Tianjin)</i>	Xiu-Mei ZHANG <i>(Ji'nan, Shandong)</i>
Junqing HAN <i>(Ji'nan, Shandong)</i>	Jikai LIU <i>(Wuhan, Hubei)</i>	Sanjay K. SRIVASTAVA <i>(Abilene, TX)</i>	Yongxiang ZHANG <i>(Beijing)</i>
Xiaojiang HAO <i>(Kunming, Yunnan)</i>	Xinyong LIU <i>(Ji'nan, Shandong)</i>	Chandan M. THOMAS <i>(Bradenton, FL)</i>	Jian-hua ZHU <i>(Guangzhou, Guangdong)</i>
Kiyoshi HASEGAWA <i>(Tokyo)</i>	Yuxiu LIU <i>(Nanjing, Jiangsu)</i>	Li TONG <i>(Xining, Qinghai)</i>	
Waseem HASSAN <i>(Rio de Janeiro)</i>	Hongxiang LOU <i>(Jinan, Shandong)</i>	Murat TURKOGLU <i>(Istanbul)</i>	<i>(As of February 2019)</i>
Langchong HE <i>(Xi'an, Shaanxi)</i>	Xingyuan MA <i>(Shanghai)</i>	Hui WANG <i>(Shanghai)</i>	

Review

- 177 - 182 **Induction of signal transduction pathways related to the pathogenicity of *Cryptococcus neoformans* in the host environment.**
Yasuhiko Matsumoto, Saki Azami, Haruka Shiga, Tae Nagamachi, Hikari Moriyama, Yuki Yamashita, Asami Yoshikawa, Takashi Sugita

Original Article

- 183 - 188 **Utility of an adverse drug event database based on the narrative accounts of patients with breast cancer.**
Kei Kikuchi, Akiko Miki, Hiroki Satoh, Noriko Iba, Rika Sato-Sakuma, Hirokuni Beppu, Yasufumi Sawada
- 189 - 197 **Repositioning of an anti-depressant drug, agomelatine as therapy for brain injury induced by craniotomy.**
Krishna A. Lad, Anurag Maheshwari, Bhagawati Saxena
- 198 - 206 **Cur2004-8, a synthetic curcumin derivative, extends lifespan and modulates age-related physiological changes in *Caenorhabditis elegans*.**
Bo-Kyoung Kim, Sung-A Kim, Sun-Mi Baek, Eun Young Lee, Eun Soo Lee, Choon Hee Chung, Chan Mug Ahn, Sang-Kyu Park
- 207 - 211 **Detection of *Trichophyton* spp. from footwear of patients with tinea pedis.**
Sanae A. Ishijima, Masataro Hiruma, Kazuhisa Sekimizu, Shigeru Abe
- 212 - 221 **Effects of naringenin on vascular changes in prolonged hyperglycaemia in fructose-STZ diabetic rat model.**
Nurul Hannim Zaidun, Sahema Zar Chi Thent, Mardiana Abdul Aziz, Santhana Raj L, Azian Abd Latiff, Syed Baharom Syed Ahmad Fuad

Brief Report

- 222 - 227 **Anti-virulence activities of biflavonoids from *Mesua ferrea* L. flower.**
Xiaochun Zhang, Rongrong Gao, Yan Liu, Yuhe Cong, Dongdong Zhang, Yu Zhang, Xuefei Yang, Chunhua Lu, Yuemao shen

Case Report

- 228 - 231 **Neurovascular compression syndrome of the brain stem with opsoclonus-myoclonus syndrome combined with vestibular paroxysmia and autonomic symptoms.**
Yusuke Morinaga, Kouhei Nii, Kimiya Sakamoto, Ritsuro Inoue, Takafumi Mitsutake, Hayatsura Hanada

CONTENTS

(Continued)

- 232 - 238 **A case of drug-induced hypersensitivity syndrome induced by salazosulfapyridine combined with SIADH caused by interstitial pneumonia.**
Yusuke Morinaga, Ichiro Abe, Tomohiro Minamikawa, Yusuke Ueda, Kouhei Nii, Kimiya Sakamoto, Ritsurou Inoue, Takafumi Mitsutake, Hayatsura Hanada, Jun Tsugawa, Kanako Kurihara, Toshio Higashi
- 239 - 243 **Focus on diagnosis, treatment, and problems of Barré-Lièou syndrome: Two case reports.**
Yusuke Morinaga, Kouhei Nii, Kimiya Sakamoto, Ritsurou Inoue, Takafumi Mitsutake, Hayatsura Hanada

Guide for Authors

Copyright

Induction of signal transduction pathways related to the pathogenicity of *Cryptococcus neoformans* in the host environment

Yasuhiko Matsumoto*, Saki Azami, Haruka Shiga, Tae Nagamachi, Hikari Moriyama, Yuki Yamashita, Asami Yoshikawa, Takashi Sugita

Department of Microbiology, Meiji Pharmaceutical University, Tokyo, Japan.

Summary

Cryptococcus neoformans, a human pathogenic fungus, infects immunocompromised humans and causes serious diseases such as cerebral meningitis. *C. neoformans* controls the expression of virulence factors in response to the host environment via various signal transduction pathways. Understanding the molecular mechanisms involved in *C. neoformans* infection will contribute to the development of methods to prevent and treat *C. neoformans*-related diseases. *C. neoformans* produces virulence factors, such as a polysaccharide capsule and melanin, to escape host immunity. Several proteins of *C. neoformans* are reported to regulate production of the virulence factors. In this review, on the basis of studies using gene-deficient mutants of *C. neoformans* and animal infection models, we outline the signal transduction pathways involved in the regulation of virulence factors.

Keywords: *Cryptococcus neoformans*, fungus, host factor, infection, pathogenicity, signal transduction pathway

1. Introduction

Several fungi cause various serious infections in immunocompromised patients, such as those taking immunosuppressive drugs to receive organ transplants and AIDS patients. *Cryptococcus neoformans* is an opportunistic fungal pathogen that causes respiratory diseases and cerebral meningitis (1-4). Cerebral meningitis is highly lethal and a main cause of death in AIDS patients (3). *C. neoformans* infects humans through carrier animals such as pigeons, and enters into the human blood via the nasal passages or wound sites (5). Immune cells in the human body are involved in eliminating *C. neoformans*. To resist immune systems, *C. neoformans* produces virulence factors such as a polysaccharide capsule and melanin (6).

A polysaccharide capsule surrounds the *C. neoformans* cell, thereby preventing phagocytosis, blocking antigen presentation to T cells, suppressing inflammatory cytokine production, and depleting

complement proteins (Figure 1) (7,8). Melanin is a polymer produced via catecholamine oxidation that accumulates in the cell wall of *C. neoformans* (9). Melanin protects against the oxidants produced by immune cells and decreases the porosity of the cell wall (Figure 1) (9-12). The melanin-induced decreased porosity of the cell wall plays an important role in the cell wall barrier function against host immune systems (12). Both production of the capsule and melanin by *C. neoformans* contributes to its escape from host immunity (13). Gene-deficient *C. neoformans* mutants unable to produce the capsule and melanin exhibit reduced mouse-killing ability (14,15). Therefore, regulation of the capsule and melanin production by *C. neoformans* is important for controlling its pathogenicity (16,17).

C. neoformans controls the growth and expression of its virulence factors in response to the host environment (16,17). It adapts to the host environment by regulating the expression of various genes in response to changes in environmental components such as sugars, amino acids, and metals (18).

In this review, we outline the signal transduction pathways involved in the pathogenicity of *C. neoformans* and the host factors that affect the activation of these signal transduction pathways.

*Address correspondence to:

Dr. Yasuhiko Matsumoto, Department of Microbiology, Meiji Pharmaceutical University, 2-522-1, Noshio, Kiyose, Tokyo 204-8588, Japan.

E-mail: ymatsumoto@my-pharm.ac.jp

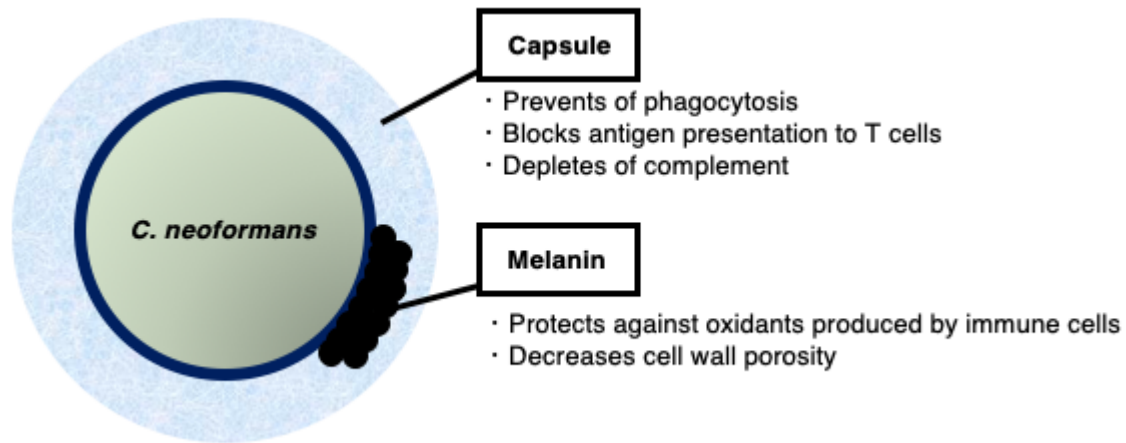


Figure 1. Functions of capsule and melanin in *C. neoformans*. *C. neoformans* produces a capsule and melanin for escaping host defense systems. The capsule contributes to preventing phagocytosis, blocking antigen presentation to T cells, and depleting complement. Melanin is involved in protecting against the oxidants produced by immune cells and decreasing cell wall porosity. *C. neoformans* cells are surrounded by a capsule layer and the cell wall is coated with melanin.

2. Signal transduction pathways related to the pathogenicity of *Cryptococcus neoformans*

C. neoformans regulates signal transduction pathways for infection in immunocompromised humans. This review focuses on the calcineurin, G-protein alpha 1 subunit (Gpa1)-cAMP, and protein kinase C 1 (Pkc1)-mitogen-activated protein kinase (MAPK) pathways, because genetic studies indicate that these three signal transduction pathways are required for the pathogenicity of *C. neoformans* (Figure 2).

2.1. Calcineurin signal transduction pathway (Figure 2A)

Calcineurin, a serine/threonine phosphatase, is present in all eukaryotes and plays an important role in the calcium-dependent signal transduction pathway (19). *C. neoformans* has a calcineurin signal transduction pathway and requires calcineurin for growth at 37°C, which is human body temperature (17,20). In *C. neoformans*, calcineurin comprises Cna1 and Cnb1. Calcium-bound calmodulin 1 (Cam1) forms a complex with Cna1 and Cnb1 by binding to the C-terminal region of Cna1 (17). The *cna1* gene-deficient *C. neoformans* mutant exhibits reduced pathogenicity in several animals, such as nematodes (*C. elegans*), wax moths (*G. mellonella*), silkworms (*Bombyx mori*), and mice (16,21-25). Therefore, the calcineurin signal transduction pathway plays an important role in the pathogenicity of *C. neoformans* by allowing *C. neoformans* to adapt to the host body temperature. Activated calcineurin complex dephosphorylates the transcription factor Crz1, which then transfers from the cytoplasm to the nucleus to regulate gene expression (26). Therefore, transcriptional regulation by Crz1 functions in the calcineurin signal transduction pathway in *C. neoformans* (26). In a *Galleria mellonella*

infection model, *crz1* gene-deficient *C. neoformans* mutants exhibit reduced pathogenicity.

The *cna1* and *crz1* gene-deficient *C. neoformans* mutants are sensitive to Congo red, an agent that induces stress to the cell wall, and the detergent sodium dodecyl sulfate, an agent that disrupts cell membranes (26). Therefore, the calcineurin signal transduction pathway regulates gene expression via the transcription factor Crz1 to protect against high temperatures, cell wall stress, and membrane damage in the host environment; and the regulatory system is required for the pathogenicity of *C. neoformans*.

2.2. Gpa1-cAMP signal transduction pathway (Figure 2B)

G-protein coupled receptors (GPCRs) respond to various stimuli, and downstream signaling molecules are regulated by G-protein activation (27). *C. neoformans* has several GPCRs on the cell membrane surface (18). Gpa1 is the alpha subunit of the G protein and is required for *C. neoformans* pathogenicity (28). Gpa1 binds to adenylyl cyclase (Cac1) and increases its enzymatic activity (17). Cac1 produces cAMP from ATP (17). The increase in the intracellular cAMP levels leads to increased cAMP binding with the protein kinase regulatory (Pkr) protein (17). Pkr binds to protein kinase A1 (Pka1), and dissociates from Pka1 by binding to cAMP (27). The dissociated Pka1 phosphorylates the transcription factors neuregulin 1 (Nrg1) and Rim101 (27). Phosphorylated Nrg1 and Rim101 regulate gene expression and promote the synthesis of melanin and the polysaccharide capsule (27). *C. neoformans* mutants deficient for *gpa1*, *pka1*, *cac1*, or *nrg1* have reduced pathogenicity in mice (28-31). On the other hand, *C. neoformans* mutants deficient for *rim101* do not exhibit increased pathogenicity in an intranasal mouse infection model (32). Therefore, Nrg1, but not Rim101, may play

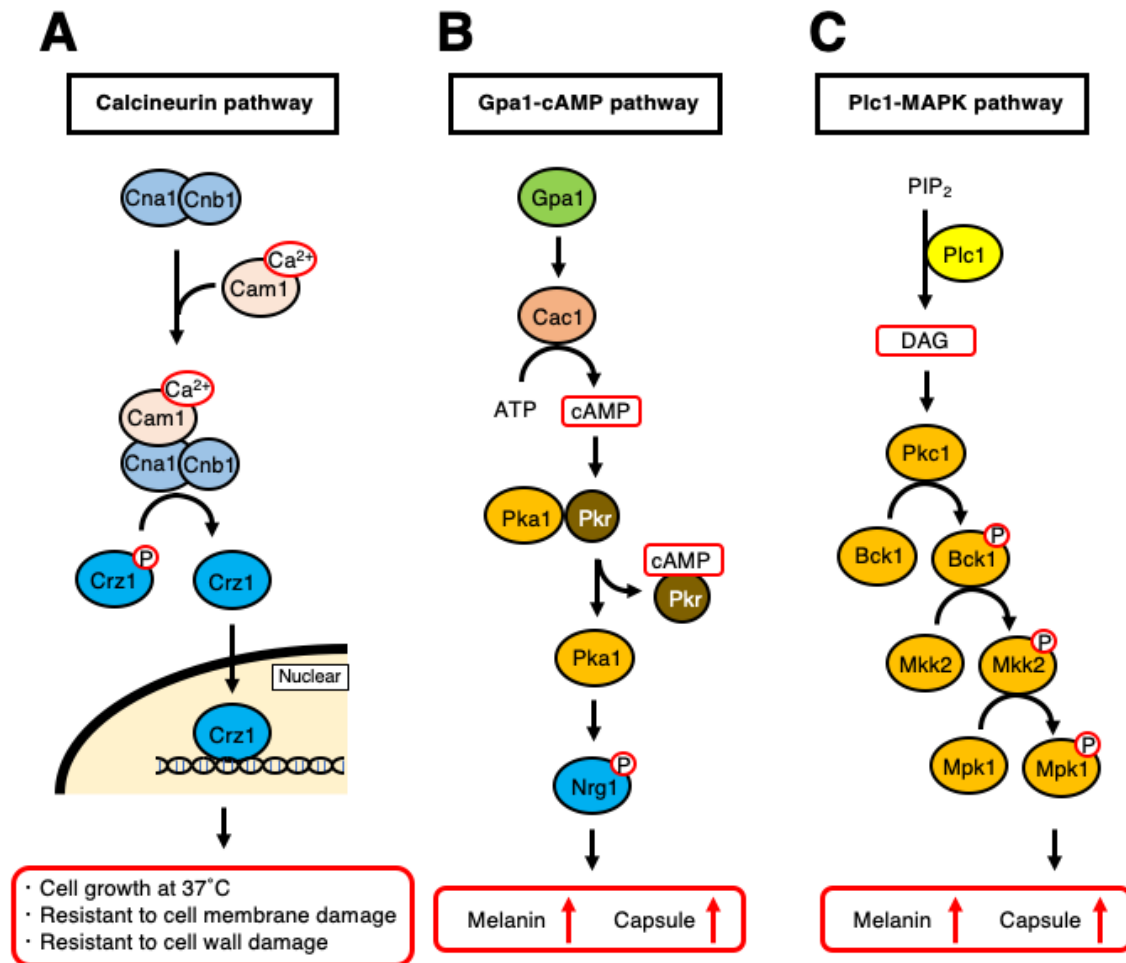


Figure 2. Signal transduction pathways related to the pathogenicity of *C. neoformans*. A. Calcineurin signal transduction pathway. Calcineurin (Cna1 and Cnb1 proteins) form a complex with calcium-bound Cam1 protein and dephosphorylates transcription factor Crz1. Dephosphorylated Crz1 regulates gene expression for resistance to high temperature, cell membrane damage, and cell wall damage. B. Gpa1-cAMP signal transduction pathway. Gpa1 protein activates Cac1 adenylyl cyclase, which produces cAMP from ATP. Intracellular cAMP binds to Pkr and releases Pka1 from the Pkr and Pka1 complex. The dissociated Pka1 phosphorylates transcription factor Nrg1, which promotes the synthesis of melanin and the polysaccharide capsule. C. Plc1-MAPK signal transduction pathway. Plc1 degrades from PIP₂ to diacylglycerol (DAG) and the produced DAG activates Pkc1 kinase, which triggers activation of the MAPK signal transduction pathway. Mpk1 is involved in the synthesis of melanin and the polysaccharide capsule.

an important role in the pathogenicity of *C. neoformans* in the Gpa1-cAMP signal transduction pathway.

2.3. Pkc1-MAPK signal transduction pathway (Figure 2C)

Phosphatidylinositol (PI) and phosphatidylinositol diphosphate (PIP₂) are lipids involved in various signal transduction pathways (17). *C. neoformans* also uses the lipid-mediated signal transduction pathway (17). PIP₂, but not PI, is degraded into diacylglycerol (DAG) by phospholipase Plc1 (33). The increase in the intracellular DAG levels leads to the phosphorylation of the MAPK kinase kinase Bck1 by the PKC Pkc1 (17,34,35). Phosphorylated Bck1 phosphorylates Mkk2, a MAPK kinase (17,34). Phosphorylated Mkk2 phosphorylates Mpk1, a MAPK (17,34). Mpk1 is a phosphorylation enzyme involved in the synthesis of

melanin and the polysaccharide capsule, and is required for the pathogenicity of *C. neoformans* (36). The *plc1* gene-deficient *C. neoformans* mutant exhibits decreased pathogenicity in invertebrate infection models (e.g., *Caenorhabditis elegans* and *Galleria mellonella*) (37,33). The *mpk1* gene-deficient *C. neoformans* mutant has reduced pathogenicity in mice infected *via* injection into the lateral tail vein (36). Therefore, the Pkc1-MAPK signal transduction pathway is essential for *C. neoformans* pathogenicity and is regulated by the intracellular levels of DAG, a lipid intermediary.

3. Environmental components related to the pathogenicity of *Cryptococcus neoformans*

Signal transduction pathways in *C. neoformans* are promoted by environmental components, including host factors (Table 1).

Table 1. Molecules that trigger signal transduction pathways related to the pathogenicity of *C. neoformans*

Signaling pathways	Calcineurin	Gpa1-cAMP	Pkc1-MAPK
Triggering molecules	Calcium Inositol	Glucose Methionine Iron Carbon dioxide	Inositol

3.1. Sugars

Glucose is a major carbon source for cells and is abundant in the human body. *C. neoformans* grows using glucose as a carbon source, and regulates the expression of virulence factors according to the glucose concentration in the environment. Glucose is a substrate for the capsule in *C. neoformans*. Moreover, glucose induces the cAMP pathway by activating Pka in *C. neoformans* (38). Therefore, factors that regulate glucose recognition and utilization may be involved in the *C. neoformans* pathogenicity. Gpr4, a receptor, and Hxt1, a hexose transporter, may regulate the recognition and utilization of glucose in *C. neoformans*. The *gpr4* gene-deficient *C. neoformans* mutant, however, does not exhibit reduced pathogenicity in mice (39). The *hxt1* gene-deficient *C. neoformans* mutant exhibits normal pathogenicity in a *C. elegans* infection model (40). Hxs1 is a high-affinity glucose transporter required for cell growth in low glucose conditions (41). The *hxs1* gene-deficient *C. neoformans* mutant exhibits reduced pathogenicity in a mouse intranasal infection model (41). Although Hxs1 contributes to melanin production, the molecular relationship between glucose transport mediated by Hxs1 and signal transduction pathways is unclear. The identification of factors that recognize or utilize glucose for modulating the pathogenicity of *C. neoformans* is an important subject for future studies.

Inositol is a sugar that many organisms can synthesize from glucose. Inositol is abundant in the human brain and is used for osmotic regulation in neuronal cells. *C. neoformans* recognizes inositol in the human brain to increase the efficiency of its blood-brain barrier penetration (42). In *C. neoformans*, inositol is taken up into cells *via* the inositol transporters ITR1a and ITR3c. *C. neoformans* mutants deficient for both *itr1a* and *itr3c* exhibit reduced pathogenicity in a mouse systemic infection model (43). Inositol activates calcineurin and MAPK signal transduction pathways after conversion to PI and PIP₂ (18). Therefore, inositol in the human brain is a host factor that enhances the pathogenicity of *C. neoformans*.

3.2. Methionine

Methionine, an amino acid, is used by all organisms for protein synthesis and abundantly exists in the human body. In *C. neoformans*, methionine activates the cAMP signal transduction pathway by increasing

the intracellular cAMP concentration (39). Gpr4 is a candidate molecule for increasing the cAMP concentration *via* the recognition of methionine. The *gpr4* gene-deficient *C. neoformans* mutant has a decreased cellular cAMP concentration and decreased capsule production (39). On the other hand, the *gpr4* gene-deficient *C. neoformans* mutant does not have reduced pathogenicity in mice (39). These findings suggest that *gpr4* contributes to the methionine response, but is not necessary for *C. neoformans* pathogenicity. Further studies are needed to investigate the gene(s) required for a response to environmental methionine and to clarify the contribution of methionine to *C. neoformans* pathogenicity using gene-deficient mutants.

3.3. Metals

Calcium is an essential metal for organisms and has various roles as an enzyme activator and signal transmitter. Microorganisms adapt to host environments *via* calcium recognition and utilization. In *C. neoformans*, calcium binds to Cam1, and the calcium-bound Cam1 forms a complex with calcineurin, leading to activation of the calcineurin signal transduction pathway (17). The *cam1* gene is required for *C. neoformans* growth (44). Therefore, calcium recognition by Cam1 is important not only for controlling pathogenicity, but also for utilizing the calcium required for survival. Moreover, the intracellular calcium concentration in *C. neoformans* is increased by inositol uptake. Activation of the calcineurin signal transduction pathway by inositol may be associated with calcium recognition *via* Cam1 (17).

Iron is required for cell growth in organisms and is abundant in human blood. *C. neoformans* alters the expression of various genes, including those involved in capsule synthesis, in response to the iron concentration in the environment (45). Iron binds to the transcription factor Cir1 and alters its transcriptional activity in *C. neoformans*. In *cir1* gene-deficient *C. neoformans* mutants, almost all of the gene expression changes caused by iron do not occur and capsule production decreases (45). Comprehensive gene expression analysis using a *cir1* gene-deficient mutant revealed that Cir1 increases the expression of genes encoding many GPCRs and the *cacl* gene, resulting in activation of the cAMP pathway (45). Furthermore, the *cir1* gene-deficient *C. neoformans* mutant exhibits

reduced pathogenicity in a mouse systemic infection model (45). Thus, iron is a host factor that regulates the *C. neoformans* pathogenicity, and Cir1 is an important factor in its recognition.

3.4. Carbon dioxide (CO₂)

CO₂ is produced by respiration and is abundant in the human body. CO₂ regulates capsule formation in *C. neoformans* (46). *C. neoformans* absorbs CO₂ and converts it to HCO₃⁻ by the β-carbonic anhydrase Can2. HCO₃⁻ binds to the adenylyl cyclase Cac1 and increases enzyme activity. Activated Cac1 increases intracellular cAMP, which leads to activation of the cAMP pathway. On the other hand, while the *can2* gene is required for growth under environmental CO₂ concentrations (0.036% CO₂), it is not required for growth at human body CO₂ concentrations (5% CO₂) (47). Moreover, the *can2* gene does not contribute to *C. neoformans* pathogenicity in mice (47). The identification of molecules that modulate pathogenicity under various CO₂ concentrations in the human body requires further study.

4. Conclusion

In this review, we described the pathogenic regulatory mechanisms of *C. neoformans*, focusing on the molecules necessary for host infection in humans. *C. neoformans* controls virulence in the host through the recognition of host factors. The contributions of several molecules to the pathogenicity of *C. neoformans* have not yet been elucidated in animal infection models. Infection models for evaluating *C. neoformans* pathogenicity have been established. The *gpa1* and *pkal* gene-deficient *C. neoformans* mutants exhibit reduced pathogenicity in invertebrate animals, such as nematodes, wax moths, and silkworms (22-24). Therefore, the importance of the Gpa1-cAMP signaling pathway for *C. neoformans* pathogenicity can be evaluated in invertebrate infection experiments. The requirement of certain factors for recognizing the host environment to control the pathogenicity of *C. neoformans* can be clarified in future studies using invertebrate infection models.

References

- Morschhauser J. Regulation of multidrug resistance in pathogenic fungi. *Fungal Genet Biol.* 2010; 47:94-106.
- Brown GD, Denning DW, Gow NA, Levitz SM, Netea MG, White TC. Hidden killers: Human fungal infections. *Sci Transl Med.* 2012; 4:165rv113.
- Park BJ, Wannemuehler KA, Marston BJ, Govender N, Pappas PG, Chiller TM. Estimation of the current global burden of cryptococcal meningitis among persons living with HIV/AIDS. *Aids.* 2009; 23:525-530.
- Kelliher CM, Haase SB. Connecting virulence pathways to cell-cycle progression in the fungal pathogen *Cryptococcus neoformans*. *Curr Genet.* 2017; 63:803-811.
- Casadevall A, Coelho C, Alanio A. Mechanisms of *Cryptococcus neoformans*-mediated host damage. *Front Immunol.* 2018; 9:855.
- Campuzano A, Wormley FL. Innate immunity against *Cryptococcus*, from recognition to elimination. *J Fungi (Basel).* 2018; 4. pii: E33.
- Zaragoza O, Rodrigues ML, De Jesus M, Frases S, Dadachova E, Casadevall A. The capsule of the fungal pathogen *Cryptococcus neoformans*. *Adv Appl Microbiol.* 2009; 68:133-216.
- Park YD, Williamson PR. Masking the pathogen: Evolutionary strategies of fungi and their bacterial counterparts. *J Fungi (Basel).* 2015; 1:397-421.
- Hamilton AJ, Holdom MD. Antioxidant systems in the pathogenic fungi of man and their role in virulence. *Med Mycol.* 1999; 37:375-389.
- Kwon-Chung KJ, Polacheck I, Popkin TJ. Melanin-lacking mutants of *Cryptococcus neoformans* and their virulence for mice. *J Bacteriol.* 1982; 150:1414-1421.
- Jacobson ES, Emery HS. Catecholamine uptake, melanization, and oxygen toxicity in *Cryptococcus neoformans*. *J Bacteriol.* 1991; 173:401-403.
- Jacobson ES, Ikeda R. Effect of melanization upon porosity of the cryptococcal cell wall. *Med Mycol.* 2005; 43:327-333.
- Kwon-Chung KJ, Rhodes JC. Encapsulation and melanin formation as indicators of virulence in *Cryptococcus neoformans*. *Infect Immun.* 1986; 51:218-223.
- Fonseca FL, Reis FCG, Sena BAG, Jozefowicz LJ, Kmetzsch L, Rodrigues ML. The overlooked glycan components of the *Cryptococcus* capsule. *Curr Top Microbiol Immunol.* 2018.
- Salas SD, Bennett JE, Kwon-Chung KJ, Perfect JR, Williamson PR. Effect of the laccase gene CNLAC1, on virulence of *Cryptococcus neoformans*. *J Exp Med.* 1996; 184:377-386.
- Steinbach WJ, Reedy JL, Cramer RA, Jr., Perfect JR, Heitman J. Harnessing calcineurin as a novel anti-infective agent against invasive fungal infections. *Nat Rev Microbiol.* 2007; 5:418-430.
- Kozubowski L, Lee SC, Heitman J. Signalling pathways in the pathogenesis of *Cryptococcus*. *Cell Microbiol.* 2009; 11:370-380.
- Rutherford JC, Bahn YS, van den Berg B, Heitman J, Xue C. Nutrient and stress sensing in pathogenic yeasts. *Front Microbiol.* 2019; 10:442.
- Rusnak F, Mertz P. Calcineurin: Form and function. *Physiol Rev.* 2000; 80:1483-1521.
- Siafakas AR, Sorrell TC, Wright LC, Wilson C, Larsen M, Boadle R, Williamson PR, Djordjevic JT. Cell wall-linked cryptococcal phospholipase B1 is a source of secreted enzyme and a determinant of cell wall integrity. *J Biol Chem.* 2007; 282:37508-37514.
- Odom A, Muir S, Lim E, Toffaletti DL, Perfect J, Heitman J. Calcineurin is required for virulence of *Cryptococcus neoformans*. *Embo J.* 1997; 16:2576-2589.
- Mylonakis E, Ausubel FM, Perfect JR, Heitman J, Calderwood SB. Killing of *Caenorhabditis elegans* by *Cryptococcus neoformans* as a model of yeast pathogenesis. *Proc Natl Acad Sci U S A.* 2002; 99:15675-15680.
- Mylonakis E, Moreno R, El Khoury JB, Idnurm A,

- Heitman J, Calderwood SB, Ausubel FM, Diener A. *Galleria mellonella* as a model system to study *Cryptococcus neoformans* pathogenesis. *Infect Immun*. 2005; 73:3842-3850.
24. Matsumoto Y, Miyazaki S, Fukunaga DH, Shimizu K, Kawamoto S, Sekimizu K. Quantitative evaluation of cryptococcal pathogenesis and antifungal drugs using a silkworm infection model with *Cryptococcus neoformans*. *J Appl Microbiol*. 2012; 112:138-146.
 25. Matsumoto Y, Sekimizu K. Silkworm as an experimental animal for research on fungal infections. *Microbiol Immunol*. 2019; 63:41-50.
 26. Chow EW, Clancey SA, Billmyre RB, Averette AF, Granek JA, Mieczkowski P, Cardenas ME, Heitman J. Elucidation of the calcineurin-Crz1 stress response transcriptional network in the human fungal pathogen *Cryptococcus neoformans*. *PLoS Genet*. 2017; 13:e1006667.
 27. Choi J, Jung WH, Kronstad JW. The cAMP/protein kinase A signaling pathway in pathogenic basidiomycete fungi: Connections with iron homeostasis. *J Microbiol*. 2015; 53:579-587.
 28. Alspaugh JA, Perfect JR, Heitman J. *Cryptococcus neoformans* mating and virulence are regulated by the G-protein alpha subunit GPA1 and cAMP. *Genes Dev*. 1997; 11:3206-3217.
 29. D'Souza CA, Alspaugh JA, Yue C, Harashima T, Cox GM, Perfect JR, Heitman J. Cyclic AMP-dependent protein kinase controls virulence of the fungal pathogen *Cryptococcus neoformans*. *Mol Cell Biol*. 2001; 21:3179-3191.
 30. Alspaugh JA, Pukkila-Worley R, Harashima T, Cavallo LM, Funnell D, Cox GM, Perfect JR, Kronstad JW, Heitman J. Adenylyl cyclase functions downstream of the Galpha protein Gpa1 and controls mating and pathogenicity of *Cryptococcus neoformans*. *Eukaryot Cell*. 2002; 1:75-84.
 31. Cramer KL, Gerrald QD, Nichols CB, Price MS, Alspaugh JA. Transcription factor Nrg1 mediates capsule formation, stress response, and pathogenesis in *Cryptococcus neoformans*. *Eukaryot Cell*. 2006; 5:1147-1156.
 32. O'Meara TR, Norton D, Price MS, Hay C, Clements MF, Nichols CB, Alspaugh JA. Interaction of *Cryptococcus neoformans* Rim101 and protein kinase A regulates capsule. *PLoS Pathog*. 2010; 6:e1000776.
 33. Lev S, Desmarini D, Li C, Chayakulkeeree M, Traven A, Sorrell TC, Djordjevic JT. Phospholipase C of *Cryptococcus neoformans* regulates homeostasis and virulence by providing inositol trisphosphate as a substrate for Arg1 kinase. *Infect Immun*. 2013; 81:1245-1255.
 34. Donlin MJ, Upadhy R, Gerik KJ, Lam W, VanArendonk LG, Specht CA, Sharma NK, Lodge JK. Cross talk between the cell wall integrity and cyclic AMP/protein kinase A pathways in *Cryptococcus neoformans*. *MBio*. 2014; 5. pii: e01573-14.
 35. Gerik KJ, Bhimireddy SR, Ryerse JS, Specht CA, Lodge JK. PKC1 is essential for protection against both oxidative and nitrosative stresses, cell integrity, and normal manifestation of virulence factors in the pathogenic fungus *Cryptococcus neoformans*. *Eukaryot Cell*. 2008; 7:1685-1698.
 36. Kraus PR, Fox DS, Cox GM, Heitman J. The *Cryptococcus neoformans* MAP kinase Mpk1 regulates cell integrity in response to antifungal drugs and loss of calcineurin function. *Mol Microbiol*. 2003; 48:1377-1387.
 37. Chayakulkeeree M, Sorrell TC, Siafakas AR, Wilson CF, Pantarat N, Gerik KJ, Boadle R, Djordjevic JT. Role and mechanism of phosphatidylinositol-specific phospholipase C in survival and virulence of *Cryptococcus neoformans*. *Mol Microbiol*. 2008; 69:809-826.
 38. Banerjee D, Bloom AL, Panepinto JC. Opposing PKA and Hog1 signals control the post-transcriptional response to glucose availability in *Cryptococcus neoformans*. *Mol Microbiol*. 2016; 102:306-320.
 39. Xue C, Bahn YS, Cox GM, Heitman J. G protein-coupled receptor Gpr4 senses amino acids and activates the cAMP-PKA pathway in *Cryptococcus neoformans*. *Mol Biol Cell*. 2006; 17:667-679.
 40. Chikamori M, Fukushima K. A new hexose transporter from *Cryptococcus neoformans*: Molecular cloning and structural and functional characterization. *Fungal Genet Biol*. 2005; 42:646-655.
 41. Liu TB, Wang Y, Baker GM, Fahmy H, Jiang L, Xue C. The glucose sensor-like protein Hxs1 is a high-affinity glucose transporter and required for virulence in *Cryptococcus neoformans*. *PLoS One*. 2013; 8:e64239.
 42. Liu TB, Kim JC, Wang Y, Toffaletti DL, Eugenin E, Perfect JR, Kim KJ, Xue C. Brain inositol is a novel stimulator for promoting *Cryptococcus* penetration of the blood-brain barrier. *PLoS Pathog*. 2013; 9:e1003247.
 43. Wang Y, Liu TB, Delmas G, Park S, Perlin D, Xue C. Two major inositol transporters and their role in cryptococcal virulence. *Eukaryot Cell*. 2011; 10:618-628.
 44. Kraus PR, Nichols CB, Heitman J. Calcium- and calcineurin-independent roles for calmodulin in *Cryptococcus neoformans* morphogenesis and high-temperature growth. *Eukaryot Cell*. 2005; 4:1079-1087.
 45. Jung WH, Sham A, White R, Kronstad JW. Iron regulation of the major virulence factors in the AIDS-associated pathogen *Cryptococcus neoformans*. *PLoS Biol*. 2006; 4:e410.
 46. Granger DL, Perfect JR, Durack DT. Virulence of *Cryptococcus neoformans*. Regulation of capsule synthesis by carbon dioxide. *J Clin Invest*. 1985; 76:508-516.
 47. Bahn YS, Cox GM, Perfect JR, Heitman J. Carbonic anhydrase and CO₂ sensing during *Cryptococcus neoformans* growth, differentiation, and virulence. *Curr Biol*. 2005; 15:2013-2020.

(Received June 27, 2019; Accepted June 29, 2019)

Utility of an adverse drug event database based on the narrative accounts of patients with breast cancer

Kei Kikuchi¹, Akiko Miki², Hiroki Satoh², Noriko Iba³, Rika Sato-Sakuma³, Hirokuni Beppu³, Yasufumi Sawada^{1,*}

¹ Faculty of Pharmaceutical sciences, The University of Tokyo, Tokyo, Japan;

² Graduate School of Pharmaceutical Sciences, The University of Tokyo, Tokyo, Japan;

³ DIPEX-Japan, Tokyo, Japan.

Summary

Patient narratives of adverse drug events (ADEs) often differ from the symptoms listed on the package inserts of pharmaceutical products using common ADE terminology and could be a source of great comfort to patients with the same disease. To explore this idea, we analyzed written narratives obtained from 48 patients with breast cancer using the NPO Corporation Database of Individual Patients' Experiences, Japan (DIPEX-Japan). Our analysis aimed to determine the utility of an "Adverse Drug Event Database" for use in clinical settings as a novel source of disease information in patients' own words. An analysis of transcripts from 29 patients, in which they recounted their treatment drugs and the time of onset and duration of ADEs in great detail, revealed several discrepancies between the language they used to describe various side effects and the standard ADE terminology on package inserts. We conclude that the language used to describe ADEs on package inserts is insufficient for helping patients as they struggle to recognize, internalize, and overcome ADEs, and argue the need for available, detailed information in the words of real patients about the nature of the ADEs predicted, as well as their clinical course and duration. Such information would be invaluable in supplementing the standardized language used on package inserts. Databases of patients' narrative accounts of ADEs are needed as information sources that can be reliably disseminated among patients.

Keywords: Package inserts, qualitative research, ADE, DIPEX-Japan

1. Introduction

Information on adverse drug events (ADEs) used to be available only from papers published by corporations and medical professionals such as doctors and pharmacists. However, since 1993, when the US Food and Drug Administration instituted a program allowing patients to submit ADEs directly to the organization, similar patient ADE reporting systems have been introduced in various countries. Japan began testing its own patient ADE reporting system in March 2012 and the program is currently operational (1). Factors driving

the introduction of ADE reporting systems include a tendency for doctors to fail to report ADEs, even when a patient's remarks strongly suggest an association with a treatment or drug (2,3), and a tendency for medical professionals to underestimate the degree and severity of ADEs (4). In addition, patients are often the first to discover side effects; certainly, they are the most sensitive to changes in their own bodies and their concern levels about these changes are the highest. Furthermore, their lack of expert-level knowledge about pharmaceuticals, paradoxically, better equips them to detect unknown and unforeseen events than medical professionals.

Nonetheless, the appropriate organization, analysis, and encoding of the vast amount of data collected in these ADE reporting systems remain to be addressed. In other words, the interpretation of the ADE-related information provided by patients with diverse

*Address correspondence to:

Dr. Yasufumi Sawada, Laboratory of Drug Lifetime Management, Graduate School of Pharmaceutical Sciences, University of Tokyo, 7-3-1 Hongo, Bunkyo-ku, Tokyo 113-0033, Japan.

E-mail: sawada@mol.f.u-tokyo.ac.jp

backgrounds by medical professionals and government experts continues to be a challenge. Studies have cautioned that the risk of discrepancies arising in ADE data with respect to the symptoms actually experienced by patients is high, particularly at the encoding stage (5,6).

In recent years, these issues and concerns have driven research interest in so-called "patient-reported outcomes" (PROs), *i.e.*, side effects as directly evaluated by patients, especially in cancer pharmacotherapy (7). ADEs are usually evaluated using the Common Terminology Criteria for Adverse Events (CTCAE) (8). Corresponding guidelines, in the form of the *Patient-Reported Outcomes Version of the CTCAE* (PRO-CTCAE), have been developed and published for PROs (9). This assessment tool covers 124 labels across 78 different adverse events, describing their potential frequency, intensity, and impairment of daily living using standardized terminology.

Systematically collecting ADE-related information in a patient-centric fashion seems a useful idea. Pharmaceutical package inserts describe ADEs using standardized medical terminology; narrative accounts, in which side effects and symptoms may be expressed in quite different terms, could be a great help to people with the same disease. To examine this idea, we analyzed a database of patient narratives maintained by the NPO Corporation Database of Individual Patients' Experiences, Japan (DIPEX-Japan) (10); the database provides free, reliable information about health issues by sharing patients' real-life experiences.

DIPEX-Japan contains narrative clips (auditory clips and or video clips) and documents presenting the thoughts and feelings of patients with various diseases and their families in a wide variety of settings, such as during diagnosis, treatment selection, and treatment, as well as side effect experiences. One feature of the data is its high reliability; individuals' stories are collected with the approval of DIPEX-Japan's internal ethics committee and advisory council from the start of the project to online publication. In the present study, using DIPEX-Japan's "Breast Cancer Story Database" (11), we evaluated how patients with breast cancer's descriptions of side effects compared and contrasted with the official ADEs (and initial symptoms) listed on the package inserts of the medications they were taking, as well as how perceptions of the events varied among patients (*i.e.*, in terms of the language used). We further assessed the utility of a hypothetical "Adverse Drug Event Database" for use in clinical settings as a novel source of disease information in breast cancer survivors' own words.

2. Methods

2.1. Data used in analysis

The original dataset consisted of narrative text data

(*i.e.*, transcripts) from survivors of breast and prostate cancer collected as part of A "Patient Stories" Database for Cancer Survivors Aimed at Instituting a Support System to Allow Cancer Patients to Choose Treatments More Independently," a 2007-2009 clinical cancer research project funded by Japan's Ministry of Health (Principal Investigator: Dr. Emiko Wada). Our analysis was confined to the transcripts of 48 patients with breast cancer.

Narrative content pertaining to adverse events or treatment was extracted and encoded into ADE categories (in patients' words). In addition to treatment history, the variables described below were encoded:

1. Patient ID: Internal identification number of the patient speaking about the side effect(s);

2. Adverse Events: Official ADEs listed on package insert(s) thought to match the patient's subjective symptoms;

3. Drug (Treatment): Name of the medication taken (or treatment received) by the patient at the time of subjective symptom onset (input as Unknown when uncertain);

4. Causality: Four-step rating of the causal link between the drug and the treatment received, according to the patient's description of their symptoms (Table S1, <http://www.ddtjournal.com/action/getSupplementalData.php?ID=46>);

5. Listed on Package Insert: How well the side effects experienced corresponded to the actual descriptions of events in the drug or treatment in package insert; also rated on a four-step scale (Table S2, <http://www.ddtjournal.com/action/getSupplementalData.php?ID=46>).

The Common Terminology Criteria for Adverse Events (CTCAE) v4.0 (Japanese version) (12) was used to classify the potential adverse events listed on the package insert. Two researchers separately read and labeled the individual transcripts, indicating information which could be registered under these variables. The labels for which a consensus was reached were compiled into the final dataset.

We adopted several conventions for reporting the results. Drugs and medications are referred to using their standard terminology, but quotations are reported verbatim (*i.e.* in the patients' own words) and included in the tables. The quotations in the tables (Tables 1,2 Tables S3, S4, <http://www.ddtjournal.com/action/getSupplementalData.php?ID=46>) are labeled with serial numbers corresponding to the 29 patients whose interviews were analyzed. In addition, since we did not analyze sentiment, interjections (*umm*, *wow*, *etc.*) that impeded reading were deleted, unless essential for context.

2.2. Ethical considerations

Our study was approved by the DIPEX-Japan Ethics

Committee (ID: 2012-1), on condition that we use only anonymized data from the original DIPEX-Japan database (*Story Archive*).

3. Results

The interviews conducted to construct DIPEX-Japan's *Story Archive* were not designed with the specific intention of obtaining information about chemotherapy. Nonetheless, our analysis of the narrative data revealed that 29 of the 48 patients with breast cancer spoke at great length about their treatment drugs, medication history, and the timing and presentation of their adverse events. Four had received pre-and post-operative chemotherapy and 16 had received postoperative radiation therapy as well. Moreover, "almost certain" causality was identified between drugs and events in 212 records. Tables S3 and S4 (<http://www.ddtjournal.com/action/getSupplementalData.php?ID=46>) contain representative excerpts of dialogue supporting drug-event causality with this high level of confidence (*i.e.*, causality ranked as "almost certain": see Table 2), in

which the patient's language matched the description of the ADEs on the package insert of the drug or treatment in question. The varied language they used to describe their side effects provided a level of detail unknowable from the standard ADE terminology on package inserts. We present the remarks of patients taking paclitaxel concerning the side effect "paresthesia" as an example (Table 1).

However, in many cases, drug-event causality was not clearly evident from patients' narratives alone. Although we did not identify any "new" ADEs *per se*, several patients who had undergone combination chemotherapy (specifically, fluorouracil/epirubicin/cyclophosphamide [FEC or CEF], adriamycin/cyclophosphamide [AC], and trastuzumab/docetaxel [TRASTU/DTX] therapy) complained of hyperosmia (a heightened sense of smell), which was not listed among the potential reactions in their respective package inserts (Table 2). We searched a database of symptom reports associated with suspected ADEs published by the Pharmaceuticals and Medical Devices Agency, an independent administrative entity, for entries that resembled the patients' reports of

Table 1. Examples of characteristic narratives of patients with breast cancer concerning paresthesia induced by paclitaxel (or taxol)

No.	Narratives	Drug name
6	There was tingling [in my arms] from the wrists down [especially in my fingertips] ... and from my lower knee down [in my legs]. The sensation was as if I had put my legs into an electric bath. I lose feeling in my legs when I sit seiza-style (<i>i.e. kneeling upright on the ground</i>). It feels like the sensation that you get when feeling starts to return to your leg after it's fallen asleep, but it started at the knee first, then spread downward. It doesn't go away, even when I try to sleep. At its worst, I just can't stay asleep, because the pins and needles wake me up after I've been lying down for about an hour.	Taxol
6	Let's say I rank how intense the tingling is from 0 to 10. From a starting point of 0, it would rise to a peak and then fall, but never back to 0, it would continue at 1. When I got my next [chemotherapy] shot, the tingling started at 1, then rose and fell again as if tracing a mountain. But this time it didn't go back to 1, it stayed at around 1.5 or 2 ... My side effects multiplied like dust as the courses of chemo piled up. [The intensity] remained at around 2, even after four courses.	Taxol
8	My hands and feet got increasingly numb. It's been 31 months since my surgery, but my first finger joints on both hands, my fingertips, and the bottoms of my toes are still numb ... When I got out of bed in the morning and planted my feet on the ground, there was this numb sensation, as if I were walking on top of something. I couldn't feel anything when I pushed down on the gas pedal when driving either. Gradually, I lost all feeling on the soles of my feet, from about the balls of my feet to the toes: it feels unpleasant. I can't feel anything when I walk barefoot on wooden flooring, either. [I have some] numbness in my fingertips. It's hard to keep a grip when I pour miso soup into a bowl, I feel like I'm going to drop something. I can't do tasks that require fine motor control of the fingers, or nerve feedback: it's difficult to open beer bottles, to put on a necklace, to press buttons, <i>etc.</i> It's like this constant tingling in the fingertips. [It] feels a little hot.	Paclitaxel
20	I felt that the numbness got worse quickly, even after finishing chemo. I started to have trouble doing various activities, and it became harder to, for example, pinch my fingers together. It's been 5 months since I finished chemo, but my hands and feet still feel numb, and my fingertips still hurt. [Always pins and needles.] I gradually lost feeling in my legs, from about my thighs down to my feet. Even today, I can barely feel the soles of my feet; [when I touch them,] it feels like someone is scratching them through rubber-soled boots. And yet when my feet bump into something, or someone steps on them, it's so painful I want to jump in the air.	Taxol (weekly)
20	I lost feeling [in my arms], [the numbness] gradually spreading from ... the shoulder area down to my fingertips. My fingers too: I have a little trouble when I try to clench my hands very forcefully. I feel like I can't take the caps off bottles, pick up slender objects, do handicrafts, and so on.	Taxol (weekly)
24	My hands and feet would start tingling continuously. The numbness would continue for a while after I'd been sitting seiza-style, even after I started walking.	Taxol

Table 2. Examples of characteristic narratives of patients with breast cancer about a "heightened sense of smell"

No.	Narratives	Treatment
7	I became very sensitive to smells. This was a side effect of the chemotherapy; it was the worst for 3-4 days [after treatment]. I couldn't handle a lot of smells – the smell when the nurse went past, of her shampoo, of the toilet of the hospital – all of them bothered me.	FEC
12	On the third day, I really couldn't tolerate any odors, it felt like I was pregnant or something.	FEC
28	My sense of smell was inhuman, like an animal's. I couldn't tolerate the smell of the hospital, the smell of meals, the smell of tea. Smells were my arch-enemy, so much so that I wished for them all to disappear from the face of the earth. When you can't tolerate smells, you can't eat food. Thousands of times worse than morning sickness (<i>laughter</i>), thousands of times worse. I developed a keen sense of smell. Most of all, I don't know if it was the medicine, but I remember that I really stank afterwards.	AC
23	Conversely, I got increasingly sensitive to smell after the third round of chemo. [Whenever I wanted to eat something,] the first thing I did was to smell it. Sometimes it would smell delicious, sometimes it would smell a bit unappetizing. After I ate something, the smell leaving my nose would make me think, "Oh I like the way this smells", or "Maybe I don't."	TRASTU/ DTX

Table 3. Characteristic narratives of patients with breast cancer concerning information on adverse drug events

Category	Narratives
<i>Information about rarely occurring adverse drug events</i>	[Vascular pain] affects very, very few people who take [Pharmorubicin]. It's not listed as a potential side effect in the information sheet that the hospital gave me. I was surprised to experience this [wide] variation from person to person. Even [assuming an incidence of] 0.1%, I think you'd likely find quite a few people like me if you searched all of Japan. It took a year and a half before they figured out that I had developed interstitial pneumonia as a side effect of the hormone drug [I was taking]. I think there are others in the country who still don't know that it's [a potential side effect].
<i>Reference material to determine whether side effects are reactions to chemotherapy, or symptoms of cancer progression</i>	Xeloda's side effects were absolutely terrible. I started to wonder, "When I received preoperative chemotherapy [adriamycin+docetaxel], I was active enough to walk and go out almost every day: why do I feel so terrible now?" Was something about my own body causing this, rather than the drug? I felt that I couldn't tell what was the medicine's fault and what wasn't. For example, there are times when the chemo causes a bunch of side effects, and you think, "Is this a side effect? Or did the cancer spread?" It's very true, something starts hurting and you think, "Could this be cancer?" There was nowhere I could ask anyone about those kinds of things.
<i>Information about side-effect severity, timing, duration, time profile, cure availability, and countermeasures</i>	The instructions document did note numbness [as a side effect of] the weekly paclitaxel. But what was written there was like, please be careful not to trip and stumble. The information wasn't clear about the healing process either: how long it would take to get better, or the available treatments. If I just knew how long the side effects would last – the joint pain, the muscle pain, the red spots on my face – I could tolerate them.

olfactory disturbance. Although we could find none for the combination drugs FEC/CEF and AC, we noted three cases for TRASTU/DTX: one of hyposmia (2007) and two of parosmia (2011 and 2012) (13). Thus, the side effects spoken of by several patients had similar symptomology to that of anosmia. This ADE was likely omitted from the package inserts because of its extremely low incidence. However, our patients' stories suggest that it was indeed an adverse event to chemotherapy drugs, something we would not have known had it not been for their narrative accounts.

Some patients also noted a desire for detailed information about the potential side effects of chemotherapy, although they were few in number.

They said that they wanted more information about rarely occurring ADEs, as well as their severity, timing, duration, time profile, cure availability, and countermeasures, and reference material to help them determine whether their side effects were reactions to chemotherapy or symptoms of cancer progression (Table 3). In addition, some patients learned about treatment efficacy and side effects via patient networking groups and internet blogs, as well as from the detailed instructions they received from nurses and pharmacists.

4. Discussion

Our analysis of narrative data from 29 breast cancer

survivors identified discrepancies between the ADEs listed on package inserts and the side effects described by the patients. We are aware of a variety of issues associated with our methodology. The study was not prospective: since interviewees had undergone different types of therapies and interview questions were not restricted to medication, their symptom narratives were likely affected by factors besides the drugs they were taking. These limitations notwithstanding, our study represents a novel attempt to extract information about drug events from individual patient dialogues in an existing database.

When planning this study, we predicted that patients' concerns about symptoms – e.g. "Does the side effect I'm experiencing now correspond to those in the medication's instructions?", "Am I the only one with this adverse event?", and "Is my condition getting worse?" – would not be adequately allayed by the bulk of the information provided today. We successfully identified discrepancies between the diverse array of symptomatic events described by patients and the incomplete descriptions on current package inserts.

Let us consider the language patients used to describe the side effect "paresthesia," an adverse event to paclitaxel mentioned by many patients. Interviewees described their symptoms using colorful and evocative language:

- *The sensation was as if I had put my legs into an electric bath.*
- *I couldn't feel anything when I pushed down on the gas pedal when driving either.*
- *Even today, I can barely feel the soles of my feet; [when I touch them,] it feels like someone is scratching them through rubber-soled boots. And yet when my feet bump into something, or someone steps on them, it's so painful I want to jump in the air.*

Readers can readily understand and/or determine the characteristics of the symptom paresthesia based on these patients' real-life experiences.

In addition, patients spoke in great detail about the various side effects they experienced:

1) Body parts

- *There was tingling [in my arms] from the wrists down [especially in my fingertips] ... and from my lower knee down [in my legs].*
- *Gradually, I lost all feeling in the soles of my feet, from about the balls of my feet to the toes.*
- *I gradually lost feeling in my legs, from about my thighs down to my feet.*

2) Conditions

- *... as if I had put my legs into an electric bath.*
- *I lose feeling in my legs when I sit seiza-style (i.e., kneeling upright on the ground). It felt like the sensation that you get when feeling starts to return to your leg after*

it's fallen asleep ...

3) Severity

- *From a starting point of 0, [the tingling] would rise to a peak and then fall, but never back to 0, it would continue at 1.*
- *My side effects multiplied like flies as the courses of chemo piled up. [The intensity] remained around 2, even after four courses.*

4) Duration

- *It's been 31 months since my surgery, but my first finger joints on both hands, my fingertips, and the bottoms of my toes are still numb.*

Paclitaxel package inserts describe adverse events using language such as "peripheral neuropathy, paralysis" and "hypoesthesia (peripheral neuropathy, such as paresthesia)." These descriptions lack information about the qualities of this "paresthesia," as well as its approximate onset and duration and the affected body part(s). One could thus expect many patients to be overwhelmed by anxiety, unable to foresee the exact side effects they should expect based on the language used in the current package inserts. In fact, a similar unease was apparent in the narratives of some patients when they relayed their feelings about the ADE information provided (Table 3). We conclude that the language used to describe ADEs on package inserts is insufficient to help patients as they struggle to recognize, internalize, and overcome drug-related side effects, especially in cancer chemotherapy settings. Detailed information in the words of real patients about the nature of the adverse events predicted, as well as their clinical course and duration, would have inestimable value in supplementing the standardized language used on package inserts.

Patient networking events, social networking services, and a variety of hospital-specific initiatives have separately been demonstrated as useful ways to gather information about individual patients. However, due to the risk of individual differences arising during data collection, we are convinced of the need to construct a database of patients' narrative accounts of ADEs as a source of information that can be reliably disseminated among patients.

We also discovered a variety of issues with our research methodology. Patient reflections were the source of the narrative data analyzed in this study. The interview structure was designed to allow participants to freely recount their personal experiences; it was not designed to investigate ADEs specifically. This made it challenging to identify the exact drug alluded to in many of the dialogues. Future studies will have the difficult task of determining causal links between different adverse events and individual medications. We believe that modifying the interview format to specifically obtain information about medications and ADEs is a necessary

step toward establishing clear causality between the drugs and their alleged side effects described in a narrative. This could be achieved by asking patients the name of their drug at the same time as asking them to describe their side effects and by checking which medications they have taken based on their medicine notebook and other sources.

Future efforts should add specific interview items that can clearly isolate events to drugs – *e.g.*, by establishing an independent line of questioning about chemo- and hormone therapy for about 10 min of the total interview – and identify and confirm with patients which medications they were actually taking using drug history handbooks and information packages. These new approaches could better explain the associations and gaps between patient narratives and the official ADEs described on package inserts.

Researchers of this topic should consider developing a specialized archive specific to adverse events to chemotherapy drugs, such as a hypothetical "Stories about Side Effects of Chemotherapy" database. With the assistance of patient caregivers (including family members) and medical professionals such as attending doctors, pharmacists, and nurses, this strategy could galvanize the construction of a highly accurate database, containing information about prescriptions, nursing care, drug history, and daily living environments. Furthermore, the utility of such a chemotherapy-specific archive for patients and related parties dealing with pharmacotherapy must be evaluated and validated. Jarernsiripornkul *et al.* reported that nervous and psychiatric symptoms and genital and breast diseases are over-represented in patient accounts of side effects (3). Similar trends could be present in patient narratives. When evaluating side effects based on patient accounts, researchers must base their analysis on the assumption that narrative information is different in many respects from the ADE reports of doctors and other professionals.

These limitations notwithstanding, we demonstrated that real patient accounts of medical treatment include copious amounts of valuable information that cannot be discovered from package inserts. Thus, an "Adverse Drug Event Database" could serve as a useful source of additional clinical information to supplement the formal, limited language on package inserts.

Conflict of interest

Kei Kikuchi, Noriko Iba, Rika Sato-Sakuma, Hirokuni Beppu: No conflicts of interest to disclose. Akiko Miki, Hiroki Satoh, Yasufumi Sawada: contributions from 10 companies in total, including five pharmaceutical companies: Shionogi & Company, Taisho Toyama Pharmaceutical, Dainippon Sumitomo Pharma, Mitsubishi Tanabe Pharma, and Nichi-Iko Pharmaceutical (AM: Project Lecturer, HS: Project Assistant Professor, YS: Project Professor). Yasufumi

Sawada: Recipient of joint research funding from eight companies including Taiho Pharmaceutical, Dainippon Sumitomo Pharma, and Wakunaga Pharmaceutical.

Supplementary materials

This manuscript includes supplementary materials (electronic resources), available online.

References

1. Pharmaceuticals and Medical Devices Agency, reported adverse events from the patients <http://www.pmda.go.jp/safety/reports/patients/0004.html> (accessed June 30, 2019). (in Japanese)
2. Golomb BA, McGraw JJ, Evan MA, Dimsdale JE. Physician response to patient reports of adverse drug effects: Implications for patient-targeted adverse effect surveillance. *Drug Saf.* 2007; 30:669-675.
3. Jarernsiripornkul N, Krska J, Capps PA, Richards RM, Lee A. Patient reporting of potential adverse drug events: A methodological study. *Br J Clin Pharmacol.* 2002; 53:318-325.
4. Basch E. The missing voice of patients in drug-safety reporting. *N Engl J Med.* 2010; 362:865-869.
5. Herxheimer A, Mintzes B. Antidepressants and adverse effects in young patients: Uncovering the evidence. *CMAJ.* 2004; 170:487-489.
6. Aagaard L, Nielsen LH, Hansen EH. Consumer reporting of adverse drug reactions: A retrospective analysis of the Danish adverse drug reaction database from 2004 to 2006. *Drug Saf.* 2009; 32:1067-1074.
7. Di Maio M, Basch E, Bryce J, Perrone F. Patient-reported outcomes in the evaluation of toxicity of anticancer treatments. *Nat Rev Clin Oncol.* 2016; 13:319-325.
8. The National Cancer Institute. Cancer Therapy Evaluation Program. Protocol Development. Adverse Events/CTCAE. https://ctep.cancer.gov/protocolDevelopment/electronic_applications/ctc.htmlDDT. (accessed June 30, 2019)
9. Patient-Reported Outcomes version of the Common Terminology Criteria for Adverse Events (PRO-CTCAE™). <https://healthcaredelivery.cancer.gov/pro-ctcae/>. (accessed June 30, 2019)
10. DIPEX-Japan. <https://www.dipex-j.org/outline/data-sharing> (accessed June 30, 2019). (in Japanese)
11. DIPEX-Japan. <https://www.dipex-j.org/breast-cancer/> (accessed June 30, 2019). (in Japanese)
12. Common Terminology Criteria for Adverse Events (CTCAE) http://www.jcog.jp/doctor/tool/CTCAEv4J_20170912_v20_1.pdf. (accessed June 30, 2019). (in Japanese)
13. Pharmaceuticals and Medical Devices Agency; http://www.info.pmda.go.jp/fsearchnew/fukusayouMainServlet?scrid=SCR_LIST&evt=SHOREI&type=1&pID=4291406%20%20%20%20%20&name=%A5C8%A5%E9%A5%B9%A5%C4%A5%BA%A5%DE%A5%D6&fuku=%D3%CC%B3%D0&root=3&srtendo=2&rdoMatch=false&page_max=100&page_no=0. (accessed June 30, 2019). (in Japanese)

(Received May 29, 2019; Revised June 30, 2019; Accepted August 21, 2019)

Repositioning of an anti-depressant drug, agomelatine as therapy for brain injury induced by craniotomy

Krishna A. Lad, Anurag Maheshwari, Bhagawati Saxena*

Department of Pharmacology and Toxicology, National Institute of Pharmaceutical Education and Research-Ahmedabad, Palaj, Gandhinagar, Gujarat, India.

Summary

Traumatic brain injury (TBI) leads to the disruption of blood-brain barrier integrity and therefore results in increased brain water content (brain edema). Brain edema is a significant factor for increased intracranial pressure (ICP), which ultimately causes functional disability and death. The decompressive craniotomy (DC) is a surgical procedure widely used for treating increased ICP following TBI. The life-saving craniotomy itself results in brain injury. The objective of this study is to investigate the effect of agomelatine against craniotomy induced brain injury. The craniotomy was performed by a variable speed micro-motor dental driller of 0.8 mm drill bit. The present study, in addition to blood-brain permeability, brain water content (edema) and histological examination of the brain, also estimated locomotor activity, oxidant, and antioxidant parameters. Results show that the craniotomy induced increase in the blood-brain barrier permeability, brain water content (edema), oxidative stress (lipid peroxide and nitric oxide) and impaired antioxidant mechanisms (superoxide dismutase, catalase, and reduced glutathione) in rats. The craniotomy was also found to increase neuronal cell death indicated by augmented chromatolysis and impaired locomotor activity. Administration of agomelatine after the craniotomy ameliorated histopathological, neurochemical and behavioral consequences of craniotomy. Thus agomelatine is effective against brain injury caused by craniotomy.

Keywords: Traumatic brain injury, craniotomy, agomelatine, blood-brain barrier permeability, brain edema, intracranial pressure

1. Introduction

Traumatic brain injury (TBI) is defined as an impairment of brain functions caused by an external mechanical impact (1). The mechanical impacts on the brain in TBI cause fracture of cranial vault bone, which sometimes depresses into the brain, leads to intracranial bleeding and hemorrhage within the brain parenchyma (2). This damage results in extracellular water accumulation due to blood-brain barrier disruption, sustained intracellular water collection, osmotic imbalances between blood and tissue, and obstruction of cerebrospinal fluid outflow.

This leads to vasogenic, cytotoxic/cellular, osmotic, and hydrocephalic/interstitial edema, respectively (3). Cerebral swelling due to edema results in the increased intracranial pressure (ICP) and the brain herniation, followed by coma and death (4).

The decompressive craniectomy (DC) is a widely used neurosurgical treatment for increased ICP following TBI (5). In DC, a part of the skull is removed to allow the swell brain to expand without being squeezed. DC caused brain injury, revealed by morphological, behavioral, and biochemical changes (6). Thus DC reduces the mortality, however, it converts fatality into survival with severe disability (7).

Brain injury results in decrease in the levels of melatonin receptors subtype 1 (MT₁) and 2 (MT₂) (8). An earlier report shows that melatonin exerts neuroprotective effects against brain injury induced by trauma (9) as well as hypoxic-ischemia (10). Melatonin attenuates TBI induced inflammation (11) and preserves the blood-brain barrier integrity and permeability *via*

*Address correspondence to:

Dr. Bhagawati Saxena, Department of Pharmacology and Toxicology, National Institute of Pharmaceutical Education and Research-Ahmedabad, Palaj, Gandhinagar 382355, Gujarat, India. Currently working as Assistant Professor at Department of Pharmacology, Institute of Pharmacy, Nirma University, S.G. Highway, Ahmedabad, 382481, India.
E-mail: bhagawati.saxena@nirmauni.ac.in

matrix metalloproteinase-9 inhibition (12). Additional studies using different experimental TBI models showed that melatonin decreases brain edema, blood-brain barrier permeability, ICP, and neuronal cell death probably due to inhibition of oxidative stress and the attenuation of nuclear factor-kappaB (NF-kappaB) (13-15). MT₁, MT₂, and melatonin receptor subtype 3 (MT₃) melatonin receptors had anti-edema effects while MT₁ and MT₂ have a role in protecting the blood-brain barrier (16).

Agomelatine is the first melatonergic antidepressant. It is a potent agonist of the melatonin receptors MT₁ and MT₂ and an antagonist at serotonin-2C (5-HT_{2C}) receptors (17). Agomelatine enhances adult hippocampal neurogenesis and increases the expression of several molecules associated with neuroplasticity (18,19). The action of agomelatine on neurogenesis is likely to reside in its antagonism to the 5HT_{2C} receptor (20). However, until now agomelatine has not been explored for its neuroprotective activity against craniotomy induced brain injury. In this study, we hypothesized that agomelatine might help in faster recovery after craniotomy *via* synergistic agonistic action on MT₁/MT₂ and antagonist on 5-HT_{2C} receptors. Therefore, the present work evaluates the neuroprotective activity of agomelatine against craniotomy induced brain injury. In addition to brain edema and its histological examination, the present study also includes estimation of locomotor activity, blood-brain permeability, oxidant and antioxidant parameters.

2. Materials and Methods

2.1. Animals

Sprague Dawley (SD) rats ($n = 90$), weighing 250 ± 10 g, of either sex were used for the study. The animals were housed 3 per cage in polypropylene cages, and the environmental conditions of the animal room were as per a specific design. A 10% air exhaust in the air conditioning unit was maintained along with a relative humidity of $60 \pm 5\%$ and a temperature of $25 \pm 3^\circ\text{C}$ was stabilized. A 12 h light/dark cycle was also regulated for the experimental animals. Food and water provided *ad libitum* to the animals during the experimental period. All experimental protocols were reviewed and accepted by the Institutional Animal Ethics Committee before the initiation of the experiment.

2.2. Drugs, reagents, and solvents

Agomelatine (Agoviz) was procured from Abbott, Mumbai, India. Isoflurane and Evans blue were purchased from Raman and Weil Pvt. Ltd. (Mumbai, India) and Sigma Aldrich (Bangalore, India), respectively. Tris buffer, ethylenediaminetetraacetic acid (EDTA), Triton X 100, pyrogallol, thiobarbituric acid (TBA), 5,5-dithiobis (2-nitrobenzoic acid) (DTNB),

naphthylendiamine dihydrochloride, sulphanilic acid, L-reduced glutathione were purchased from HiMedia laboratories Pvt. Ltd., Mumbai, India. All the other solvents and chemicals were purchased from Loba Chemie (Mumbai, Maharashtra, India).

2.3. Craniotomy

The craniotomy procedure was performed on rats as demonstrated by Cole *et al.* (6). Briefly, rats were anesthetized with 4% isoflurane and maintained with 2% in 98% oxygen. Once anesthetized, the animals were placed in a prone position with anesthesia delivered using nosecone. The animal's head and surgical site were sterilized with the application of 95% ethanol after shaving. A midline incision on the scalp exposed the skull. The craniotomy was performed by using a variable speed micro-motor dental driller of 0.8 mm drill bit. 2.5 mm radius bone flap above the right hemisphere was carefully drilled. Bone flap was removed, and the brain was exposed to the normal environment for 4 min while normal saline was continuously poured. After 4 min of exposure, the bone flap was replaced and secured with Ethicon bone wax. The incision was sutured, and Povidone Iodine solution was applied to the sutured site. Animals were returned to recovery cage with sodium lamp to provide heat and continuously monitored.

2.4. Experimental design

SD rats were divided into five groups with six animals each. All groups except normal were then subjected to craniotomy. Normal and craniotomy group rats received the 0.3% carboxymethylcellulose (CMC) (3 mL/kg, *p.o.*) suspension as the vehicle and other three groups received a single treatment of agomelatine (1, 3, and 10 mg/kg, *p.o.*) after one h of craniotomy. Alterations in the behavior of all the animals were assessed using the beam walking test, and pole test. All animals were sacrificed and brains were taken out for histopathology, estimation of brain water content, malondialdehyde (MDA), nitric oxide (NO), superoxide dismutase (SOD), catalase and reduced glutathione.

2.5. Behavioral assessment

All behavioral testing was carried out after 24 h of craniotomy and agomelatine treated animals in a sound proof room with subdued lighting.

2.5.1. Beam walking test

The beam-walk test was done to measure the loss of balance and coordination generally seen post-trauma (21). The surface of a 2.5×112 cm wooden beam was elevated 60 cm above the floor by the wooden support. A $20 \times 25 \times 24$ cm goal box with a 10 cm opening was

Table 1. Score for beam walking behavior of rat

Score	Observation
1	Rat is unable to place the affected hind paw on the horizontal surface of the beam
2	Rat places the affected hindpaw on the horizontal surface of the beam and maintains balance but is unable to traverse the beam
3	Rat traverses the beam dragging the affected hindpaw
4	Rat traverses the beam and once places the affected hindpaw on the horizontal surface of the beam
5	Rat crosses the beam and places the affected hindpaw on the horizontal surface of the beam to aid less than half its steps
6	Rat uses the affected hindpaw to aid more than half its steps
7	Rat traverses the beam with no more than two footsteps

placed at the one end of the beam. Two trials were given to each animal with 10 min interval. For each trial, the rat was placed at the start end of the beam opposite to the goal box. After two trials, the result was recorded. The performance was scored on a 7-point scale as mentioned in Table 1.

2.5.2. Pole test

Pole test was performed using the method described by Ogata *et al.* (22). The time for the rats to descend from the top of the roughly surfaced pole to the floor was recorded in all the animals of each group. Pole: 2.5 cm diameter, 100 cm height with 120 sec cut-off time.

2.6. Estimation of oxidative stress

2.6.1. Assessment of lipid peroxidation

MDA is one of the final products of the lipid peroxidation (LPO) in the cells. It was estimated as described in Draper and Hadley (23) with slight modification. Brain tissue was isolated and the cortex region was weighed 100 mg. Weighed tissue was transferred to tubes containing 5 mL Hanks' Balanced Salt Solution (HBSS) buffer and homogenized in 3 cycles of 30 sec each at 3,000 rpm with 30 sec gap. Tissue homogenate was centrifuged for 10 min at 3,000 rpm and 25°C. The supernatant was discarded and the cell pellet was taken. The cell pellet was transferred into tubes containing 0.2 mL of sodium dodecyl sulfate (SDS), 1.5 mL of acetic acid, 1.5 mL of TBA and 0.7 mL of MilliQ water. 0.1 mL HBSS was added in control tubes instead of homogenate. The tubes were kept in boiling water bath for 1 h. After boiling, 1 mL Milli Q was added to each tube. 5 mL butanol: pyridine (15:1) was added to each tube and vortexed for five mins. The organic layer was centrifuged at 3,000 rpm for 10 min at 25°C and the amount of MDA formed was measured by the absorbance of the upper organic layer at 532 nm. The concentration of MDA was calculated in $\mu\text{M}/\text{mg}$ brain tissue using a standard curve prepared with 1,1,3,3-tetraethoxypropane (TEP).

2.6.2. Assessment of nitric oxide

The nitrite level is the marker of nitric oxide (NO).

Nitrite level in brain tissues were estimated using the method described by Hevel and Marletta (24) with slight modification. Brain tissue was isolated and 100 mg cortex region was homogenized in 5 mL of ice-cold phosphate buffer at 3,000 rpm for 2 min in 2 cycles with 30 sec gap. In a separate tube containing freshly prepared 100 μL of Griess reagent and 2 mL of phosphate buffer, 300 μL of the homogenized solution was added. Tubes were incubated at room temperature for 30 min and absorbance was measured at 548 nm. The total nitrite concentration was calculated in mM/mg of tissue from a standard curve prepared with sodium nitrite.

2.6.3. Assessment of superoxide dismutase (SOD)

The SOD levels were estimated using the method described by Marklund and Marklund (25) with slight modification. Brain tissue was isolated, and 100 mg cortex region was homogenized in 4 mL Tris-EDTA (chilled) buffer by three cycles of 30 sec each at 3,000 rpm with 30 sec gap. In each tube, 1 mL of 1% Triton-X-100 was added. The tube was vortexed and incubated for 20 min at 4-8°C. The content was transferred to microcentrifuge tubes and centrifuged at 10,000 rpm at 4°C for 30 min. The supernatant was taken for the spectroscopic analysis. Zero time absorbance was taken at 420 nm followed by recording the absorbance reading every 60 sec for 10 min at 25°C. The above-mentioned reaction mixtures without the brain homogenate served as control. The rate of increase in absorbance units (A) per minute for the control and the test sample(s) was determined, and the percentage inhibition for the test sample(s) was calculated by the following formula:

$$\% \text{ inhibition} = \left\{ \frac{[(\Delta A_{420} \text{ nM/min})_{\text{control}} - (\Delta A_{420} \text{ nM/min})_{\text{test}}]}{(\Delta A_{420} \text{ nM/min})_{\text{control}}} \right\} \times 100$$

Units of the SOD activity were expressed as the amount of enzyme required to inhibit the reduction of pyrogallol by 50%, and the activity was expressed in units per g of brain tissue.

2.6.4. Estimation of catalase

The catalase levels were estimated using the method described by Sinha (26) with slight modifications. Brain tissue was isolated, and 100 mg cortex region was

homogenized in 5 mL phosphate buffer at 1,800 rpm in 3 cycles for 30 sec with 30 sec gap each. 1 mL tissue homogenate was diluted up to 5 mL using phosphate buffer and from diluted homogenate 1 mL was mixed with 2 mL of hydrogen peroxide (H₂O₂) (100 mM) and absorbance was noted for 0-10 min at 240 nm. Catalase activity was calculated per min per mg of brain tissue using the standard curve of H₂O₂.

2.6.5. Estimation of reduced glutathione

The reduced glutathione levels were estimated using the method described by Ellman (27) with slight modification. Brain tissue was isolated and 100 mg cortex region was homogenized in 5 mL of ice-cold phosphate buffer. In tissue homogenate, 0.1 mL of trichloroacetic acid was added. Centrifuged at 3,900 g at 25°C for 10 min. 1 mL of the supernatant was mixed with 1 mL DTNB and 1 mL phosphate buffer. It was vortexed for 1 min and incubated for 5 min at room temperature. Absorbance was noted at 412 nm. 1 mL DTNB with 2 mL phosphate buffer was taken as blank. Reduced glutathione levels were calculated as μM/mg of brain tissue using a standard curve.

2.7. Estimation of brain water content

The brain water content was used to estimate edema, which forms as a consequence of the blood-brain barrier breakdown. Brain water content was estimated using the method described by Shigeno *et al.* (28) with slight modifications. Briefly, after decapitating the rats, the brains were removed. The injured hemisphere was weighed (wet weight), dipped in absolute alcohol for 30 min, dried at 55 ± 5°C for 24 h and reweighed (dry weight). The brain water content was determined by following equation:

% Brain water content = [(Wet weight – Dry weight)/wet weight] × 100 and expressed as % brain water content per 100 gm body weight of the animal.

2.8. Estimation of blood-brain barrier integrity

For estimation of blood-brain barrier integrity, in the rats of all the groups, Evans blue (2% W/V) was injected intraperitoneally (2 mg/kg, *i.p.*) as per Manaenko *et al.* (29) 30 min before craniotomy. All groups except normal were then subjected to craniotomy. The normal as well as craniotomy control group were given vehicle (0.3 % CMC) while the other three groups received single oral administration of agomelatine (1, 3, and 10 mg/kg). After 24 h, all the animals were anesthetized using thiopentone sodium (40 mg/kg, *i.p.*) and transcardially perfused with ice-cold heparinized saline. The brain was isolated, and Evans blue in each hemisphere was estimated as described in Katayama *et al.* (30) with slight modifications. Briefly, each hemisphere was

soaked in 0.5 N KOH overnight at 37°C. 2.5 mL of a mixed solution of 4 N H₃PO₄ and acetone (3:15) was added to each tube. The tube was vortexed for a minute and centrifuged at 3,000 rpm for 15 min at 25°C. The absorbance of the blue layer was taken at 620 nm. Evans blue concentration in the brain was calculated using the standard curve prepared from Evans blue.

2.9. Histopathological study

The brain tissues were excised, washed with ice-cold 0.9% saline solution and fixed for 24 h in 10% buffered formalin for histopathological studies. The tissues were washed with running tap water to remove any additional fixative. The tissues were finally cleaned with methyl benzoate and embedded in paraffin wax after dehydrating through a graded series of alcohol. Tissue sections of 5 μm thickness were cut, deparaffinized and hydrate to water followed by cresyl violet (0.5% W/V) staining for 3-5 min. After staining tissue sections were dehydrated and fixed by DPX mountant. Sections were examined under a light microscope (200×).

2.10. Statistical analysis

Statistical analysis was done using GraphPad Prism 4 (San Diego, California). All the results were expressed as the mean ± SEM (*n* = 6). All the data were statistically analyzed by one-way ANOVA, followed by Newman-Keuls multiple comparisons test. *p* < 0.05 was considered statistically significant.

3. Results

3.1. Effect of agomelatine on behavioral performance in craniotomy rats

Figure 1A illustrates the effect of agomelatine treatment on the score assessed in beam walking in craniotomy induced brain injury model. Results were statistically analyzed using one way ANOVA which indicates significant differences in score among the different groups [F (4, 29) = 17.23, *p* < 0.0001]. In craniotomy exposed rats, score decreased significantly compared to the normal control group. A single treatment with agomelatine increased craniotomy induced decreased score at all the doses. Agomelatine in all doses showed significant improvement in performance as compared with craniotomy group.

Figure 1B depicts the effect of agomelatine treatment on the performance of rats on pole test in the craniotomy induced brain injury model. Statistical analysis was done using one way ANOVA [F (4, 29) = 33.16, *p* < 0.0001]. A significant difference was found in performance with pole test between normal and craniotomy animals. Agomelatine in a dose of 1, 3, and 10 mg/kg had shown significant improvement in performance compared with

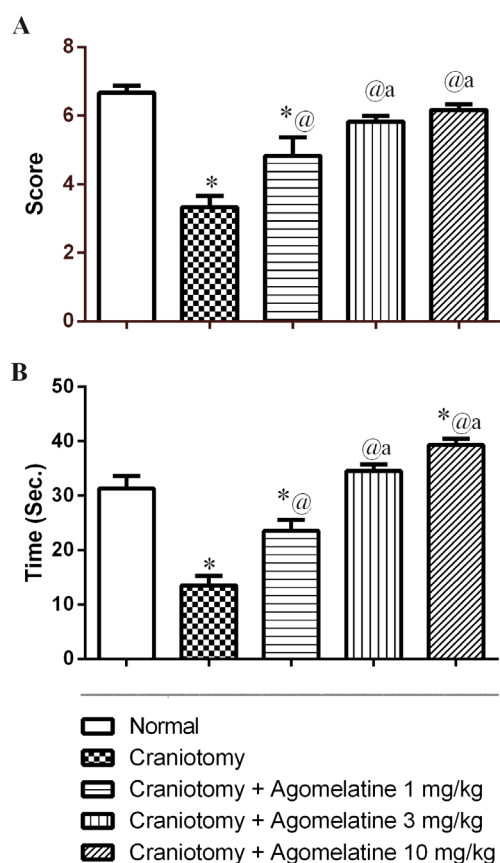


Figure 1. Effect of agomelatine on motor defects induced by craniotomy in rats using beam walking test (A) and pole test (B). Data were expressed as mean \pm SEM ($n = 6$). * $p < 0.05$ compared to normal, @ $p < 0.05$ compared to craniotomy, # $p < 0.05$ compared to agomelatine 1 mg/kg using one way ANOVA (Newman-Keuls multiple comparison test).

the craniotomy group.

3.2. Effect of agomelatine on oxidative stress and antioxidant parameters

Figure 2A aptly demonstrates the effect of agomelatine treatment on the level of MDA, a marker of lipid peroxidation. One-way ANOVA revealed significant differences in MDA level among various groups [$F(4,29) = 12.40$; $p < 0.0001$]. Craniotomy did increase MDA level in brain significantly while agomelatine treatment effectively attenuated the craniotomy-induced increase in LPO at the doses of 3 and 10 mg/kg.

Figure 2B represents the effect of agomelatine treatment on nitrite level. One-way ANOVA revealed a significant differences in nitrite level among various groups [$F(4,29) = 6.105$; $p < 0.005$]. It was observed that craniotomy had increased the nitrite level significantly and agomelatine treatment attenuated the increased nitrite level at the doses of 3 and 10 mg/kg.

The results of agomelatine treatment on superoxide dismutase (SOD) levels in craniotomy induced brain injury model were analyzed by one-way ANOVA [$F(4,29) = 7.220$, $p < 0.0005$] (Figure 3A). A significant

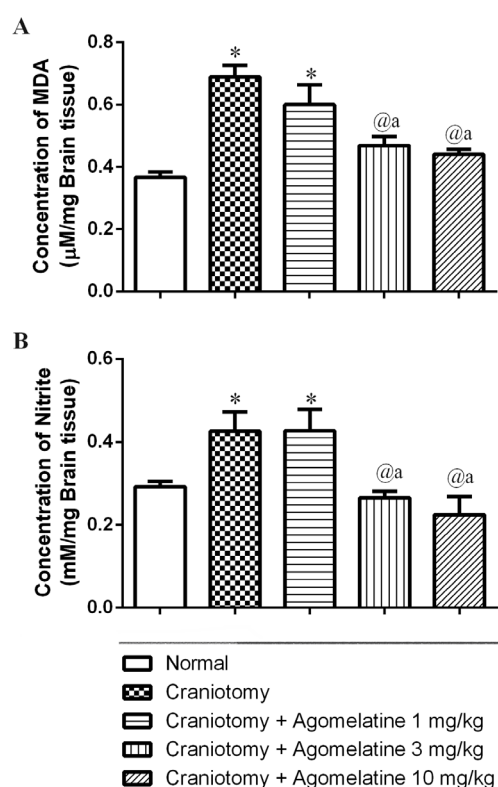


Figure 2. Effect of agomelatine on MDA level (LPO) (A) and nitrite level (B) rats against craniotomy induced brain injury. Data were expressed as mean \pm SEM ($n = 6$). * $p < 0.05$ compared to normal, @ $p < 0.05$ compared to craniotomy, # $p < 0.05$ compared to agomelatine 1 mg/kg using one way ANOVA (Newman-Keuls multiple comparison test).

decrease in SOD levels was observed in craniotomy animals compared to the normal. Agomelatine at all the doses had shown no significant effect on SOD levels compared to the craniotomy group.

The effect of agomelatine treatment on the catalase activity in craniotomy induced brain injury model is shown in Figure 3B. One-way ANOVA revealed a significant differences in catalase activities between groups [$F(4, 29) = 12.01$, $p < 0.0001$]. Post-hoc analysis showed that craniotomy significantly increased catalase activity. Agomelatine (1, 3, and 10 mg/kg, *p.o.*) significantly decreased the catalase activity compared to the craniotomy group.

Figure 3C elucidates the effect of agomelatine treatment on the reduced glutathione in craniotomy induced brain injury. The results were analyzed by one way ANOVA [$F(4,29) = 3.361$, $p < 0.05$]. The significant decrease in reduced glutathione levels was observed in craniotomy animals as compared to normal animals. Agomelatine in the dose of 3 and 10 mg/kg had significantly modulated the reduced glutathione due to craniotomy.

3.3. Effect of agomelatine on brain water content

Figure 4 illustrates the effect of agomelatine treatment

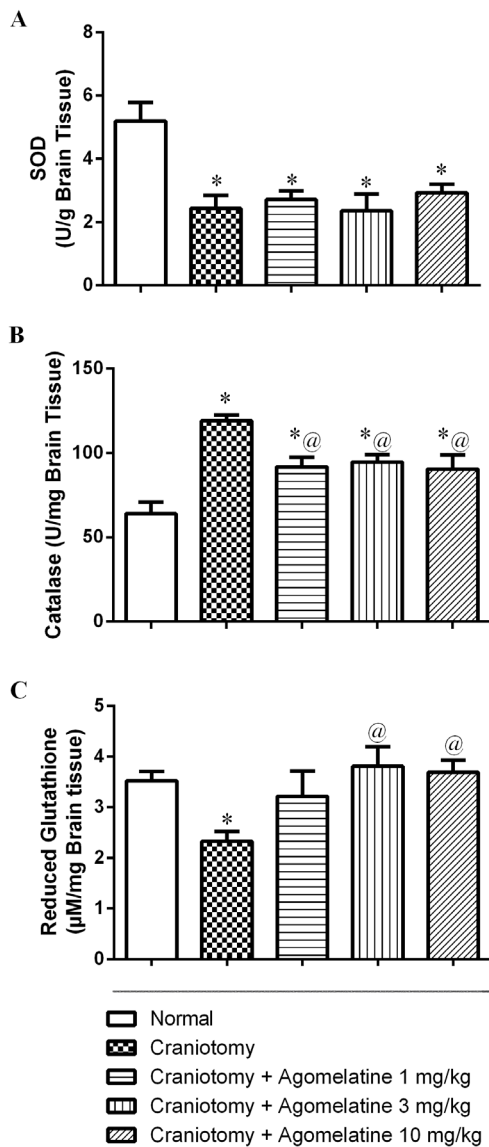


Figure 3. Effect of agomelatine on SOD (A), catalase (B) and reduced glutathione (C) levels in rats against craniotomy induced brain injury. Data were expressed as mean \pm SEM ($n = 6$). * $p < 0.05$ compared to normal, [@] $p < 0.05$ compared to craniotomy, ^a $p < 0.05$ compared to agomelatine 1 mg/kg using one way ANOVA (Newman-Keuls multiple comparison test).

on the water content of brain in animals underwent craniotomy. One-way ANOVA [$F(4,29) = 5.753$, $p < 0.005$] showed that the brain water content increased significantly in the rats undergone craniotomy compared with normal rats without craniotomy. Brain water content was attenuated with the agomelatine treatment at all the doses.

3.4. Effect of agomelatine on blood-brain barrier integrity

The effect of agomelatine treatment on the Evans blue concentration in the right brain hemispheres of all the rats was studied and the results were analyzed by one-way ANOVA (Figure 5). Significant differences were

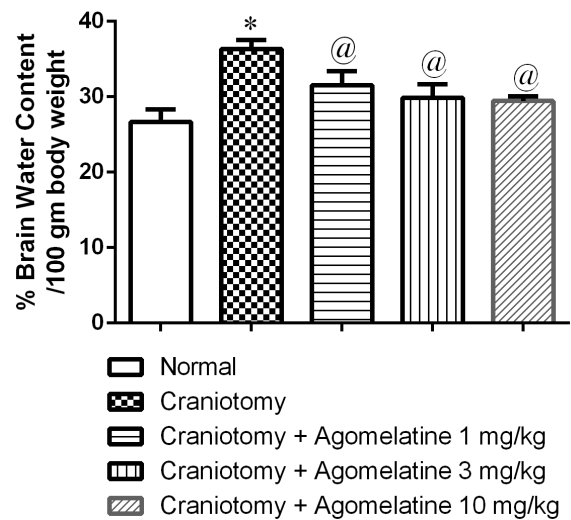


Figure 4. Effect of agomelatine on edema (% brain water content/100 g of body weight) in rats against craniotomy induced brain injury. Data were expressed as mean \pm SEM ($n = 6$). * $p < 0.05$ compared to normal, [@] $p < 0.05$ compared to craniotomy, ^a $p < 0.05$ compared to agomelatine 1 mg/kg using one way ANOVA (Newman-Keuls multiple comparison test).

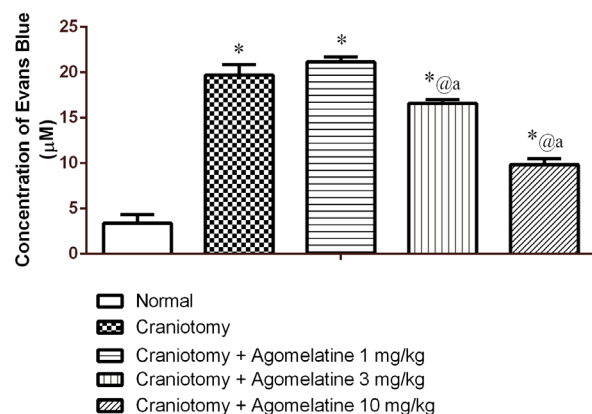


Figure 5. Effect of agomelatine on blood brain barrier (Evans blue concentration) in left and right brain hemisphere of rats against craniotomy induced brain injury. Data were expressed as mean \pm SEM ($n = 6$). * $p < 0.05$ compared to normal, [@] $p < 0.05$ compared to craniotomy, ^a $p < 0.05$ compared to agomelatine 1 mg/kg using one way ANOVA (Newman-Keuls multiple comparison test).

observed in the Evans blue concentration among the groups [$F(4, 29) = 89.11$, $p < 0.0001$]. A significant increase in Evans blue concentration was observed in craniotomy animals than normal. Agomelatine in the doses of 3 and 10 mg/kg had shown a significant decrease in Evans blue concentration as compared with craniotomy group.

3.5. Effect of agomelatine on Nissl staining

Nissl staining was performed on brain sections from a normal group, craniotomy group, and agomelatine in 1, 3, and 10 mg/kg dose. Sections were stained with cresyl

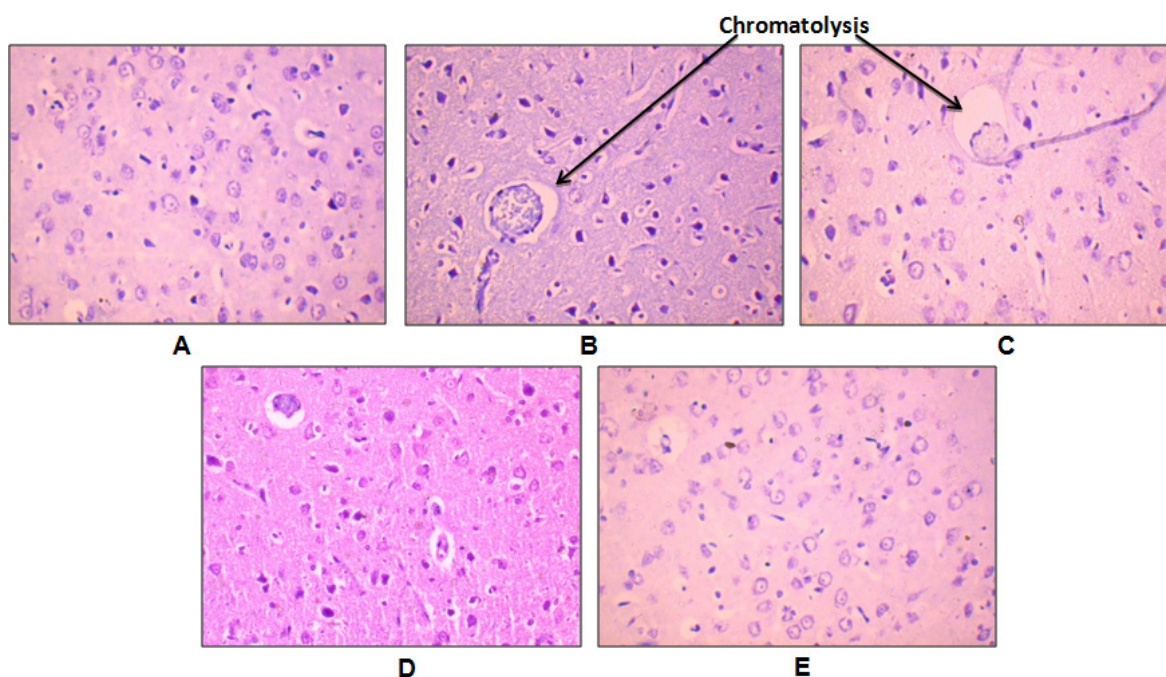


Figure 6. Nissl staining of brain sections of different groups. Normal (A), craniotomy (B), agomelatine 1 mg/kg (C), agomelatine 3 mg/kg (D), agomelatine 10 mg/kg (E).

violet. Nissl staining using cresyl violet was done in brain sections for detection of neuronal death and damage. Cresyl violet specifically stains the Nissl bodies which are large granular bodies in neurons. Chromatolysis (indicated by arrow), *i.e.*, dissolution of Nissl bodies was found in craniotomy (Figure 6B) and agomelatine 1 mg/kg groups (Figure 6C). Chromatolysis is an induced response of cell triggered by axotomy, neurotoxicity, cell exhaustion. Chromatolysis is a precursor to apoptosis.

4. Discussion

The key findings of the present investigation are as follows: (1) craniotomy in rats induced increased brain water content (edema), blood-brain barrier permeability, oxidative stress (LPO and NO), impaired antioxidant mechanisms (SOD, catalase and reduced glutathione) and increased neuronal cell death indicated by augmented chromatolysis, (2) craniotomy also induced impairment in locomotor activity (behavioral consequence) and (3) administration of agomelatine after the craniotomy ameliorated histopathological, neurochemical and behavioral consequences of craniotomy.

Brain edema occurs in TBI. Edema results in increased ICP, which causes death (4). The DC is a surgical procedure done to treat increased ICP following TBI. However, DC causes considerable damage to the brain (6). The complications after DC are subdural hygroma and hydrocephalus, postoperative hematoma expansion and infection of the surgical site. Consequent cranioplasty has the risk of infection, cerebral edema, and bone flap reabsorption (31). Results of present study also shows craniotomy induced brain injury which is

evident by increased brain water content (edema), blood-brain barrier permeability, oxidative stress (LPO and NO), impaired antioxidant mechanisms (SOD, catalase, and reduced glutathione) and increased neuronal cell death indicated by augmented chromatolysis visible in Nissl stained histopathological slide.

TBI results in neuromotor impairment that causes disabilities affecting mobility, and motor coordination (32,33). To elucidate the effect of agomelatine on impairment in mobility, balance and motor coordination induced by craniotomy, we performed two functional tests, the pole test and beam walk test. The craniotomy results in sustained neurological motor dysfunction, as indicated by decreased performance when transverse the beam and the decreased latency time to descend from the top of roughly surfaced pole to the floor. Thus craniotomy induced motor dysfunction. Maier (34) noted the cortical area associated with coordinated walking in the rat and a cortical lesion results in a motor abnormality when the rats were transverse a narrow elevated beam. Beam-walking test in rats is an excellent tool for studying the functional recovery of locomotor ability after sensorimotor cortex injury (35). Similarly, pole test is a useful method for evaluating the movement disorder (36). Hence craniotomy causes the cortical lesions and thus abnormality in mobility and motor coordination as observed with beam walking and pole test. The present study showed that agomelatine in the doses of 1, 3, and 10 mg/kg attenuated craniotomy induced motor deficit in beam walking and pole test. Thus agomelatine increases functional recovery after craniotomy.

Existing evidence suggests that free radicals play a significant role in the pathophysiology of brain injury

(37). In the present study, results showed a significant increase in MDA and NO levels in animals underwent the craniotomy. Thus, craniotomy increased overall oxidative stress. Agomelatine attenuated the increase in oxidative stress in craniotomy animals. The brain has many defense mechanisms to protect itself from free radicals. SOD and catalase are antioxidant enzymes, which are involved in the elimination of free radicals, whereas small-molecule antioxidants such as glutathione can repair oxidizing radicals directly (38). Results of this investigation show the alteration in anti-oxidants level in craniotomy animals. Agomelatine treatment increased the anti-oxidants level in the brain. Melatonin has been reported to exert direct free radical scavenging activity and indirect antioxidant enzymes stimulatory activity (39). Thus, agomelatine normalizes the balance between oxidative stress and anti-oxidants mechanisms impaired by craniotomy *via* its melatonin agonistic activity.

Neural membranes consist of phospholipids in large amount, which are characterized by their high content of some polyunsaturated fatty acids (PUFA) like arachidonic, docosatetraenoic (adrenic), and docosahexaenoic acids. These are essential for normal vascular permeability. Phospholipid peroxidation results in loss of membrane PUFA and contributes to increased membrane rigidity and loss of vascular permeability (38). Oxidative-free radicals generated in brain injury are most likely to play a crucial role in increased cerebral vascular permeability and thus in vasogenic brain edema (40). The present study showed that the % brain water content/100 g animal body weight was significantly increased in animals underwent craniotomy. This increased brain water content indicates craniotomy induced brain edema. Agomelatine treatment followed by craniotomy attenuated the % brain water content/100 g of body weight of animal thus reduced the brain edema. Blood-brain barrier breakdown and increase of vascular endothelium permeability can result in brain edema and eventually ICP increase, which may be fatal (41). The Evans blue is not able to cross the blood-brain barrier. Blood-brain barrier disruption results in increased permeability of Evans blue to the brain. Hence, Evans blue concentration in the brain is indicative of the blood-brain barrier disruption. Craniotomy has shown a marked increase in Evans blue level in the brain. Agomelatine, in a dose of 10 mg/kg, has shown a significant decrease in brain Evans blue concentration. Thus agomelatine mitigated the disturbed blood-brain barrier integrity and increased brain edema caused by craniotomy. MT₁, MT₂, and MT₃ melatonin receptors had anti-edema effects, while MT₁ and MT₂ have a role in protecting the blood-brain barrier (16). This beneficial effect of agomelatine on disturbed blood-brain barrier integrity and increased brain edema due to craniotomy might be due to its melatonin agonistic activity.

Free radical generations, reduced antioxidant mechanism, disrupted the blood-brain barrier and

increased brain edema results in the neuronal loss. Nissl-staining is a widely used method to study morphology and pathology of neuronal tissue. Histopathological examination of Nissl stained brain sections reveals the chromatolysis in animals underwent craniotomy, which indicates neuronal cell death. The absence of chromatolysis was observed in the nissl stained brain sections of animal treated with agomelatine (3 and 10 mg/kg doses) followed by craniotomy. Thus agomelatine decreased neuronal cell death.

5. Conclusion

In the present investigation, the pharmacological evaluation of single treatment agomelatine post craniotomy showed that it possesses promising neuroprotective activity as it mitigates the craniotomy induced histopathological, neurochemical, and behavioral consequences.

Acknowledgments

Authors acknowledge Department of Pharmaceuticals, Ministry of Chemical and Fertilizers, Government of India and National Institute of Pharmaceutical Education and Research (NIPER) Ahmedabad, Gandhinagar, India for financial support. The manuscript is based on M.S. (Pharm.) Dissertation project work done by Ms. Krishna A. Lad from July 2014 to June 2015 at the Department of Pharmacology and Toxicology, NIPER-Ahmedabad. The authors also acknowledge B. V. Patel PERD Centre, Ahmedabad for institutional support.

References

1. Menon DK, Schwab K, Wright DW, Maas AI. Position statement: Definition of traumatic brain injury. *Arch Phys Med Rehabil.* 2010; 91:1637-1640.
2. Mustafa AG, Alshboul OA. Pathophysiology of traumatic brain injury. *Neurosciences (Riyadh).* 2013; 18:222-234.
3. Unterberg AW, Stover J, Kress B, Kiening KL. Edema and brain trauma. *Neuroscience.* 2004; 129:1021-1029.
4. Tomosvari A, Mencser Z, Futo J, Hortobagyi A, Bodosi M, Barzo P. Preliminary experience with controlled lumbar drainage in medically refractory intracranialhypertension. *Orv Hetil.* 2005; 146:159-164.
5. Bor-Seng-Shu E, Figueiredo EG, Fonoff ET, Fujimoto Y, Panerai RB, Teixeira MJ. Decompressive craniectomy and head injury: Brain morphometry, ICP, cerebral hemodynamics, cerebral microvascular reactivity and neurochemistry. *Neurosurg Rev.* 2013; 36:361-370.
6. Cole JT, Yarnell A, Kean WS, Gold E, Lewis B, Ren M, McMullen DC, Jacobowitz DM, Pollard HB, O'Neill JT, Grunberg NE, Dalgard CL, Frank JA, Watson WD. Craniotomy: True sham for traumatic brain injury, or a sham of a sham? *J Neurotrauma.* 2011; 28:359-369.
7. Honeybul S. Decompressive craniectomy for severe traumatic brain injury reduces mortality but increases survival with severe disability. *Evid Based Med.* 2017; 22:61.

8. Osier ND, Pham L, Pugh BJ, Puccio A, Ren D, Conley YP, Alexander S, Dixon CE. Brain injury results in lower levels of melatonin receptor subtypes MT1 and MT2. *Neurosci Lett.* 2017; 650:18-24.
9. Naseem M, Parvez S. Role of melatonin in traumatic brain injury and spinal cord injury. *ScientificWorldJournal.* 2014; 2014:1-13.
10. Sinha B, Wu Q, Li W, *et al.* Protection of melatonin in experimental models of newborn hypoxic-ischemic brain injury through MT1 receptor. *J Pineal Res.* 2018; 64.
11. Lin C, Chao H, Li Z, Xu X, Liu Y, Hou L, Liu N, Ji J. Melatonin attenuates traumatic brain injury-induced inflammation: A possible role for mitophagy. *J Pineal Res.* 2016; 61:177-186.
12. Alluri H, Wilson RL, Anasooya Shaji C, Wiggins-Dohlvik K, Patel S, Liu Y, Peng X, Beeram MR, Davis ML, Huang JH, Tharakan B. Melatonin preserves blood-brain barrier integrity and permeability *via* matrix metalloproteinase-9 inhibition. *PLoS One.* 2016; 11:e0154427.
13. Dehghan F, Khaksari Hadad M, Asadikram G, Najafipour H, Shahrokhi N. Effect of melatonin on intracranial pressure and brain edema following traumatic brain injury: Role of oxidative stresses. *Arch Med Res.* 2013; 44:251-258.
14. Beni SM, Kohen R, Reiter RJ, Tan DX, Shohami E. Melatonin-induced neuroprotection after closed head injury is associated with increased brain antioxidants and attenuated late-phase activation of NF-kappaB and AP-1. *FASEB J.* 2004; 18:149-151.
15. Ozdemir D, Uysal N, Gonenc S, Acikgoz O, Sonmez A, Topcu A, Ozdemir N, Duman M, Semin I, Ozkan H. Effect of melatonin on brain oxidative damage induced by traumatic brain injury in immature rats. *Physiol Res.* 2005; 54:631-637.
16. Shahrokhi N, Khaksari M, AsadiKaram G, Soltani Z, Shahrokhi N. Role of melatonin receptors in the effect of estrogen on brain edema, intracranial pressure and expression of aquaporin 4 after traumatic brain injury. *Iran J Basic Med Sci.* 2018; 21:301-308.
17. Guardiola-Lemaitre B, De Bodinat C, Delagrangé P, Millan MJ, Muñoz C, Mocaer E. Agomelatine: Mechanism of action and pharmacological profile in relation to antidepressant properties. *Br J Pharmacol.* 2014; 171:3604-3619.
18. Banasr M, Soumier A, Hery M, Mocaer E, Daszuta A. Agomelatine, a new antidepressant, induces regional changes in hippocampal neurogenesis. *Biol Psychiatry.* 2006; 59:1087-1096.
19. Paizanis E, Renoir T, Lelievre V, Saurini F, Melfort M, Gabriel C, Barden N, Mocaer E, Hamon M, Lanfumey L. Behavioural and neuroplastic effects of the new-generation antidepressant agomelatine compared to fluoxetine in glucocorticoid receptor-impaired mice. *Int J Neuropsychopharmacol.* 2010; 13:759-774.
20. AlAhmed S, Herbert J. Effect of agomelatine and its interaction with the daily corticosterone rhythm on progenitor cell proliferation in the dentate gyrus of the adult rat. *Neuropharmacology.* 2010; 59:375-379.
21. Goldstein LB, Davis JN. Beam-walking in rats: Studies towards developing an animal model of functional recovery after brain injury. *J Neurosci Methods.* 1990; 31:101-107.
22. Ogata A, Tashiro K, Nukuzuma S, Nagashima K, Hall WW. A rat model of Parkinson's disease induced by Japanese encephalitis virus. *J Neurovirol.* 1997; 3:141-147.
23. Draper H, Hadley M. Malondialdehyde determination as index of lipid peroxidation. *Methods Enzymol.* 1990; 186:421-431.
24. Hevel JM, Marletta MA. Nitric-oxide synthase assays. *Methods Enzymol.* 1994; 233:250-258.
25. Marklund S, Marklund G. Involvement of the superoxide anion radical in the autoxidation of pyrogallol and a convenient assay for superoxide dismutase. *Eur J Biochem.* 1974; 47:469-474.
26. Sinha AK. Colorimetric assay of catalase. *Anal Biochem.* 1972; 47:389-394.
27. Ellman GL. Tissue sulfhydryl groups. *Arch Biochem Biophys.* 1959; 82:70-77.
28. Shigeno T, Brock M, Shigeno S, Fritschka E, Cervos-Navarro J. The determination of brain water content: Microgravimetry versus drying-weighing method. *J Neurosurg.* 1982; 57:99-107.
29. Manaenko A, Chen H, Kammer J, Zhang JH, Tang J. Comparison Evans blue injection routes: Intravenous versus intraperitoneal, for measurement of blood-brain barrier in a mice hemorrhage model. *J Neurosci Methods.* 2011; 195:206-210.
30. Katayama S, Shionoya H, Ohtake S. A new method for extraction of extravasated dye in the skin and the influence of fasting stress on passive cutaneous anaphylaxis in guinea pigs and rats. *Microbiol Immunol.* 1978; 22:89-101.
31. Moon JW, Hyun DK. Decompressive craniectomy in traumatic brain injury: A review article. *Korean J Neurotrauma.* 2017; 13:1-8.
32. Foster J. Predicting resource use for patients with traumatic brain injury. *AACN Clin Issues.* 1996; 7:168-174.
33. Walker WC, Pickett TC. Motor impairment after severe traumatic brain injury: A longitudinal multicenter study. *J Rehabil Res Dev.* 2007; 44:975-982.
34. Maier NRF. The cortical area concerned with coordinated walking in the rat. *J Comp Neurol.* 1935; 61:395-405.
35. Goldstein LB. Model of recovery of locomotor ability after sensorimotor cortex injury in rats. *ILAR J.* 2003; 44:125-129.
36. Matsuura K, Kabuto H, Makino H, Ogawa N. Pole test is a useful method for evaluating the mouse movement disorder caused by striatal dopamine depletion. *J Neurosci Methods.* 1997; 73:45-48.
37. Hall ED, Braughler JM. Central nervous system trauma and stroke. II. Physiological and pharmacological evidence for involvement of oxygen radicals and lipid peroxidation. *Free Radic Biol Med.* 1989; 6:303-313.
38. Farooqui AA, Horrocks LA. Lipid peroxides in the free radical pathophysiology of brain diseases. *Cell Mol Neurobiol.* 1998; 18:599-608.
39. Reiter RJ, Tan DX, Fuentes-Broto L. Melatonin: A multitasking molecule. *Prog Brain Res.* 2010; 181:127-151.
40. Ikeda Y, Long DM. The molecular basis of brain injury and brain edema: The role of oxygen free radicals. *Neurosurgery.* 1990; 27:1-11.
41. Shlosberg D, Benifla M, Kaufer D, Friedman A. Blood-brain barrier breakdown as a therapeutic target in traumatic brain injury. *Nat Rev Neurol.* 2010; 6:393-403.

(Received August 15, 2019; Revised August 19, 2019; Accepted August 21, 2019)

Cur2004-8, a synthetic curcumin derivative, extends lifespan and modulates age-related physiological changes in *Caenorhabditis elegans*

Bo-Kyoung Kim¹, Sung-A Kim¹, Sun-Mi Baek¹, Eun Young Lee^{2,3}, Eun Soo Lee⁴, Choon Hee Chung⁴, Chan Mug Ahn⁵, Sang-Kyu Park^{1,*}

¹Department of Medical Biotechnology, Soonchunhyang University, Asan, Chungnam, Republic of Korea;

²Department of Internal Medicine, Soonchunhyang University Cheonan Hospital, Cheonan, Chungnam, Republic of Korea;

³Institute of Tissue Regeneration, College of Medicine, Soonchunhyang University, Cheonan, Chungnam, Republic of Korea;

⁴Department of Internal Medicine, Wonju College of Medicine, Yonsei University, Wonju, Gangwon, Republic of Korea;

⁵Department of Basic Science, Wonju College of Medicine, Yonsei University, Wonju, Gangwon, Republic of Korea.

Summary

Curcumin, a compound found in Indian yellow curry, is known to possess various biological activities, including anti-oxidant, anti-inflammatory, and anti-cancer activities. Cur2004-8 is a synthetic curcumin derivative having symmetrical bis-alkynyl pyridines that shows a strong anti-angiogenic activity. In the present study, we examined the effect of dietary supplementation with Cur2004-8 on response to environmental stresses and aging using *Caenorhabditis elegans* as a model system. Dietary intervention with Cur2004-8 significantly increased resistance of *C. elegans* to oxidative stress. Its anti-oxidative-stress effect was greater than curcumin. However, response of *C. elegans* to heat stress or ultraviolet irradiation was not significantly affected by Cur2004-8. Next, we examined the effect of Cur2004-8 on aging. Cur2004-8 significantly extended both mean and maximum lifespan, accompanying a shift in time-course distribution of progeny production. Age-related decline in motility was also delayed by supplementation with Cur2004-8. In addition, Cur2004-8 prevented amyloid-beta-induced toxicity in Alzheimer's disease model animals which required a forkhead box (FOXO) transcription factor DAF-16. Dietary supplementation with Cur2004-8 also reversed the increase of mortality observed in worms treated with high-glucose-diet. These results suggest that Cur2004-8 has higher anti-oxidant and anti-aging activities than curcumin. It can be used for the development of novel anti-aging product.

Keywords: Curcumin, Cur2004-8, oxidative stress, aging, *Caenorhabditis elegans*

1. Introduction

Aging is one of the most complex biological phenomena. It exhibits various physiological and pathological changes in organisms. To understand aging process, many theories have been suggested. Among them, the most cited and studied one is the free radical theory introduced by Dr. Herman (1). According to this free

radical theory, when free radicals are accumulated with aging, they cause cellular damages and dysfunction of cellular biomolecules, eventually leading to organism's death. Major free radicals found in cells are reactive oxygen species (ROS) that can cause oxidative damages to DNA, protein, and lipid. A lot of studies have focused on role of anti-oxidant genes in aging. In *C. elegans*, although knockout of anti-oxidant genes could reduce resistance of *C. elegans* to oxidative stress and lifespan, over-expression of anti-oxidant genes failed to extend lifespan (2). Simultaneous over-expression of both Cu/Zn-superoxide dismutase and catalase significantly increased lifespan of *Drosophila melanogaster* (3). However, the longevity phenotype

*Address correspondence to:

Dr. Sang-Kyu Park, Department of Medical Biotechnology, Soonchunhyang University, 22 Soonchunhyang-ro, Asan, Chungnam 31538, Republic of Korea.

E-mail: skpark@sch.ac.kr

conferred by double transgenic animals was observed only in short-lived strain, not in long-lived strain of *Drosophila melanogaster* (4). Transgenic mice having additional copy of anti-oxidant genes showed no lifespan extension (5). Over-expression of human catalase with mitochondrial target signal in mice induced significant lifespan extension (6). The role of anti-oxidant genes in lifespan remains elusive.

Effects of dietary supplementation with various anti-oxidants on aging have been reported. Resveratrol, a polyphenol compound found in red wine, can extend lifespans of many experimental organisms. In *C. elegans*, treatment with resveratrol increased its lifespan to 18% and reduced its susceptibility to oxidative stress (7). The increase in lifespan induced by resveratrol is accompanied by reduced fecundity as a trade-off (8). The lifespan-extending effect of resveratrol was also observed in yeast and fruit fly (9,10). Polyphenol extracted from blueberry can increase resistance of *C. elegans* to heat stress, delay age-related decline of pharyngeal pumping, and confer 28% increase of its lifespan (11). Vitamin E has lifespan-extending effects in nematode and mice (12,13). Genomic transcriptional profiling study has revealed tissue-specific transcriptional biomarkers of aging (14). In addition, dietary supplementation with anti-oxidants such as lipoic acid, coenzyme Q10, lycopene, and tempol can markedly block age-related transcriptional changes in mice (14).

Curcumin is a bio-active ingredient found in turmeric, *Curcuma longa*. It has been used as a traditional therapeutic compound due to its anti-inflammatory, anti-oxidant, and chemo-preventive activities. In recent

years, curcumin has been shown to possess anti-cancer activities. It can reduce tumor formation and progression (15). Curcumin also shows protective effect against many chronological diseases, including cardiovascular and neurological diseases (16). A recent study has shown that curcumin can mediate lifespan extension and modulate many age-related biomarkers, including accumulation of lipofuscin, fertility, response to environmental stressors, and cellular ROS production in *C. elegans* (17). Curcumin can also inhibit amyloid beta (A β)-induced pathology in Alzheimer's disease (AD) model mice (18).

In the present study, we examined effect of curcumin derivative Cur2004-8 on aging using *C. elegans* as a model system. Cur2004-8, a synthetic curcumin derivative produced by Sonogashira reaction, has symmetrical bis-alkynyl pyridines connected by aromatic linker (Figure 1A). A previous study has shown that Cur2004-8 has stronger anti-angiogenic activity *in vitro* than curcumin (19). We compared the anti-stress effect of Cur2004-8 to that of curcumin and examined the anti-aging activity of Cur2004-8. Effect of dietary supplementation with Cur2004-8 on age-related diseases was also monitored. Results of this study support the free radical theory of aging and suggest that Cur2004-8 can be useful for the development of novel anti-aging therapeutics.

2. Materials and Methods

2.1. *C. elegans* strains and maintenance

Bristol N2 strain of *C. elegans* was used as a wild-type

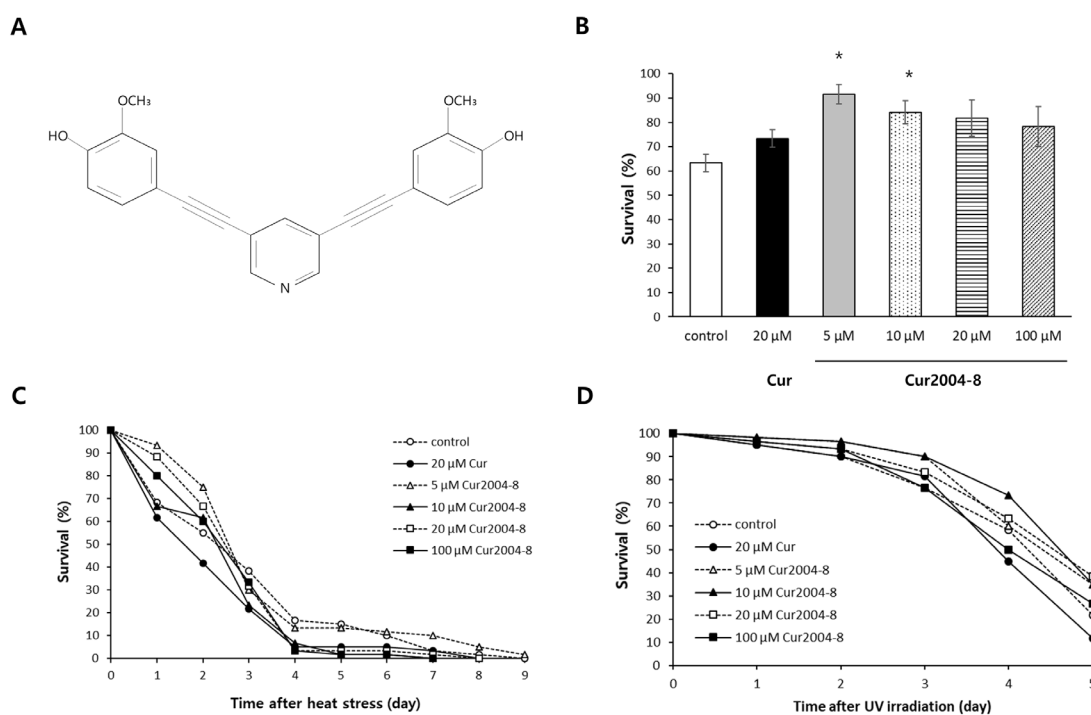


Figure 1. Effect of Cur2004-8 on response to environmental stressors. (A) Structure of Cur2004-8. Survival after oxidative stress (B), heat stress (C), or UV irradiation (D) was compared between untreated control and curcumin- or Cur2004-8-treated group. Cur, curcumin; *, significantly different from untreated control ($p < 0.05$).

control in all experiments. The CL4176 strain expressing muscle-specific human A β_{1-42} (*dvl527 [myo-3/A β_{1-42} /let UTR, rol-6]*) was used for A β -induced toxicity assay. All strains were purchased from the *Caenorhabditis elegans* Genetics Center (CGC, Minneapolis/St. Paul, MN, USA). Worms were maintained on solid Nematode Growth Media (NGM) (25 mM NaCl, 1.7% agar, 2.5 mg/mL peptone, 50 mM KH₂PO₄ (pH 6.0), 5 μ g/mL cholesterol, 1 mM CaCl₂, and 1 mM MgSO₄) plates at 20°C. *Escherichia coli* OP50 was provided as food source.

2.2. Resistance to oxidative stress

For age-synchronization, five young adult worms obtained from 3-day-old mothers were transferred to a fresh NGM plate and permitted to lay eggs for 6 h. After removing these five adult worms from the plate, remaining eggs were incubated at 20°C for 3 days to hatch and grow. Three-day-old age-synchronized worms ($n = 30$) were transferred to fresh NGM plates treated with curcumin or Cur2004-8 and incubated at 20°C for 1 day. These worms were then placed under oxidative stress condition with 2 mM hydrogen peroxide (H₂O₂) (Sigma-Aldrich, St. Louis, MO, USA) in S-basal without cholesterol (5.85 g sodium chloride, 1 g potassium phosphate dibasic, and 6 g potassium phosphate monobasic for 1 L sterilized distilled-water) for 6 h in 96-well plates.

2.3. Response to heat stress

Three-day-old age-synchronized worms ($n = 60$) were transferred to fresh NGM plates containing curcumin or Cur2004-8. After adapting for 24 h, worms were placed in a 35°C incubator for 7 h to be exposed to heat stress. These worms were then transferred back to 20°C and incubated for 24 h. The survival of worms was recorded daily until all worms were dead.

2.4. Survival after ultraviolet (UV) irradiation

Sixty age-synchronized young adult worms were treated with curcumin or Cur2004-8 for 24 h at 20°C and irradiated with 20 J/cm²/min of UV for 1 min in a UV crosslinker (BLX-254, VILBER Lourmat Co., Torcy, France). The survival of worms on NGM plates containing curcumin or Cur2004-8 was then monitored daily until all worms were dead.

2.5. Measurement of lifespan

Three-day-old age-synchronized worms ($n = 60$) were transferred to NGM plates containing curcumin or Cur2004-8. Live and dead worms were scored daily. Worms lost, killed, or having internal hatching were excluded. During the assay, worms were transferred

to fresh NGM plates every day during gravid period and every 2-3 days after gravid period. 5-Fluoro-2'-deoxyuridine (Sigma-Aldrich, St. Louis, MO, USA) (12.5 mg/L) was added to NGM plates to prevent internal hatching.

2.6. Assessment of fertility

Five L4/young adult worms were placed on a fresh NGM plate containing curcumin or Cur2004-8 at 20°C for 5 h to lay eggs. After removing all adult worms from the plate, eggs were maintained at 20°C for 2 days. Ten randomly selected worms were transferred individually to fresh NGM plates treated with curcumin or Cur2004-8 every day until worms no longer produced eggs. Hatched progeny from an individual worm on each day were counted after incubation at 20°C for 48 h.

2.7. Measurement of motility

Age-synchronized worms ($n = 100$) were grown on NGM plates containing curcumin or Cur2004-8. Change of motility was measured on 15 and 20 days after egg-hatching. Each worm was classified into one of three groups: 1) Phase 1, a worm that could move spontaneously without any mechanical stimuli; 2) Phase 2, a worm that moved only when mechanical stimuli were given; and 3) Phase 3, a worm that could only move its head part with mechanical stimuli.

2.8. A β -induced toxicity

Age-synchronized young adult CL4176 worms ($n = 30$) were permitted to lay eggs on NGM plates containing curcumin or Cur2004-8 for 2 h at 15°C. After removing all adult worms, the progeny was incubated at 15°C for 24 h. Randomly selected worms ($n = 60$) were then incubated for 24 h at 25°C to induce the expression of human A β transgene in muscle. The number of paralyzed worms was recorded every hour after A β induction.

2.9. RNA interference (RNAi)

To repress the expression of *daf-16*, we used *daf-16* RNAi clone obtained from the Ahringer RNAi library (20). Induction of *daf-16* double-stranded RNA was done by adding 0.4 mM isopropyl- β -D-thiogalactoside (IPTG, Sigma-Aldrich, St. Louis, MO, USA) to culture media after OD₆₀₀ reached 0.4. After culturing for additional 4 h, bacteria were used as food source for RNAi knockdown. RNAi clone carrying empty vector (EV) was used as a negative control.

2.10. Lifespan with high-glucose diet (HGD)

Sixty age-synchronized worms were randomly selected from 3-day-old young adult worms. These worms were

then transferred to a fresh NGM plate containing both OP50 and high-glucose (100 μ L of 40 mM glucose). The survival of worms was recorded daily until all worms were dead.

2.11. Statistical analysis

For comparison of resistance to oxidative stress and fertility between untreated control and curcumin- or Cur2004-8-treated group, we used the standard two-tailed Student's *t*-test. For statistical analysis of survival after heat stress or UV irradiation, lifespan, paralysis assay, and survival under HGD, we employed the log-rank test (21). The log-rank test is a non-parametric Mantel-Cox test widely used for statistical comparison between two survival curves. A *p*-value lower than 0.05 was considered as statistically significant.

3. Results

3.1. Cur2004-8 specifically increases resistance of *C. elegans* to oxidative stress

In order to examine the effect of Cur2004-8 on response of *C. elegans* to environmental stressors, survival of

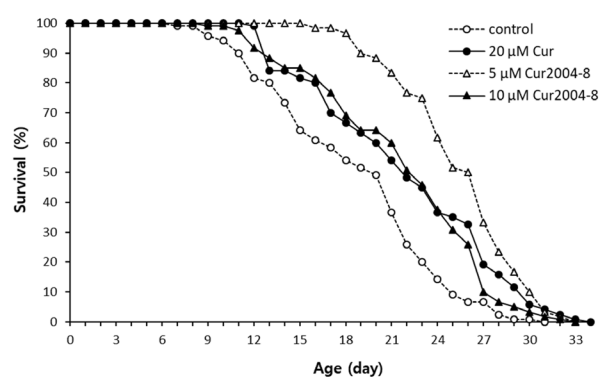


Figure 2. Lifespan extension by supplementation with Cur2004-8. Effect of dietary supplementation with curcumin or Cur2004-8 on lifespan of *C. elegans* was examined using age-synchronized animals ($n = 60$). Cur, curcumin.

worms was monitored after oxidative stress, heat stress, or UV irradiation. We compared the effect of different concentration of Cur2004-8 with that of 20 μ M of curcumin reported to be able to increase resistance of *C. elegans* to oxidative stress and its lifespan (19). Resistance to oxidative stress was significantly increased by supplementation with Cur2004-8 (Figure 1B). Mean survival rate of wild-type control was $63.3 \pm 3.60\%$ (mean of three replicates \pm SE) after 6 h of oxidative stress. Survival rate for the group supplemented with 20 μ M of curcumin was $73.3 \pm 3.60\%$ ($p = 0.097$), which was slightly increased compared to that of the wild-type control after 6 h of oxidative stress. However, mean survival rates for groups supplemented with 5 and 10 μ M of Cur2004-8 were significantly increased to $91.7 \pm 3.97\%$ ($p = 0.002$) and $84.2 \pm 4.79\%$ ($p = 0.014$), respectively. Although concentration of Cur2004-8 higher than 10 μ M increased the survival rate, the survival rate was not significantly different from that of the wild-type control ($p > 0.05$). However, there was no significant difference in response to heat stress or UV irradiation between control and Cur2004-8-treated groups (Figures 1C and 1D). These findings suggest that Cur2004-8 is more effective than curcumin in increasing resistance of *C. elegans* to oxidative stress and that its effect is specific for oxidative stress.

3.2. Supplementation with Cur2004-8 significantly extends lifespan of *C. elegans*

The free radical theory of aging emphasizes the role of oxidative stress in determination of organism's lifespan (1). Having observed anti-oxidative-stress effect of Cur2004-8, we next examined its effect on lifespan. Since 5 and 10 μ M of Cur2004-8 showed a significant increase in resistance to oxidative stress, we chose those two concentrations for the following experiments. Dietary supplementation with Cur2004-8 significantly extended both mean and maximum lifespan (Figure 2). Mean lifespan of untreated control (20.1 days) was increased to 24.6 days after supplementation with 5 μ M Cur2004-8 ($p < 0.001$). It was increased to 23.5

Table 1. Effect of Cur2004-8 on lifespan of *C. elegans*

Items	Mean lifespan (d)	Maximum lifespan (d)	<i>p</i> -value ^a	% effect ^b
1 st experiment				
control	20.1	30		
20 μ M Cur	25.4	33	< 0.001	26.6
5 μ M Cur2004-8	24.6	32	< 0.001	22.6
10 μ M Cur2004-8	23.5	32	< 0.001	17.4
2 nd experiment				
control	15.5	27		
20 μ M Cur	16.6	25	0.791	7.6
5 μ M Cur2004-8	24.6	32	0.001	59.1
10 μ M Cur2004-8	18.1	28	0.051	16.9

^a*p*-value was calculated using the log-rank test by comparing the survival of control group to that of Cur- or Cur2004-8-treated group. ^b % effects were calculated by $(C-T)/C \times 100$, where *T* is the mean lifespan of curcumin- or Cur2004-8-treated group and *C* is the mean lifespan of control group. Cur, curcumin.

days after supplementation with 10 μM Cur2004-8 ($p < 0.001$). Mean lifespans were increased 22.6 and 17.4% by 5 and 10 μM Cur2004-8, respectively. Maximum lifespan was also increased from 30 days to 32 days after treatment with Cur2004-8. An independent replicative experiment showed a positive effect of Cur2004-8 on lifespan (Table 1). The percent effect on mean lifespan was 59.1% with 5 μM Cur2004-8 ($p = 0.001$) while it was only 16.9% with 10 μM Cur2004-8 ($p = 0.051$). Unlike consistent lifespan-extending effect of Cur2004-8, 20 μM curcumin showed a significant lifespan-extending effect in the first experiment but failed to induce lifespan extension in the second experiment (Table 1). Our results indicate that Cur2004-8 can confer a longevity phenotype and that its lifespan-extending activity is greater than curcumin.

3.3. Cur2004-8 modulates reproduction of adult worms

Previous studies have reported that many lifespan-extending genetic or dietary interventions are

accompanied by reduced fertility as a trade-off (9,22,23). In the present study, dietary supplementation with Cur2004-8 did not affect total number of progeny produced during the gravid period (Figure 3A). There was a slight decrease in total number of progeny compared to untreated control, although the difference was not statistically significant ($p > 0.05$). However, time-course distribution of progeny produced was significantly modulated by curcumin or Cur2004-8 (Figure 3B). At 3 days after hatching, 89.7 ± 9.73 (mean of 10 individual worms \pm SEM) progeny were produced by the untreated control. The number of progeny produced was decreased by curcumin or Cur2004-8: 68.0 ± 3.25 ($p = 0.066$) for 20 μM curcumin-treated worms, 67.2 ± 2.49 ($p = 0.040$) for 5 μM Cur2004-8-treated worms, and 70.2 ± 3.74 ($p = 0.086$) for 10 μM Cur2004-8-treated worms. Statistically significant decreases in the number of progeny produced were detected in all curcumin- and Cur2004-8-treated groups on 4th day after hatching. The number of progeny was reduced from 122.4 ± 6.74 in the untreated control

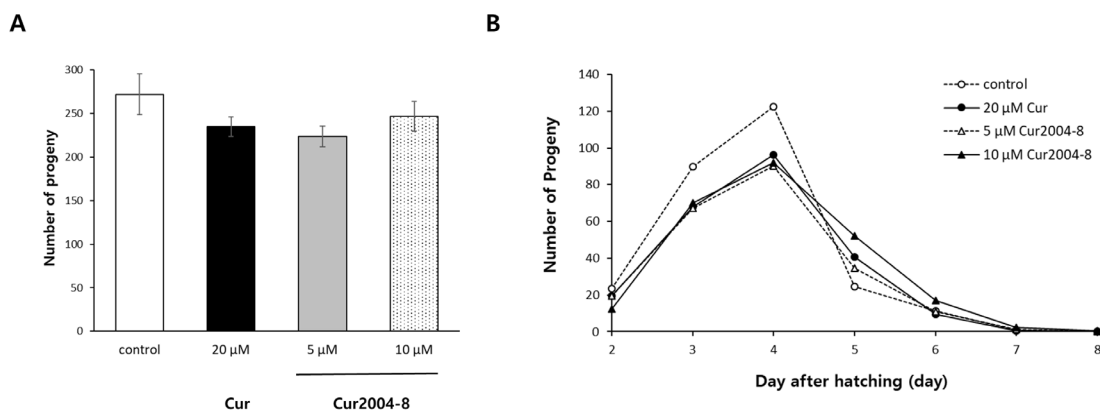


Figure 3. Effect of Cur2004-8 on reproduction. (A) Total number of progeny produced during the gravid period was counted ($n = 10$). Error bar indicates standard error of mean. (B) Time-course distribution of progeny in untreated control, curcumin-treated, and Cur2004-8-treated group. Cur, curcumin.

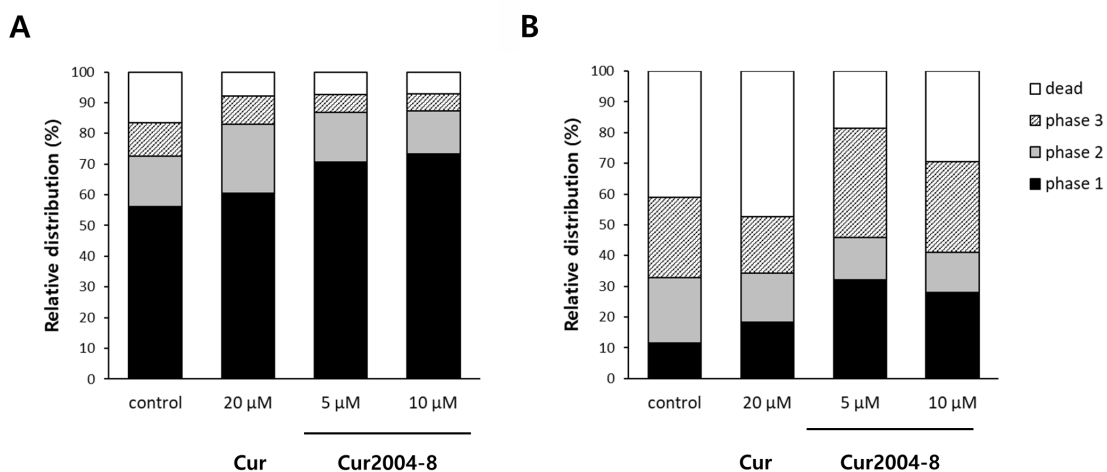


Figure 4. Delayed decline of motility by Cur2004-8. Effect of curcumin or Cur2004-8 on motility was determined in 15-day-old (A) and 20-day-old animals (B) ($n = 100$). Worms were classified into three phases according to their locomotive activity: Phase 1, a worm that could move spontaneously without any mechanical stimuli; Phase 2, a worm that moved only when mechanical stimuli were given; and Phase 3, a worm that could only move its head part with mechanical stimuli. Cur, curcumin.

to 96.4 ± 2.46 ($p = 0.005$), 90.3 ± 2.82 ($p < 0.001$), and 92.1 ± 2.59 ($p = 0.001$) in 20 μM curcumin-, 5 μM Cur2004-8-, and 10 μM Cur2004-8-treated group, respectively. However, the number of progeny produced in curcumin- or Cur2004-8-treated group was higher than that in the untreated control on 5 days after hatching. Numbers of progeny in worms treated with 20 μM curcumin, 5 μM Cur2004-8, and 10 μM Cur2004-8 were 40.5 ± 2.69 ($p = 0.016$), 34.5 ± 3.65 ($p = 0.108$), and 52.0 ± 5.02 ($p = 0.001$), respectively, compared to the number of progeny produced in the untreated control (24.4 ± 3.53) (Figure 3B). These data suggest that dietary supplementation with curcumin or Cur2004-8 does not affect the reproducibility of *C. elegans*, although it can induce a significant shift in time-course distribution of progeny during the gravid period.

3.4. Age-related decline of motility is delayed by Cur2004-8

Next, we determined the effect of Cur2004-8 on change of motility with time to elucidate its role in muscle aging. At 15 days after hatching, 56% of the untreated control worms and 61% of worms treated with 20 μM curcumin showed spontaneous motility without any mechanical stimuli (phase 1) while more worms (71% with 5 μM Cur2004-8 and 73% with 10 μM Cur2004-8) were classified as phase 1 (Figure 4A). Bigger difference in motility was observed on 20th day. In the untreated control, only 11% of worms could move spontaneously and 18% of worms showed 'phase 1' phenotype in 20 μM curcumin-treated group. However, percentages of worms categorized as 'phase 1' were increased to 32% and 29% by supplementation with 5 and 10 μM Cur2004-8, respectively (Figure 4B). In addition, percentages of dead worms showing no motility was reduced by Cur2004-8. In untreated control and 20 μM curcumin-treated group on day 20, 41% and 47% of worms were not moving at all, respectively. Percentages of worms showing no motility were

reduced to 19% and 30% by dietary supplementation with 5 and 10 μM Cur2004-8, respectively (Figure 4B). These results suggest that Cur2004-8 could slow down age-related dysfunction of muscle in *C. elegans*.

3.5. Cur2004-8 suppresses A β -induced toxicity via DAF-16

To examine the effect of Cur2004-8 on age-related disease, we employed a transgenic AD model expressing human A β . Accumulation of transgenic human A β in muscle is known to induce paralysis and lead to death (24). Mean survival time of the untreated control was 4.1 h. Dietary supplementation with Cur2004-8 significantly delayed paralysis. Cur2004-8 at 5 and 10 μM increased mean survival time to 6.6 h ($p < 0.001$) and 5.7 h ($p = 0.003$), respectively (Figure 5A). Treatment with 20 μM curcumin also reduced A β -induced toxicity (mean survival time 5.8 days, $p = 0.004$). Thus, 20 μM curcumin, 5 μM Cur2004-8, and 10 μM Cur2004-8 increased mean survival time by 42.6%, 61.1%, and 41.0%, respectively (Table 2). A previous study has reported that DAF-16 is required for the inhibition of A β -induced toxicity (25). Interestingly, increased survival after A β induction by Cur2004-8 completely disappeared when the expression of *daf-16* was knocked down (Figure 5B). Thus, we conclude that Cur2004-8 can reduce A β -induced toxicity more efficiently than curcumin and that it requires DAF-16 for its preventive effect.

3.6. Decreased survival with HGD is recovered by supplementation with Cur2004-8

Since HGD can reduce survival of *C. elegans*, it can be used as a nutritional model of diabetes mellitus (26). In the present study, HGD reduced the lifespan of *C. elegans* compared to the untreated control. Mean lifespan was significantly decreased from 16.7 days in the untreated control to 13.5 days in the HGD group ($p = 0.001$) (Figure 6). However, decreased lifespan by

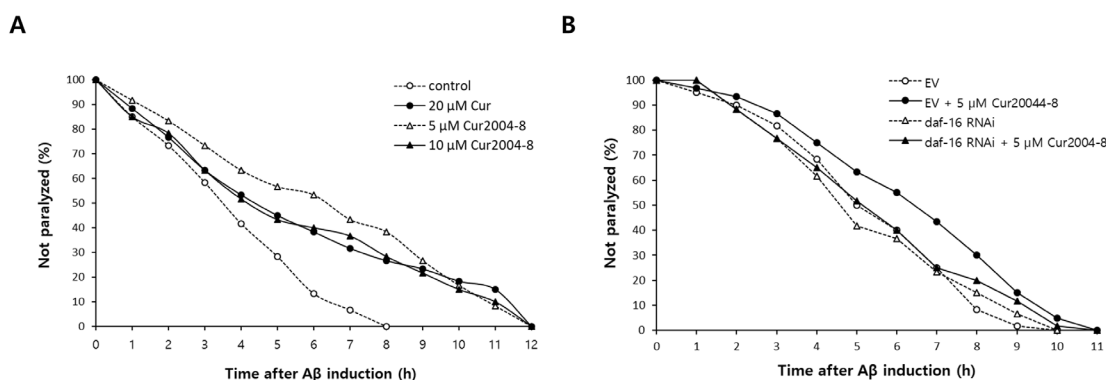


Figure 5. Reduced susceptibility to A β -induced toxicity by Cur2004-8. (A) Paralysis caused by muscle-specific expression of human A β was monitored. **(B)** Effect of *daf-16* knockdown on protective effect of Cur2004-8 against A β -induced paralysis was determined using RNAi. Cur, curcumin; EV, empty vector.

Table 2. Effect of Cur2004-8 on A β -induced toxicity in *C. elegans*

Items	Time when 50% of worms were paralyzed (h)	p-value ^a	% effect ^b
1 st experiment			
control	4.1		
20 μ M Cur	5.8	< 0.01	42.6
5 μ M Cur2004-8	6.6	< 0.001	61.1
10 μ M Cur2004-8	5.7	< 0.01	41.0
2 nd experiment			
control	5.1		
20 μ M Cur	6.2	< 0.05	23.0
5 μ M Cur2004-8	6.2	< 0.05	22.0
10 μ M Cur2004-8	6.0	0.075	19.1

^ap-value was calculated using the log-rank test by comparing the survival of control group to that of Cur- or Cur2004-8-treated group. ^b% effects were calculated by $(C-T)/C*100$, where T is the mean lifespan of curcumin- or Cur2004-8-treated group and C is the mean lifespan of control group. Cur, curcumin.

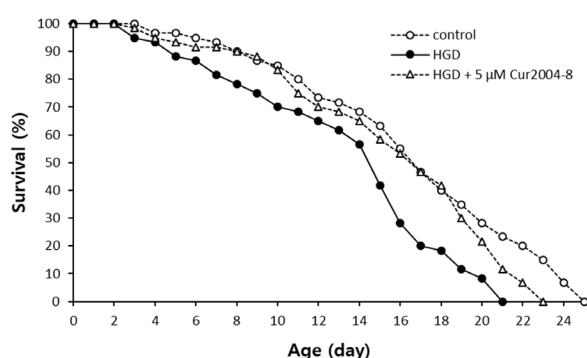


Figure 6. Effect of Cur2004-8 on HGD-induced toxicity. Survival of animals was compared between untreated control and worms fed with HGD, and preventive effect of Cur2004-8 on decrease in survival by HGD was examined. Cur, curcumin; HGD, high-glucose diet.

HGD was markedly restored by supplementation with Cur2004-8. Mean lifespan was increased up to 15.8 days for HGD-worms treated with 5 μ M Cur2004-8, which was 71.9% increase compared to worms treated with HGD alone ($p = 0.009$). Maximum lifespan was also decreased by HGD and restored for worms treated with both HGD and Cur2004-8 (Figure 6). These results suggest that Cur2004-8 has a preventive effect on HGD-induced toxicity in addition to its effect on A β -induced toxicity in *C. elegans*.

4. Discussion

An increasing number of aging studies have been focused on the identification of anti-aging dietary interventions. The most effective intervention identified so far is dietary restriction (DR) which retards age-related physiological changes and extends lifespan in many model organisms (27). However, due to difficulty in practicing DR in daily life, people are searching for nutritional interventions that can delay aging process without DR. Anti-oxidants are believed to be the most promising compounds based on the free radical theory. Curcumin is a well-known anti-oxidant with anti-aging effect. Dietary supplementation with

curcumin can reduce intracellular ROS and increase resistance to oxidative stress (28). Expression levels of stress-responsive genes are significantly induced by curcumin (28). Curcumin can modulate activities of anti-oxidant enzymes and reduced protein oxidation (29,30). Lifespan extension after supplementation with curcumin has also been reported with 20 μ M and there was no significant difference in lifespan with higher dose (200 μ M) of curcumin (17). Results of the present study showed that Cur2004-8 as a synthetic curcumin derivative had higher anti-oxidant and lifespan-extending effects than free curcumin. Recent studies have reported that trimethoxystilbene derivative of resveratrol showed better bioavailability and elevated anti-cancer activity than resveratrol (31). Resveratrol-maltol hybrids inhibited aggregation of A β (32). In addition, resveratrol peptidyl derivatives exhibited strong anti-oxidant and anti-cancer activities (33). Further studies revealing the molecular basis of improved activities of Cur2004-8 and anti-aging effect in higher organisms should be followed in the near future.

Many studies have reported that there is a trade-off for lifespan extension by genetic or dietary intervention. Longevity phenotype observed in *daf-2* mutants is accompanied by delayed development and reduced reproduction (22). The *age-1* mutation also exhibited reduced fertility as a trade-off for long lifespan (23). Resveratrol resulted in early onset of egg-laying and extended the gravid period with increased lifespan (8). In case of blueberry polyphenols, long-lived worms showed delayed decline of pharyngeal pumping rate with aging (11). We observed a shift in time-course distribution of progeny in worms supplemented with Cur2004-8, suggesting that Cur2004-8 might induce allocation of cellular limited resource from reproduction toward survival and maintenance. The disposable soma theory of aging emphasizing role of fitness cost paid for lifespan extension supports our findings (34).

Muscle cells are among the most energy-demanding cells and aging muscle is characterized by loss of mass and reduced strength (35). A previous study has

shown that transgenic mice carrying additional copy of mitochondrial catalase have delayed dysfunction of mitochondria (6). Dietary supplementation with antioxidants including silymarin and phycoerythrin can enhance locomotion rate and increase lifespan (36,37). Lifespan-extending selenocysteine can also significantly delay age-related decline of motility in *C. elegans* (38). Here, we observed enhanced motility in aged animals treated with Cur2004-8. Our findings suggest that Cur2004-8 can retard muscle aging possibly through its anti-oxidant activity.

Effects of curcumin on age-related diseases have been reported. Treatment with tetrahydrocurcumin can reduce ROS production caused by A β in rat hippocampal cells (39). α -Synuclein-induced cell death is significantly inhibited by curcumin (40). In AD model mice, curcumin reduced lipid peroxidation and restored motor function (41). Encapsulated curcumin nanoparticle rescued neuromotor deficits observed in Huntington's disease model animals (42). Our results showed that Cur2004-8 could ameliorate A β -induced toxicity in *C. elegans* genetic model of AD and that its effect required DAF-16. Additionally, dietary supplementation with Cur2004-8 completely blocked the toxic effect of HGD which was used as a nutritional model of diabetes mellitus.

In conclusion, Cur2004-8 has anti-oxidant and anti-aging activities and protective activity against toxicities involved in age-related diseases. Cur2004-8 shows improved bioactivities compared to free curcumin. The effect of 5 μ M Cur2004-8 was higher than that of 20 μ M free curcumin in oxidative stress, lifespan, motility, and A β -induced toxicity assays. Further studies identifying downstream molecular targets of Cur2004-8 and determining its *in vivo* effect in higher organisms such as mice are necessary.

Acknowledgements

This work was supported by the Soonchunhyang University Research Fund and the Basic Science Research Program through the National Research Foundation of Korea funded by the Ministry of Education (2018R1D1A1B07043414).

References

1. Harman D. Aging: A theory based on free radical and radiation chemistry. *J Gerontol.* 1956; 11:298-300.
2. Salmon AB, Richardson A, Perez VI. Update on the oxidative stress theory of aging: Does oxidative stress play a role in aging or healthy aging? *Free Radic Biol Med.* 2010; 48:642-655.
3. Orr WC, Sohal RS. Extension of life-span by overexpression of superoxide dismutase and catalase in *Drosophila melanogaster*. *Science.* 1994; 263:1128-1130.
4. Mockett RJ, Sohal BH, Sohal RS. Expression of multiple copies of mitochondrially targeted catalase or genomic

- Mn superoxide dismutase transgenes does not extend the life span of *Drosophila melanogaster*. *Free Radic Biol Med.* 2010; 49:2028-2031.
5. Perez VI, Van Remmen H, Bokov A, Epstein CJ, Vijg J, Richardson A. The overexpression of major antioxidant enzymes does not extend the lifespan of mice. *Aging Cell.* 2009; 8:73-75.
6. Schriener SE, Linford NJ, Martin GM, Treuting P, Ogburn CE, Emond M, Coskun PE, Ladiges W, Wolf N, Van Remmen H, Wallace DC, Rabinovitch PS. Extension of murine life span by overexpression of catalase targeted to mitochondria. *Science.* 2005; 308:1909-1911.
7. Baur JA. Resveratrol, sirtuins, and the promise of a DR mimetic. *Mech Ageing Dev.* 2010; 131:261-269.
8. Gruber J, Tang SY, Halliwell B. Evidence for a trade-off between survival and fitness caused by resveratrol treatment of *Caenorhabditis elegans*. *Ann N Y Acad Sci.* 2007; 1100:530-542.
9. Wood JG, Rogina B, Lavu S, Howitz K, Helfand SL, Tatar M, Sinclair D. Sirtuin activators mimic caloric restriction and delay ageing in metazoans. *Nature.* 2004; 430:686-689.
10. Howitz KT, Bitterman KJ, Cohen HY, Lamming DW, Lavu S, Wood JG, Zipkin RE, Chung P, Kisielewski A, Zhang LL, Scherer B, Sinclair DA. Small molecule activators of sirtuins extend *Saccharomyces cerevisiae* lifespan. *Nature.* 2003; 425:191-196.
11. Wilson MA, Shukitt-Hale B, Kalt W, Ingram DK, Joseph JA, Wolkow CA. Blueberry polyphenols increase lifespan and thermotolerance in *Caenorhabditis elegans*. *Aging Cell.* 2006; 5:59-68.
12. Harrington LA, Harley CB. Effect of vitamin E on lifespan and reproduction in *Caenorhabditis elegans*. *Mech Ageing Dev.* 1988; 43:71-78.
13. Navarro A, Gómez C, Sánchez-Pino MJ, González H, Bández MJ, Boveris AD, Boveris A. Vitamin E at high doses improves survival, neurological performance, and brain mitochondrial function in aging male mice. *Am J Physiol Regul Integr Comp Physiol.* 2005; 289:R1392-1399.
14. Park SK, Kim K, Page GP, Allison DB, Weindruch R, Prolla TA. Gene expression profiling of aging in multiple mouse strains: Identification of aging biomarkers and impact of dietary antioxidants. *Aging Cell.* 2009; 8:484-495.
15. Duvoix A, Blasius R, Delhalle S, Schnekenburger M, Morceau F, Henry E, Dicato M, Diederich M. Chemopreventive and therapeutic effects of curcumin. *Cancer Lett.* 2005; 223:181-190.
16. Abrahams S, Haylett WL, Johnson G, Carr JA, Barden S. Antioxidant effects of curcumin in models of neurodegeneration, aging, oxidative and nitrosative stress: A review. *Neuroscience.* 2019; 406:1-21.
17. Liao VH, Yu CW, Chu YJ, Li WH, Hsieh YC, Wang TT. Curcumin-mediated lifespan extension in *Caenorhabditis elegans*. *Mech Ageing Dev.* 2011; 132:480-487.
18. Lim GP, Chu T, Yang F, Beech W, Frautschy SA, Cole GM. The curry spice curcumin reduces oxidative damage and amyloid pathology in an Alzheimer transgenic mouse. *J Neurosci.* 2001; 21:8370-8377.
19. Ahn CM, Shin WS, Bum Woo H, Lee S, Lee HW. Synthesis of symmetrical bis-alkynyl or alkyl pyridine and thiophene derivatives and their antiangiogenic activities. *Bioorg Med Chem Lett.* 2004; 14:3893-3896.
20. Kamath RS, Fraser AG, Dong Y, Poulin G, Durbin R,

- Gotta M, Kanapin A, Le Bot N, Moreno S, Sohrmann M, Welchman DP, Zipperlen P, Ahringer J. Systematic functional analysis of the *Caenorhabditis elegans* genome using RNAi. *Nature*. 2003; 421:231-237.
21. Peto R, Peto J. Asymptotically efficient rank invariant test procedures. *J R Statist Soc A*. 1972; 135:185-207.
 22. Gems D, Sutton AJ, Sundermeyer ML, Albert PS, King KV, Edgley ML, Larsen PL, Riddle DL. Two pleiotropic classes of daf-2 mutation affect larval arrest, adult behavior, reproduction and longevity in *Caenorhabditis elegans*. *Genetics*. 1998; 150:129-155.
 23. Larsen PL, Albert PS, Riddle DL. Genes that regulate both development and longevity in *Caenorhabditis elegans*. *Genetics*. 1995; 139:1567-1583.
 24. Link CD. *C. elegans* models of age-associated neurodegenerative diseases: Lessons from transgenic worm models of Alzheimer's disease. *Exp Gerontol*. 2006; 41:1007-1013.
 25. Cohen E, Dillin A. The insulin paradox: Aging, proteotoxicity and neurodegeneration. *Nat Rev Neurosci*. 2008; 9:759-767.
 26. Schlotterer A, Kukudov G, Bozorgmehr F, et al. *C. elegans* as model for the study of high glucose-mediated life span reduction. *Diabetes*. 2009; 58:2450-2456.
 27. Mair W, Dillin A. Aging and survival: The genetics of life span extension by dietary restriction. *Annu Rev Biochem*. 2008; 77:727-754.
 28. Yu CW, Wei CC, Liao VH. Curcumin-mediated oxidative stress resistance in *Caenorhabditis elegans* is modulated by *age-1*, *akt-1*, *pdk-1*, *osr-1*, *unc-43*, *sek-1*, *skn-1*, *sir-2.1*, and *mev-1*. *Free Radic Res*. 2014; 48:371-379.
 29. Banji D, Banji OJ, Dasaroju S, Kranthi KC. Curcumin and piperine abrogate lipid and protein oxidation induced by D-galactose in rat brain. *Brain Res*. 2013; 1515:1-11.
 30. Kumar A, Prakash A, Dogra S. Protective effect of curcumin (*Curcuma longa*) against D-galactose-induced senescence in mice. *J Asian Nat Prod Res*. 2011; 13:42-55.
 31. Traversi G, Staid DS, Fiore M, Percario Z, Trisciuglio D, Antonioletti R, Morea V, Degrassi F, Cozzi R. A novel resveratrol derivative induces mitotic arrest, centrosome fragmentation and cancer cell death by inhibiting gamma-tubulin. *Cell Div*. 2019; 14:3.
 32. Cheng G, Xu P, Zhang M, Chen J, Sheng R, Ma Y. Resveratrol-maltol hybrids as multi-target-directed agents for Alzheimer's disease. *Bioorg Med Chem*. 2018; 26:5759-5765.
 33. Mrkus L, Batinić J, Bjeliš N, Jakas A. Synthesis and biological evaluation of quercetin and resveratrol peptidyl derivatives as potential anticancer and antioxidant agents. *Amino Acids*. 2019; 51:319-329.
 34. Kirkwood TB. Evolution of ageing. *Nature*. 1977; 270:301-304.
 35. Gomes MJ, Martinez PF, Pagan LU, Damatto RL, Cezar MDM, Lima ARR, Okoshi K, Okoshi MP. Skeletal muscle aging: Influence of oxidative stress and physical exercise. *Oncotarget*. 2017; 8:20428-20440.
 36. Kumar J, Park KC, Awasthi A, Prasad B. Silymarin extends lifespan and reduces proteotoxicity in *C. elegans* Alzheimer's model. *CNS Neurol Disord Drug Targets*. 2015; 14:295-302.
 37. Sonani RR, Singh NK, Awasthi A, Prasad B, Kumar J, Madamwar D. Phycoerythrin extends life span and health span of *Caenorhabditis elegans*. *Age (Dordr)*. 2014; 36:9717.
 38. Kim JS, Kim SH, Park SK. Selenocysteine modulates resistance to environmental stress and confers anti-aging effects in *C. elegans*. *Clinics (Sao Paulo)*. 2017; 72:491-498.
 39. Mishra S, Mishra M, Seth P, Sharma SK. Tetrahydrocurcumin confers protection against amyloid beta-induced toxicity. *Neuroreport*. 2011; 22:23-27.
 40. Liu Z, Yu Y, Li X, Ross CA, Smith WW. Curcumin protects against A53T alpha-synuclein-induced toxicity in a PC12 inducible cell model for Parkinsonism. *Pharmacol Res*. 2011; 63:439-444.
 41. Seo JS, Leem YH, Lee KW, Kim SW, Lee JK, Han PL. Severe motor neuron degeneration in the spinal cord of the Tg2576 mouse model of Alzheimer disease. *J Alzheimers Dis*. 2010; 21:263-276.
 42. Sandhir R, Yadav A, Mehrotra A, Sunkaria A, Singh A, Sharma S. Curcumin nanoparticles attenuate neurochemical and neurobehavioral deficits in experimental model of Huntington's disease. *Neuromolecular Med*. 2014; 16:106-118.

(Received July 16, 2019; Revised August 20, 2019; Accepted August 21, 2019)

Detection of *Trichophyton* spp. from footwear of patients with tinea pedis

Sanae A. Ishijima¹, Masataro Hiruma², Kazuhisa Sekimizu¹, Shigeru Abe^{1,*}

¹Teikyo University Institute of Medical Mycology, Hachioji, Tokyo, Japan;

²Hiruma Clinic, Hidaka-shi, Saitama, Japan.

Summary

The prevalence of tinea pedis (also known as athlete's foot) in Japanese workers as well as contamination of their footwear by pathogenic filamentous fungi were investigated. Health checks by a dermatologist at a factory located in the Kanto region (Japan) led to a clinical and morphologic diagnosis of tinea pedis in 9 of 19 workers. Scales obtained from the feet and dust obtained from the protective footwear (safety shoes) worn daily in the factory were obtained from these nine subjects and tested using a mycological culture technique. Scales obtained from six of the nine subjects indicated pathogenic filamentous fungi, not only *Trichophyton* spp., but also *Acremonium*, which causes symptoms similar to tinea pedis or onychomycosis. Similarly, culture of the dust obtained from the safety shoes yielded pathogenic filamentous fungi in six of the nine subjects, and in four samples *Trichophyton* spp. was also identified. These findings suggest that cultivable *Trichophyton* spp. can be detected in approximately 40% of the safety shoes of workers with tinea pedis. The risk of reinfection by pathogenic filamentous fungi is likely increased by wearing dermatophyte-contaminated shoes.

Keywords: Tinea pedis, dermatophyte, reinfection, microbial pollution

1. Introduction

Although recently developed antifungal agents have a high capacity to cure tinea pedis, the population of patients with tinea pedis has not decreased – at least in Japan (1). Some potential reasons for the steady number of patients with tinea pedis despite the availability of effective antifungal agents are: 1) viable dermatophytes remain in the infected lesions when the application of therapeutic agents is discontinued prior to eradication of the dermatophytes, 2) reinfection by dermatophytes from other sites, such as a patient's onychomycosis, and 3) reinfection by dermatophytes remaining in the environment.

In the present study, we focused on the third possibility – reinfection from dermatophytes in the environment. Several reports indicate that viable dermatophytes are distributed in the houses in which individuals with tinea pedis live; cultivable

dermatophytes are detectable from various areas in the house (2), such as from room-dust (3) and bath mats (4). Dermatophytes are also detected at high frequency in shoes deposited by prisoners in USA upon entry into prison (5). Dermatophytes were isolated from the footwear using tape strips in 41% of 34 patients with clinically active tinea pedis (6). Recently, we found viable dermatophytes attached to the shoes of patients with tinea pedis visiting a dermatology clinic (7). These findings suggest that reinfection from not only the indoor environment, but also from footwear is responsible for the steady number of patients with tinea pedis, as predicted by Bonifaz (8).

We hypothesized that the detection ratio of viable *Trichophyton* spp. from worker's shoes, who didn't recognize one's infection of dermatophytes, might be high because their footwear is generally not washed or sanitized. Recently, dermatologic examinations of workers' feet was performed as part of a health support program for a factory. In parallel with this health examination, we checked the inside of the workers' safety shoes for fungal contamination. Here we report that viable *Trichophyton* spp. was detected in the safety shoes in 4 of 9 cases in which the workers were diagnosed with

*Address correspondence to:

Dr. Shigeru Abe, Teikyo University Institute of Medical Mycology, 359 Otsuka, Hachioji, Tokyo 192-0395, Japan.
E-mail: sabe@main.teikyo-u.ac.jp

dermatophyte infection by a professional dermatologist.

2. Materials and Methods

2.1. Dermatologic examination and collection of fungi from shoes

A clinical dermatologist experienced with medical treatment for dermal mycosis performed the dermatologic examination. He performed an examination of the feet of 19 workers (men) and collected desquamated skin scales to check for fungal filament using the KOH test. The skin samples of KOH-test positive participants were cultured as described below. In this examination procedure, their shoes were donated for collection of materials adhering to the inside of the shoe. To protect the privacy of the individuals, an opt-out policy was instituted; a notice regarding the opt-out policy was posted in the factory and the study was conducted with consent from all of the factory workers.

The methods in detail of these tests were as follows. By scraping the affected area, a large amount of scales was collected on slide glass. KOH test solution (20%) was dropped on the scales. The KOH-treated preparation on the slide glass was heated by exposure to the upper edge of the flame of an alcohol lamp for approximately 1 min to properly clear the keratin. After microscopic confirmation, KOH-positive specimens were cultured on Mycosel agar plates (Becton Dickinson, Franklin Lakes, NJ, USA).

2.2. Method for collecting dermatophytes from inside the footwear

Most of the workers wear safety shoes while at work, changing into personal shoes before leaving the factory at the end of the day. The work shoes were not washed and were worn almost every day. To collect fungi from the shoes, sealing tape for enzyme-linked immunosorbent assay (ELISA, Sumitomo Bakelite Co., Ltd., Japan) (7) was cut into a circle that was slightly smaller in size ($\varphi = 7.5$ cm) than the inner diameter of a petri dish ($\varphi = 9$ cm). The circular piece of tape containing both fungi and dust was incubated at 30°C on a Mycosel agar plate, so that the surface containing the dust and fungi was in contact with the medium surface. After 24 h culture, the tape was removed and culture was continued at 30°C. Six days after culture, we selected white fungus from the petri dishes where many fungal colonies were densely grown, gently touched the fungus with the tip of a micropipette, and cloned the fungus into a fresh agar plate. The cloning procedure was repeated at least twice.

2.3. Morphologic observation of fungi

Fungi-Tape (Scientific Device Lab. Inc., Des Plaines,

IL, USA) was pressed against the surface of the fungal colony to adsorb hypha and spores. The staining solution, Myco Perm Blue (Scientific Device Laboratory Inc., USA), was dropped on a slide glass, and Fungi-Tape with the hypha attached was adhered onto the slide glass, and stained. After staining, it was observed with a microscope and photographed.

2.4. Determination of nucleotide sequences of the DNA of the filamentous fungi and identification of the species

Using the obtained DNA as a template, the nucleotide sequence of the Internal Transcribed Spacer 1 (9) region located between 18S and 5.8S ribosomal DNA was amplified by polymerase chain reaction (PCR) using the primers shown below (9).

Internal Transcribe Spacer 1 primer sequences: #18SF1: AGGTTTCCGTAGGTGAACCT; #58SR1: TTCGCTGCGTTCCTTCATCGA

The PCR conditions were as follows: After dissociating double stranded DNA at 94°C for 10 min, we performed 30 cycles of 94°C for 30 s, 60°C for 30 s, and 72°C for 60 s. The temperature was then reduced to 4°C. The PCR product was purified using a QIAquick PCR Purification Kit (Qiagen, Germany). To determine the base sequence, samples were prepared with the two primers using the BigDye Terminator cycle sequence (Thermo Fisher Scientific, Waltham, MA, USA) method, and the base sequence was determined using an ABI sequencer 3130 (Applied Biosystems, Foster City, CA, USA). The sequence was obtained using the SEQUENCHER v4.10.1 (Gene Codes Corporation, Ann Arbor, MI, USA) and assembled from both directions. The resulting sequence was compared with the existing fungal base sequence using NCBI's BLAST, allowing for identification of the fungal species.

3. Results

Of 19 men, 9 were diagnosed with tinea pedis by clinical and mycological examination by a dermatologic expert. The diagnosis was made on the basis of not only clinical symptoms, but also the microscopical detection of filamentous fungi from scales. Table 1 shows the prevalence of tinea pedis, the age distribution of the subjects, and the rate of symptom awareness in 19 male subjects on the basis of the examination and inquiry results of the examinees. No person under the age of 35 had tinea pedis. Table 1 shows that the infection rates tended to be higher with increased age (maximum age 61). Although tinea pedis seemed to preferentially affect older people compared with younger people, the mean age of those without tinea pedis (43.9 ± 16.1 years old) is not significantly different from that of subjects with tinea pedis (52.4 ± 10.1 years old).

For 9 of the 19 participants of the dermatology health examination found to have filamentous fungi

Table 1. Characteristics of male workers who underwent a dermatology medical checkup

Items	n	Age (average)	Age (distribution)	Rate of men with symptom awareness related to tinea pedis
Person undergoing medical examination	19	47.9 ± 14.0	19-61	26.3%
Healthy person	10	43.9 ± 16.1	19-59	0%
Tinea pedis	9	52.4 ± 10.1	36-61	55.6%

Table 2. Identification of white filamentous fungi isolated from patient foot scales and dust from their footwear

No.	Age	From patient's scales	From shoes
1	56	<i>T. mentagrophytes</i>	<i>T. rubrum</i> , <i>T. mentagrophytes</i>
2	36	<i>T. interdigitale</i>	ND
3	60	ND	ND
4	40	<i>T. interdigitale</i>	<i>T. interdigitale</i> , <i>Acremonium sclerotigenum</i>
5	57	<i>T. rubrum</i>	<i>T. rubrum</i> , <i>Acremonium spp</i>
6	59	<i>T. interdigitale</i>	<i>Fusarium solani</i>
7	61	ND	<i>Arthrographis kalrae</i>
8	61	<i>Acremonium sclerotigenum</i>	<i>Acremonium sclerotigenum</i>
9	42	ND	<i>T. rubrum</i> , <i>Acremonium sclerotigenum</i>

ND, not detected

on the basis of the KOH-test, we cultured scraped and sliced keratinized samples on agar medium. After the primary culture, the samples prepared from six of the nine participants positive for filamentous fungi were re-culture for cloning. Genetic methods were used to identify the samples as *Trichophyton interdigitale* ($n = 3$), *T. rubrum* ($n = 1$), *T. mentagrophytes* ($n = 1$), and *Acremonium sclerotigenum* ($n = 1$; Table 2). Questionnaires completed by the workers diagnosed with filamentous fungi in the skin revealed that four of the nine subjects (44.4%) were unaware of their dermatologic infection (subjective symptoms) or did not know they had a skin abnormality (Table 1).

Filamentous fungi collected from the right and left shoes of the nine people diagnosed with tinea pedis were cultured. The plates were cultured for 1 week at 30°C. A wide variety of fungal colonies was observed on the cultured agar plates, including *Acremonium*, *Alternaria*, *Aspergillus*, *Arthrographis*, *Cladosporium*, *Fusarium*, *Penicillium*, and *Trichophyton*. We cloned small white colonies thought to be *Trichophyton*, which has a relatively slow growth rate. After two rounds of cloning the obtained colonies, microscopic observation and DNA analyses were performed. Three species of *Trichophyton* detected in the shoes were *T. rubrum*, *T. mentagrophytes*, and *T. interdigitale* (Table 2). The same species of fungi was identified in the scales and shoes obtained from four patients (Nos. 1, 4, 5, and 8; Table 2).

Figure 1 shows the typical images of *T. interdigitale* isolated from the scales (Figure 1A) and shoe (Figure 1 B) of patient No. 4. We wish to note that *T. mentagrophytes* was detected from the scales of the left foot and the left shoe of patient No. 1, and *T. rubrum* was detected from both the left and right shoes of the same patient. *T. rubrum* was also detected in the shoe of patient No. 9, but could not be cultured from the scales (Table 2). *Acremonium sclerotigenum* was detected in both the scales and shoes from patient No. 8, and

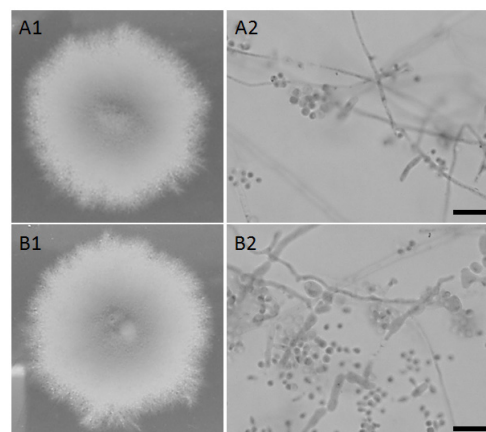


Figure 1. Typical images of *Trichophyton* obtained from the scales of the feet and dust from the shoes of examinee No. 4 in Table 2. (A) *T. interdigitale* from scales, (B) *T. interdigitale* from the dust of the shoe, 1; colony images grown on agar medium, 2; microscopic images of hyphae and conidia stained by MYCO PERM BLUE (Scientific Device Lab. Inc.). Bar represents 10 µm.

Acremonium was also detected from the shoes of three other workers (No. 4, 5, and 9; Table 2).

4. Discussion

The dermatologic examination at the factory in the present study revealed two major findings. First, 9 of 19 workers in the factory were diagnosed with tinea pedis (47%). This number is more than double that reported in Japanese in 1999/2000 (18.6%) (1), in 2006 (24.1%) (1), and 2007 (21.6%) (10). Second, the rate of detection of dermatophytes from the shoes of the workers with tinea pedis was also high (4 of 9, 44%).

The dermatologic examination in this study was conducted by an experienced dermatologist. Of 19 workers examined, 9 (47.4%) were diagnosed with tinea pedis and had a high infection rate; the youngest subject was 36 years old and none of the infected

subjects was under 35 years of age. We found a higher tinea pedis-positive rate in comparison with a previous study reported by Watanabe *et al.* (1). But, they also reported that persons between 50 and 60 years old having tinea pedis comprised 35% (1999/2000) and 36% (2006) of the subjects (1).

Although information regarding the existence of viable pathogenic fungi in footwear is very limited, we think that the detection rate of *Trichophyton* spp. in the shoes may be dependent on several factors. In our preceding study, the detection rate of *Trichophyton* spp. from the shoes of patients visiting the dermatology clinic for diseases other than tinea pedis was very low (7%), even the rate of patients with tinea pedis was high (7). We noted that the one of the reason for low detection rate may result from short wearing period of the patients visiting the clinic. In this study reported here, we studied workers who wore safety shoes almost every day for more than one year had the highest detection rate of *Trichophyton* spp. (44%) among the studies (5-7): The difference may depend on the wearing period.

The rate of *Trichophyton* spp. detected in the shoes may also be related to the severity of the tinea pedis-symptoms of the person wearing the shoes. In this connection, Knudsen reported that 41% of the footwear worn by patients with tinea pedis are dermatophyte-positive (6).

Trichophyton spp. was detected from shoes at a relatively high rate in this study, suggesting that fungal detection methods should be improved. Compared with skin samples, shoe dust was more often contaminated with mold, which grew faster, making it difficult to determine the causative *Trichophyton* spp. of tinea pedis among the various species found in the shoes. Actually, in this study, multicolored fungal colonies began to form on the plate on day 4 of culture, but *Trichophyton* spp. was not detected until after day 7 of culture. A method that could selectively cultivate *Trichophyton* spp. alone would enable a higher rate of collection of *Trichophyton* spp. from shoes. We plan to develop a selective nutrient media and clarify the culture temperatures to more efficiently detect *Trichophyton* spp.

Trichophyton spp. detected from inside the shoe might derive from a patient's scales through the socks or from contamination by the outside of the socks, because all persons providing the shoes tested in this study wore cotton socks. All subjects changed into their safety shoes from their personal shoes in the morning, but wore the same socks in both the work and personal shoes. With regard to dermatophyte penetration through socks, not only nylon stockings, but also cotton socks are reported to transmit *Trichophyton* spp. (11). *Trichophyton* spp. may attach to the outside of the socks from the environment, e.g., when they take their shoes off at home.

If the same species of *Trichophyton* are obtained from the scales and from the shoes, it is highly likely that the origin was the same. Cases in which *Trichophyton* spp. was detected only in the shoes may be due to contamination of the shoes from the environment or the detection efficiency of *Trichophyton* spp. in the scales of the patient by the KOH method may depend on the area of the foot selected for scraping.

Filamentous fungi other than *Trichophyton* spp. were also detected. *Acremonium*, which is not normally considered to be a common cause of tinea pedis with the exception of a recent report (12), was detected from patient No.8's scales. We think that *Acremonium* was the cause of infection in this patient due to the fact that the scales were obtained after the patient's skin was almost entirely disinfected with ethanol and the same filamentous fungus was collected from the patient's shoe. In addition to *Acremonium*, several kinds of fungi that cause skin mycoses and onychomycosis were detected and identified among the shoes, e.g., *Arthrographis* (13) and *Fusarium* (14), as shown in Table 2. The rate of infection increases, especially in immunocompromised persons, when mold, including *Trichophyton* spp., grows abundantly in environments such as shoes.

The findings of this study suggest a high risk of reinfection by tinea pedis from footwear and an increased risk of spreading *Trichophyton* spp. from shared footwear. Frequent eradication of the fungi inside of shoes to prevent infection by other dermatophytes as well as reinfection by tinea pedis is important, as well as for preventing the spread of *Trichophyton* spp. in other environments, such as the home.

Acknowledgements

The author sincerely thanks the workers at the factory who volunteered for this research. This work was supported in part by JSPS KAKENHI Grant Numbers JP15H05783 (Grant-in-Aid for scientific research (S)) to KS.

References

1. Watanabe S, Harada T, Hiruma M, Iozumi K, Katoh T, Mochizuki T, Naka W; Japan Foot Week Group. Epidemiological survey of foot diseases in Japan: results of 30,000 foot checks by dermatologists. *J Dermatol.* 2010; 37:397-406.
2. Katoh T. Dermatophytosis and environment. *Jpn J Med Mycol.* 2006; 47:63-67.
3. Shimamura Y. Isolation of dermatophytes from human cases of dermatophytosis and from house dust. *Jpn J Med Mycol.* 1984; 26:74-80.
4. Sano T, Taniguchi H, Yokozeki H, Katoh T, Nishioka K. The dissemination and adhesion of dermatophytes and

- a treatment to decrease collecting them on the various materials in daily life. *Jpn J Dermatol.* 2005; 115:1315-1319.
5. Ajello L, Getz ME. Recovery of dermatophytes from shoes and shower stalls. *J Invest Derm.* 1954; 22:17-24.
 6. Knudsen EA. Isolation of dermatophytes from footwear with adhesive tape strips. *J Med Vet Mycol.* 1987; 25:59-61.
 7. Ishijima SA, Hiruma M, Yamada A, Abe S. Detection and identification of *Trichophyton* living cells in footwear of patients with tinea pedis. *Med Mycol Res.* 2017; 8:17-23.
 8. Bonifaz A, Vázquez-González D, Hernández MA, Araiza J, Tirado-Sánchez A, Ponce RM. Dermatophyte isolation in the socks of patients with tinea pedis and onychomycosis. *J Dermatol.* 2013; 40:504-505.
 9. Makimura K, Mochizuki T, Hasegawa A, Uchida K, Saito H, Yamaguchi H. Phylogenetic classification of *Trichophyton mentagrophytes* complex strains based on DNA sequences of nuclear ribosomal internal transcribed spacer 1 regions. *J Clin Microbiol.* 1998; 36:2629-2633.
 10. Naka W. Foot Check 2007. *J. JOCD (Journal of the Japan Organization of Clinical Dermatologists).* 2009; 26:27-36. (in Japanese)
 11. Watanabe K, Taniguchi H, Nishioka K, Maruyama R, Katoh T. Preventive effects of various socks against adhesion of dermatophytes to healthy feet. *Jpn J Med Mycol.* 2000; 41:183-186.
 12. Chan GF, Sinniah S, Idris TI, Puad MS, Abd Rahman AZ. Multiple rare opportunistic and pathogenic fungi in persistent foot skin infection. *Pak J Biol Sci.* 2013; 16:208-218.
 13. Ramli SR, Francis AL, Yusof Y, Khaithir TM. A severe case of *arthrographis kalrae* keratomycosis. *Case Rep Infect Dis.* 2013; 2013:851875.
 14. Diongue K, Diallo MA, Ndiaye M, Seck MC, Badiane AS, Ndiaye D. Interdigital tinea pedis resulting from *Fusarium* spp. in Dakar, Senegal. *J Mycol Med.* 2018; 28:227-231.

(Received August 19, 2019; Accepted August 22, 2019)

Effects of naringenin on vascular changes in prolonged hyperglycaemia in fructose-STZ diabetic rat model

Nurul Hannim Zaidun¹, Sahema Zar Chi Thent¹, Mardiana Abdul Aziz¹, Santhana Raj L², Azian Abd Latiff¹, Syed Baharom Syed Ahmad Fuad^{1,*}

¹ Faculty of Medicine, Universiti Teknologi MARA (UiTM), Selangor, Malaysia;

² Institute of Medical Research, Jalan Pahang, Kuala Lumpur, Malaysia.

Summary

Chronic uncontrolled hyperglycaemia leads to increased oxidative stress and lipid peroxidation resulting in vascular complications and accelerates the progression of diabetic atherosclerosis. Though varieties of modern drugs used in the treatment of diabetes, the complications of diabetes are increasing. Naringenin (NG), has been reported to have potent antioxidant and anti-atherosclerotic properties. However, the effects of NG as vasculoprotective agent in prolonged hyperglycaemia are not well documented. Thus, this study was aimed to determine the effect of NG against vascular changes after prolonged hyperglycaemia in a diabetic rat model. Thirty adult male Sprague-Dawley rats were induced with fructose and streptozotocin to develop the diabetic rat model. After 4 weeks, the rats were randomly divided into 5 groups each group consisting of 6 animals: control, control treated with NG, non-treated diabetes mellitus (DM), DM treated with NG and metformin-treated DM. The treatment with NG (50 mg/kg) and metformin were continued for 5 weeks. The results showed that consumption of NG at 4 weeks post diabetic did not improved blood sugar, blood pressure and serum lipid profile. However, NG did significantly improve oxidative stress parameters in the aortic tissue like malondialdehyde (MDA). Analysis through light microscopy and transmission electron microscope (TEM) reverted the histological changes caused by prolonged hyperglycaemia. The findings thus demonstrated that introduction of NG after prolonged exposure to hyperglycaemia improved the vascular deterioration in diabetic group by decreasing oxidative stress evident by the reduced in the lipid peroxidation activity. Thus, this study showed the potential use of NG as adjunct in managing the diabetic condition during late presentation.

Keywords: Diabetes Mellitus (DM), naringenin, vascular complications, malondialdehyde (MDA), transmission electron microscope (TEM)

1. Introduction

The global prevalence of diabetes mellitus (DM) in 2017 has reached 425 millions and this figure is expected to rise in the coming years (1). Chronic uncontrolled hyperglycaemia leads to macrovascular and microvascular complications of diabetes such as vasculopathy. Vascular changes related-DM causes increase morbidity and mortality that significantly

contributes to the overall health economics and productivity of a country (2).

The pathogenesis of diabetic complications is complex (3). Many hypothesized aetiologies had attributed it to the disease process including overproduction of free radicals (4). The imbalance between oxidant and antioxidant reactions produces excessive reactive oxygen species and reactive nitrogen species thus increase in oxidative stress. Exposure of vascular wall to the free radicals in chronic hyperglycaemia causes injury to the endothelial cells. Chronic hyperglycaemia also causes reduction in the circulating nitric oxide (NO) secreted by the endothelial cells which triggers endothelial injury by altering the

*Address correspondence to:

Dr. Syed Baharom Syed Ahmad Fuad, Faculty of Medicine, Universiti Teknologi MARA (UiTM), Sungai Buloh Campus, 47000 Selangor, Malaysia.
E-mail: sbsaf11@gmail.com

vascular tone (5) and increased peroxynitrite, a potent free radical derived from nitric oxide (6).

Dyslipidaemia as a result of chronic DM has contributed to the development of atherosclerosis in diabetics (7). Increased thickness of tunica intima due to endothelial injury is further enhanced by increase in the low density lipoprotein (LDL) and reduction in the high density lipoprotein (HDL) levels in diabetes. Thickening of both tunica intima and media in type 2 diabetes mellitus (T2DM) leads to increased cardiac output which later can be resulted in hypertension (8), in addition to the impaired vascular tone secondary to the reduced availability of circulating NO.

Over the years, modern drugs have been the mainstay of treatment for DM for example, in T2DM, metformin remains as one of the first line drugs in treating DM. Nevertheless, the side effects which include lactic acidosis from metformin can be fatal to patients especially the elderly (9). Newer antidiabetic drugs such as thiazolidinedione is also associated with increased risk of developing cardiac disease (10). Despite the availability of various antidiabetic drugs, the complications of DM is still increasing (11). Furthermore, untoward side effects of the drugs warrant an alternative treatment that must be explored.

Naringenin (NG), one of the flavonoid which is found in plants and citrus fruits, has been studied widely in due to its potential actions against diabetes (12). NG is found in daily local diet in Malaysia and possesses multiple therapeutics properties such as anti-hypertensive, anti-inflammatory (13), anti-dyslipidaemia (13), anti-atherosclerotic (14) and anti-oxidative (15). Effects of NG in diabetic vessels has also been investigated. For an example, Bei Ren *et al.* had showed that NG improved glucose and lipid metabolism and as well as ameliorated endothelial dysfunction in type 2 diabetic rat model when given 1 week after confirmation of DM (16). Many other studies have also investigated the effects of NG on various organs and reported positive outcomes when NG treatment was started immediately from the time of DM development. Nevertheless, its effect on the diabetic vessels after prolonged exposure to uncontrolled hyperglycaemia is not known. Therefore, the aim of the study is to investigate the effects of NG on the diabetic vessels in prolonged (4 weeks) uncontrolled diabetic.

2. Materials and Methods

2.1. Animals

This study was approved by Universiti Teknologi MARA Animal Ethics Committee. Thirty ($n = 30$), Sprague-Dawley rats weighing 200-250 g were used. Each rat was caged individually in a controlled temperature and humidity. The temperature was set between 25-28°C with 12 h light/dark cycle. The rats

were fed with commercially available rat chow diet (Gold coin, Malaysia) and drinking water *ad libitum*.

2.2. Research framework

After 1 week of acclimatization, rats were randomly divided into control ($n = 12$) and experimental groups ($n = 18$). Weight, blood pressure and random blood glucose were measured as baseline values. In experimental group, all the rats were induced with diabetes according to the method described by Wilson *et al.* in 2012 (17). Briefly, 10% of fructose was given to the experimental group of rats in drinking water for 2 weeks and then, a single intramuscular injection of 40 mg/kg body weight of streptozotocin (STZ) (98% from Santa Cruz, USA) diluted in citrate buffer (18) was given. Control groups received normal drinking water and was injected with citrate buffer as placebo. Three days following STZ injection, a random blood glucose (RBG) was measured using glucometer (Oncall-plus, Germany) at the tail vein. Rats with RBG level of more than 16.5 mmol/L was considered as diabetics (19). After 4 weeks of DM induction, the rats were further subdivided into 5 groups; control (Ctr) and control-treated with naringenin (Ctr-NG), non-treated diabetic (DM-Ctr), diabetic treated with metformin (DM-MTF) as positive control group and diabetic treated with naringenin (DM-NG). Weight, blood pressure and random blood glucose were measured prior to treatment as pre-treatment values. The treatment was continued for 5 weeks using oral gavage. The dose of NG 50 mg/kg (20) and metformin 150 mg/kg (21) were used in the present study. One day before the end of the experiment, weight, random blood sugar and blood pressure were measured as post-treatment values. At the end of the experiment, the rats were fasted overnight and anaesthetized with diethyl ether. Cardiac puncture was performed to collect the blood for fasting lipid profile. Overdose diethyl ether was used for euthanasia. The aorta were harvested from the rats for further biochemical and histological examinations.

2.3. Blood pressure measurement

Systolic blood pressure (SBP) and diastolic blood pressure (DBP) measurements were taken at after 4 weeks of hyperglycaemia as pre-treatment and at 5 weeks following treatment as post-treatment time. Non-invasive tail-cuffed method was used using CODA system (Kent Scientific, USA). All rats were acclimatized prior to BP measurement by putting the rats in the BP tube 15 min before to the procedure in conscious state. An average of 3 readings were taken for each measurement.

2.4. Measurement of fasting serum lipid profile

Fasting lipid profile which consists of total cholesterol

(TC), triglycerides (TG), high density lipoprotein (HDL) and low density lipoprotein (LDL) were measured at post-treatment and compared between each group. Blood was taken via cardiac puncture following anaesthesia with diethyl ether. The collected blood samples were sent to Gribbles Sdn Bhd Malaysia for further analysis.

2.5. Collection of tissues

After 5 weeks of treatment, all rats were euthanised using overdose diethyl ether. Both arch of aorta and thoracic aorta were taken for histological and biochemical analyses, respectively. For the arch of aorta, approximately 2 mm³ of the proximal part was taken for transmission electron microscope analysis.

2.6. Microscopic analysis

2.6.1. Light microscopy

The arch of aorta was fixed in 10% formaldehyde and all the samples were processed for histological analysis. Tissue was cut using the microtome (Microm, USA) at 5 µm thickness and stained with haematoxylin and eosin for standard histological observation, and alcian blue to observe mucopolysaccharides deposit in the aortic tissues. For histomorphological analysis, the thickness of tunica intima (TI), tunica media (TM) and the ratio between TI and TM were measured by using an image analyzer software (ImageJ, an open resource developed by National Institutes of Health). Four measurements per image were obtained at 0°, 90°, 180° and 270° and the means were calculated (22).

2.6.2. Transmission electron microscopy (TEM)

Arch of aorta from all rats was cut into 2 mm³ size. The tissues were washed with 0.9% normal saline and fixed with 2.5% glutaraldehyde in phosphate buffer solution (PBS). Then, the tissue was rinsed with distilled water and 2% osmium tetroxide in distilled water. The tissues were dehydrated using a series of different concentrations of acetone. Infiltration and polymerisation were performed using acetone/resin and pure resin respectively. After polymerization, the specimens were sectioned with a glass knife, stained with toluidine blue solution and further sectioned with diamond knife at 90 nm cut. The specimens were viewed under transmission electron microscope (Tecnai G2 model, FEI, USA).

2.7. Biochemical analysis

2.7.1. Determination of malondialdehyde (MDA)

MDA was measured as oxidative marker in the aortic

tissue using a commercial kit (Sigma-Aldrich, German). The assay is based on the reaction of MDA with thiobarbituric acid (TBA) to form a colorimetric product which is proportional to the MDA present. Aortic tissue was collected, weighed and was homogenized in 300 mL of the MDA lysis buffer and 3 mL of butylated hydroxytoluene (BHT). The solution was centrifuged at 13,000× g for 10 min. The supernatant (200 µL) from each homogenized sample were placed into a microcentrifuge tube and proceeded to assay reaction. MDA standard solution was prepared according to the manufacturer protocol. MDA standard solution (600 µL) was added into each vial containing homogenised tissue sample. The samples were incubated at 95°C for 60 min and cooled to room temperature in an ice bath for 10 min. Approximately 200 µL of reaction mixture was pipetted into a 96 well plate for analysis. The absorbance was measured at 532 nm (A532) using Perkin Elmer 2030 Multilabel Reader Victor TM X5 machine and expressed in nanomoles per gram of protein.

2.7.2. Determination of nitric oxide (NO)

Nitric oxide was determined using Quantichrome Nitric oxide Assay Kits (BioAssay System, USA). Aortic tissue samples (10 mg) were homogenised in phosphate buffer solution and centrifuged at 14,000 rpm at 4°C. The supernatant were taken and deproteinated using 8 µL ZnSO₄. The mixture of 150 µL supernatant of sample were vortexed and 8 µL NaOH and vortexed again. The mixture were centrifuged for 10 min at 14,000 rpm. The final 100 µL of supernatant were collected and used for the reaction assay. Working reagent (WR) and standard solution were prepared according to manufacturer protocol. WR was added to every standard solution and samples. The mixture of WR and samples or standards in reaction tubes were incubated for 10 min at 60°C. Then, the reaction tubes were centrifuged and 250 µL of each reaction were separated to the 96 well plate. The optical density (OD) was read at 540 nm using Perkin Elmer 2030 Multilabel Reader Victor TM X5 machine.

2.8. Statistical analysis

The data are presented as the means ± standard deviation (SD). Statistical analysis was carried out by using ANOVA followed by Bonferroni post-hoc test. A value of $p < 0.05$ was considered to be significant. All statistical analysis was performed using the SPSS statistical package version 24.0 (SPSS Inc., Chicago, USA).

3. Results

3.1. Confirmation of diabetes

After induction of diabetes, all rats exhibited clear signs

of overt diabetes in comparison with non-induced rats. The induced rats suffered frequent urination (polyuria) and high fluids and food intake *i.e.* polydipsia and hyperphagia respectively. They were also noticed to become hypoactive and more lethargic, evidenced by the reduced activity upon handling and less movement upon changing of bedding. It was observed that treatment with NG did not improved the morphology, character and behaviour of the diabetic rats. The weights in diabetic rats were not increased in treated and untreated rats as shown in Figure 1.

At post-treatment time (Figure 2), RBG in the DM-Ctr group (27 ± 4.85 mmol/L) remained significantly high ($p < 0.05$) compared to Ctr group (4.98 ± 0.28 mmol/L). Treatment with NG however, did not significantly reduced RBG level in DM-NG (26.7 ± 4.70 mmol/L) group when compared to DM-Ctr group (27 ± 4.85 mmol/L). Metformin also did not significantly reduce the level of RBG ($p > 0.05$) but a reducing trend was seen in DM-MTF group (24.43 ± 4.67 mmol/L) compared to DM-Ctr group. Neither hypoglycaemia nor hyperglycaemia was observed at post-treatment time in Ctr-NG group compared to Ctr group.

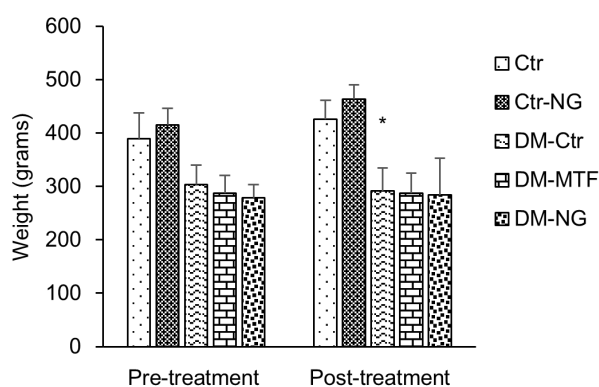


Figure 1. The changes of weight of the rats at different interval. (*) significant weight loss was seen in DM-Ctr group compared to Ctr group.

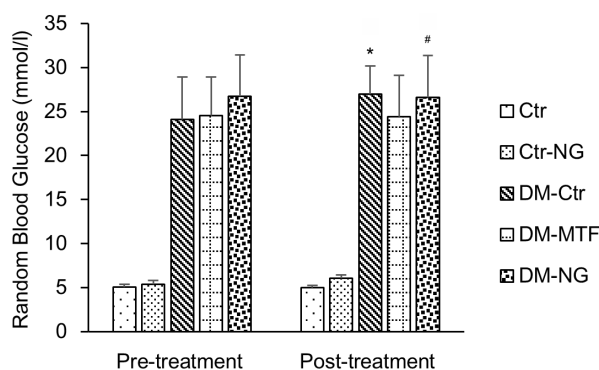


Figure 2. Effects of NG on RBG level when NG was introduced after 4 weeks of uncontrolled hyperglycemia. (*) significant increase in RBG, $p < 0.05$, in DM-Ctr group compared to Ctr-group. (#) no significant changes observed in DM-NG compared to DM-Ctr group.

3.2. Blood pressure

During pre-treatment time, DM-Ctr group showed significant ($p < 0.05$) changes in SBP (143.78 ± 10.79 mmHg) and DBP (101.00 ± 8.13 mmHg) when compared to Ctr group. However, after 5 weeks of treatment, DM-NG group showed no significant changes ($p > 0.05$) in either SBP (130.17 ± 19.68 mmHg) and DBP (85.72 ± 13.51 mmHg) when compared to DM-Ctr (SBP: 145.22 ± 7.79 mmHg; DBP: 89.11 ± 20.37 mmHg) group (Figure 3).

3.3. Fasting serum lipid profile

Fasting lipid profiles were evaluated following 5 weeks of treatment with NG when it was consumed at 4 weeks post diabetic. There were no significant changes observed in all diabetic rats groups in terms of total cholesterol, triglycerides, low density lipoprotein and high density lipoprotein levels when compared to the untreated diabetic rats (DM-Ctr group) ($p > 0.05$). The lipid profiles of non-diabetic rats treated with NG (Ctr-NG) also showed no significant difference ($p > 0.05$) compared with the untreated non-diabetic rats (Ctr). These finding suggest that consumption of NG at 4 weeks post diabetic for 5 weeks had no significant effect on fasting serum lipid profile in diabetic animals

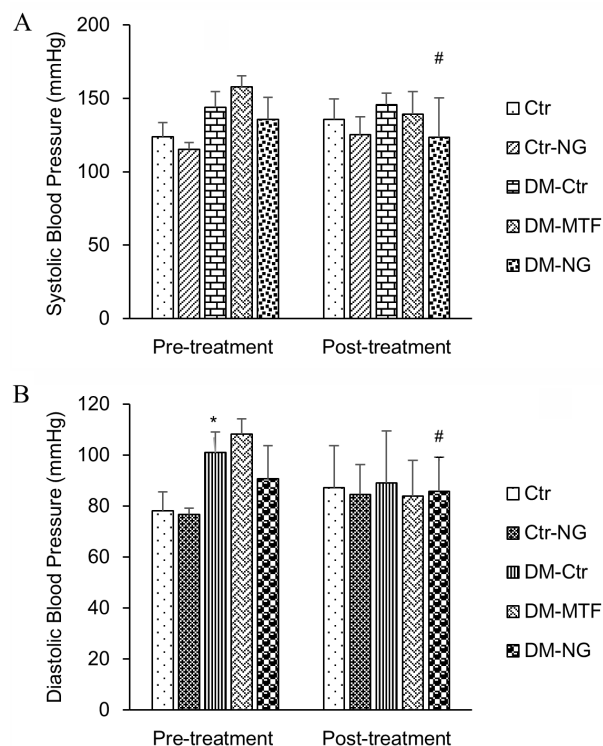


Figure 3. Changes in the systolic (A) and diastolic (B) blood pressure at different time. No significant change (#) was observed in systolic and diastolic blood pressure when NG introduced to experimental rats at 4 weeks post diabetic for 5 weeks. (*) significant changes observed in DM-Ctr group compared to Ctr group prior the start of treatment.

Table 1. Effect of NG when introduced after 4 weeks of diabetes to the fasting serum lipid profile

Group	Total Cholesterol (TC)	Triglycerides (TG)	High Density Lipoprotein (HDL)	Low Density Lipoprotein (LDL)
Ctr	1.82 ± 0.26	0.805 ± 0.14	0.48 ± 0.28	0.97 ± 0.09
Ctr-NG	2.47 ± 0.22	0.69 ± 0.11	0.305 ± 0.06	1.84 ± 0.22
DM-Ctr	2.64 ± 0.14	1.21 ± 0.04	0.84 ± 0.32	1.27 ± 0.31
DM-MTF	2.7 ± 0.26	0.80 ± 0.04	0.89 ± 0.11	1.49 ± 0.28
DM-NG	2.77 ± 0.20#	1.19 ± 0.29#	0.97 ± 0.18#	1.25 ± 0.10#

(#) showed no significant changes in fasting serum lipid profile in DM-NG compared to DM-Ctr group.

(Table 1).

3.4. MDA and NO levels of aortic tissue

MDA level was measured in the aortic tissue (thoracic aorta) as an indicator for lipid peroxidation activity. DM-NG group exhibited significantly decreased ($p < 0.05$) MDA level ($0.79 \text{ nmol} \pm 0.02 \text{ nmol/mg}$) compared to the DM-Ctr group ($0.84 \pm 0.02 \text{ nmol/mg}$). However, the diabetic group treated with metformin (DM-MTF) showed no significant difference compared to DM-Ctr group. No significant changes were observed between NG-treated and untreated non-diabetic rats group (Table 2).

NO level in aortic tissue (thoracic aorta) was measured at the end of the study according to the protocol described by the manufacturer. It was observed that NG-treated DM rats (DM-NG group) showed no significant changes in NO level compared to the untreated group (DM-Ctr) ($p > 0.05$). Similarly, DM-MTF group also showed insignificant change in NO level ($p > 0.05$) compared to control. In the non-DM rats (Ctr and Ctr-NG), treatment with NG did not show any significant changes in NO level (Table 2).

Table 2. Effect of NG on MDA and NO levels in the aortic tissue when introduced at 4 weeks post diabetic, for 5 weeks.

Group	MDA level (nmol/mg)	NO level ($\mu\text{M/mg}$)
Ctr	0.82 ± 0.02	30.95 ± 1.26
Ctr-NG	0.79 ± 0.01	38.10 ± 6.12
DM-Ctr	0.83 ± 0.03	35.80 ± 3.72
DM-MTF	0.82 ± 0.02	33.98 ± 3.08
DM-NG	0.79 ± 0.02*	37.38 ± 6.47#

Significant changes were only seen in MDA level (*) but no significant changes were observed in NO level (#) when compared to the DM-Ctr group.

Table 3. Effect of NG on the thickness of TI and TM when NG introduced at 4 weeks post diabetic

Group	Ctr	Ctr-NG	DM-Ctr	DM-MTF	DM-NG
Thickness of TI (μm)	8.71 ± 0.65	9.71 ± 1.39	11.93 ± 1.67	9.36 ± 1.04**	9.04 ± 1.82*
Thickness of TM (μm)	317.58 ± 67.14	398.22 ± 59.09	470.58 ± 92.12	388.48 ± 93.46	306.36 ± 85.18*
Ratio (TI:TM)	0.03	0.02	0.03	0.02	0.03

Thickness of TI and TM was significantly reduced in DM-NG group when compared to DM-Ctr group (*). Treatment with metformin in DM-MTF group showed significant reduced in the thickness of TI, but not seen in TM (**).

3.5. Histomorphometry and histological analysis

In the present study, the thickness of tunica intima (TI) and tunica media (TM) were measured under haematoxylin eosin (H&E) staining which is routine histological staining to observe the morphological feature of a tissue. The measured thickness TI and TM were compared with untreated diabetic group (DM-Ctr) and the ratio between TI:TM were calculated. There was significant increase ($p < 0.05$) in TI thickness in the untreated diabetic rats (DM-Ctr group). Following 5 weeks of treatment with NG, the thickness of TI and TM were reduced in the diabetic rats compared to DM-Ctr group. Similarly, treatment with metformin reduced the TI thickness but not the TM. In addition, there was no significant difference observed in the ratio between TI and TM in all groups (Table 3).

There was loss of endothelial cells and disruption of internal elastic lamina in TI observed in the untreated DM rats on H&E staining (Figure 4). TM elastin was also observed to be less tortuous compared to the untreated non diabetic group. Sublamina area showed high proliferation of vascular smooth muscle cells. After treatment with NG, these distorted morphological features seen in the untreated diabetic rats were lessen, and instead similar features to the non-diabetic rats were observed. The DM-NG group showed presence of normal endothelial cells in TI, prominent internal elastic lamina along with increased in the tortuosity of the elastin. Similar features were also observed in DM-MTF group.

Alcian blue staining was used to stain the connective tissue particularly acid mucopolysaccharides. In the present study, there was increased deposition of acid mucopolysaccharides (blue in colour) in DM-Ctr group (Figure 5). However, DM-NG group showed less deposition of acid mucopolysaccharides along with normal architecture of aortic tissue. Similar

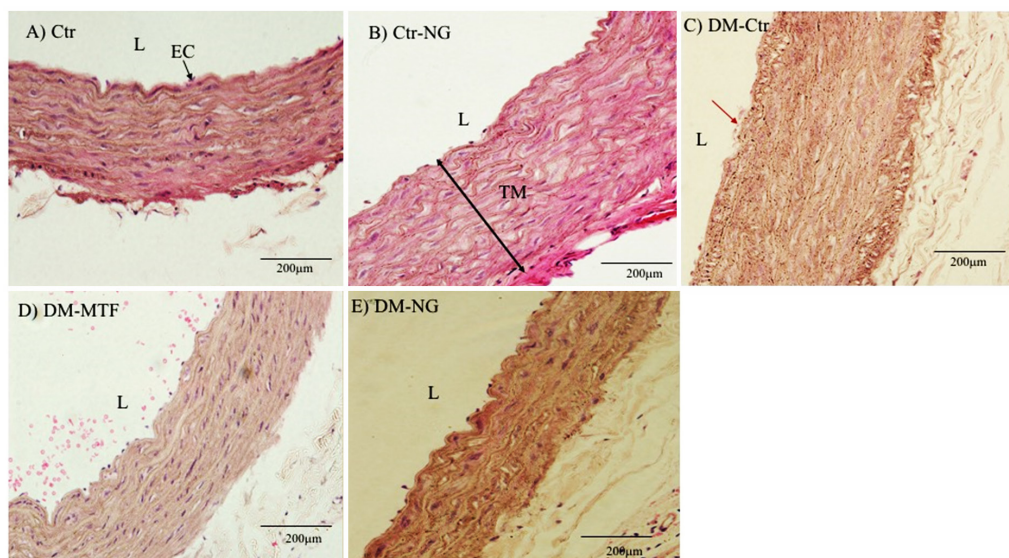


Figure 4. Photomicrograph of transverse sections of the arch of aorta under H&E staining $\times 40$. Thickened TI and TM was observed in DM-Ctr compared to Ctr group. Consumption of the NG by the diabetic group in DM-NG after 4 weeks post diabetic group showed improvement in the histological features compared to DM-Ctr group. Arrow head (red) showed injury on intimal layer on the DM-Ctr group. TI, tunica intima; TM, tunica media; EC, endothelial cell; L, lumen.

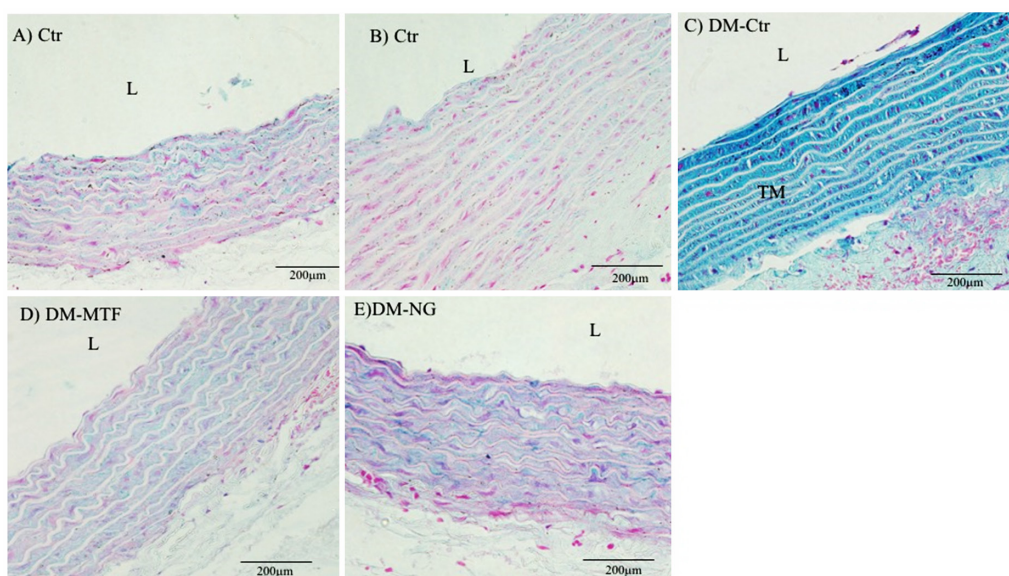


Figure 5. Photomicrograph of transverse sections of the arch of aorta under Alcian Blue staining $\times 40$. Increased deposition of acid mucopolysaccharides (blue stain) in both TI and TM was observed in DM-Ctr group compared to Ctr group. In DM-NG group, reduced in mucopolysaccharides was seen compared to DM-Ctr group. TM, tunica media; L, lumen.

features were observed in the DM-MTF group. These histological findings revealed that treatment with NG after 4 weeks exposure to the uncontrolled hyperglycaemia improved the morphological deterioration of aortic tissue in diabetic rats.

3.6. TEM analysis

The ultrastructural features of endothelial cells in tunica intima, extracellular matrix in the subendothelial region, internal elastic lamina and smooth muscle cells in tunica media were observed under TEM and the results

are shown in Figure 6. There were no ultrastructural differences observed in treated and untreated non-diabetic rats (Ctr-NG and Ctr, respectively). Endothelial cells were intact and internal elastic lamina was not disturbed. Smooth muscles cells were normally distributed. However, DM-Ctr group showed some area of desquamation along the intimal region. Retracted endothelial cells were seen and possessed irregular distributions. The notable morphological changes in the intimal layer showed endothelial injury. The appearance normal structure of internal elastic lamina layer was loss. Irregular shaped of smooth muscle

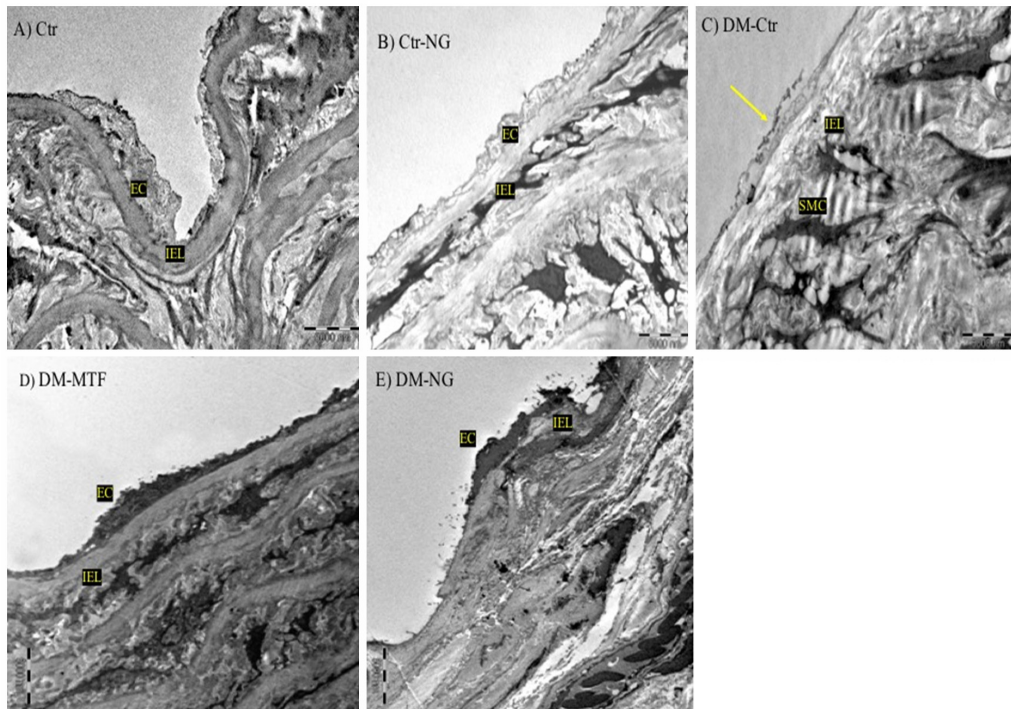


Figure 6. Micrograph ($\times 8,500$) of aorta under TEM. Noted the disruption of IEL in DM-Ctr compared to Ctr group. Lifting of EC, migration of SMC to intimal layer was noticeable in DM-Ctr which was absent in DM-NG group. EC, endothelial cells; IEL, internal elastic lamina; SMC, smooth muscle cells.

cells was observed in proximity to the internal elastic lamina, migrating to the TI. Nonetheless, DM-NG group showed less ultrastructural deteriorations both in the intimal and media regions. Consumption of NG after 4 weeks of uncontrolled hyperglycaemia improved the diabetic changes. Presence of normal endothelial cells, less disrupted and well-arranged lamina area was observed in DM-NG group. Smooth muscle cells were restored to its normal shape. Similar finding was found in DM-MTF group.

4. Discussion

Studies on prolonged hyperglycaemia in diabetic rats has used various duration to define chronic hyperglycaemia. Some studies defined chronic hyperglycaemia as 2 weeks (23), 4 weeks (24), 8 weeks (25) and up to 16 weeks (26). In this current study, 4 weeks of prolonged hyperglycaemia is chosen to define chronic DM as no study of NG had been done to investigate the effects of NG on vascular changes in chronic hyperglycaemia. Studies involving the effect of NG on vascular changes had demonstrated NG to effectively prevent abnormal changes in the diabetic vessels through nitric oxide by introducing NG at 1 week post diabetes (27). A study on NG by Bei Ren *et al.* had demonstrated NG to significantly regulate glucose and lipid metabolism, and ameliorate vascular dysfunction after introducing NG at 1 week post diabetes in type 2 diabetic rat model (16). The longest duration of chronic hyperglycaemia prior the

introduction of NG had been reported by Salim *et al.* and Dosari *et al.*, where both studies defined 2 weeks as their cut off point prior introducing NG to diabetic group to investigate the effect of diabetic retinopathy and neuropathy (20,23). Thus this study was aimed to evaluate the effectiveness of NG at a longer post diabetic period *i.e.* 4 weeks before the introduction of treatment.

The present study used an established diabetic model described by Wilson *et al.* using fructose and low dose STZ (28). All the rats in the experimental groups (DM-Ctr, DM-NG and DM-MTF) remained diabetic where the RBG was persistently more than 16.5 mmol/L throughout the experiment prior introduction of NG. The rats were left in non-treated condition for 4 weeks prior starting the treatment. Treatment with NG in the diabetic group did not significantly reduced the blood glucose level. This finding is in contrast to other reported result where immediate treatment with NG on diabetic experimental animal significantly reduced the blood sugar (29). Delay in starting treatment had proven to take a longer time to regulate the blood glucose (30). Therefore, longer exposure of the cells to the hyperglycaemic condition caused increased in oxidative stress thus more difficult in treating the hyperglycaemic conditions (31). Prolonged hyperglycaemia is also known to affect the prognosis and outcome of patients as delay in the intensification of treatment might increase risk in developing cardiac event that could lead to fatality (32). In this study, metformin treatment also showed no significant reduction in blood glucose.

This may suggest the possible need for multiple drugs modalities to treat prolonged hyperglycaemia. There is also a need to determine if a higher dose of NG could reduce the blood sugar in chronic state of diabetes.

Complications of DM was reported to result from the imbalance between antioxidant and oxidant reactions. Increased in secondary metabolites due to chronic hyperglycaemia lead to the overproduction of superoxide in the endothelial cells (7) thus triggering the oxidative stress in the tissue. Such increase in oxidative stress condition causes endothelial cells injury and promote vascular injury and later on atherosclerosis. On the other hand, NG is one of the flavonoids abundantly found in citrus fruits. It has multiple therapeutics properties against chronic diseases like DM. Apart from being able to improve diabetic condition (33), NG is also known to be effective against atherosclerosis accelerated by diabetic condition (34). However, in such experiment, NG was being introduced at different intervals from the time of the confirmation of diabetes. In this present study, effects of NG on the general condition including weight, blood pressure, serum lipid profile and histological changes of diabetic aortic tissue in a prolonged diabetic were evaluated.

Immediate introduction of NG to the experimental animal seem to report different results. A study by Sandeep *et al.* (35) showed that NG attenuated the loss of weight in the diabetic animal while another study had shown NG to have no significant effect on the weight (16). At 2 week post diabetic, NG administration showed no improvement of weight in the diabetic animal (23). In this present study, introduction of NG at 4 weeks post diabetic did not significantly affect the weight of the diabetic animal. This result might be due to the condition of the affected animals whereby chronic hyperglycaemia has put the experimental animals into catabolic state. The imbalance between catabolic and anabolic state caused the diabetic rats to lose muscle weight with addition of dehydration hence preventing weight gain.

Blood pressure in diabetic patients tend to rise with prevalence of 30% and 60% for type 1 DM and type 2 DM respectively (36). This is partly due to the atherosclerotic process which is accelerated in diabetes (37). Consumption of NG in diabetic rats as part of the prevention of hypertension, did not show significant changes on the blood pressure (14). However, another study had found that, naringin (aglycone NG) did significantly reduce systolic blood pressure in diabetic animals when it was introduced immediately in metabolic syndrome rat model (38). The present study showed that introduction of NG at 4 weeks post diabetic did not significantly improved either systolic or diastolic blood pressure.

Serum lipid profile is commonly affected in diabetes (39). Uncontrolled hyperglycaemia causes increased in the glycosylation and oxidation which affect the

lipoproteins and contributes to the development of atherosclerosis in diabetes (36). Effects of NG on serum lipid profile had shown positive outcomes whereby consumption of NG by the diabetic animal immediately from the time of diagnosis improved serum lipid profile compared to non-treated diabetic animals (16). At 10 days post diabetic, consumption of NG by the type 2 diabetic animal model caused alleviation of triglycerides and high density lipoprotein (40). However, in this study, 5 weeks of NG consumption by the diabetic animal did not significantly improve lipid profile caused by prolonged uncontrolled hyperglycaemia.

The effects on NG on MDA and NO levels in diabetic aortic tissue were determined. MDA is one of the final products of lipid peroxidation of the unsaturated fatty acids in the cell membrane. It is commonly known as a marker for oxidative stress (41). In a diabetic setting, imbalance of antioxidant and oxidant reaction increases the production of MDA. NG is a well-known antioxidant that was shown to reduce lipid peroxidation in the liver, kidney, and pancreas (15,42). However, the effects of NG on the level of MDA in the diabetic aortic tissue when the given earlier than 4 weeks post diabetic is not yet available up to the time of writing. In this study, we had found that consumption of NG at 4 weeks post diabetic reduced MDA level in the diabetic aortic tissue. This result supports the existing facts on NG which is not only effective as antioxidant when introduced immediately after the confirmation of diabetes, but may be useful in the managing diabetes when the patients presented late.

NO is secreted by the vascular endothelial cells and acts as key regulator in maintaining the vessel tone (5,6). However, NO may interact with superoxide radicals which is increased in hyperglycemia to produce peroxynitrite, a potent oxidant radical. Accumulation of peroxynitrite may trigger endothelial injury and accelerate atherosclerotic process (43). *In vitro* studies on NO had shown that NG prevented the decrease in NO level in diabetic cells (16,44). Introduction of NG at 1 week post diabetes showed improvement in the availability of NO in the diabetic aorta compared to non-treated diabetic aorta (27). Another report showed that consumption of 50 mg/kg body weight of NG after 2 weeks of confirmation of diabetes, had reduced the level of NO in diabetic sciatic tissue (20). Similar results was shown in another study where NG introduced at 4 weeks post diabetic showed reduction in the NO level in the diabetic brain tissue (24). The present study showed that the effect of NG on the diabetic aortic tissue after consumption of NG at 4 weeks post diabetic to be not significant. Looking at the various reports on the effect of NO when introduced at different interval post diabetes, we can observe the paradox phenomenon of NO in diabetic setting. It was reported that superoxide produced following hyperglycaemia activated other

pathway that caused increased in the expression of inducible nitric oxide (iNOS), thus the net production of NO. However, in chronic hyperglycaemia, more superoxide anions is produced and present in high concentrations. Superoxides interact promptly with newly produced NO to form stronger oxidant which is peroxynitrite and cause decline in the availability of NO in the endothelial cell itself (45).

NG that was introduced to the experimental animal at different intervals once the metabolic abnormality was confirmed exhibit positive results in histomorphometrical analysis. For instance, the effect of NG when introduced as supplementation prior the development of the metabolic syndrome rat model had demonstrated improved endothelial injury effect on the vessel wall (14,34). Similar result was reported when NG was introduced at 1 week post diabetic, whereby histological analysis by light microscopy and TEM showed less injury to the aorta of the diabetic rats compared to untreated diabetic group (16). In this study, consumption of NG for 5 weeks at 4 weeks post diabetic caused significant reduction in the thickness of tunica intima and media with reduced the collagen deposition in the vessel wall of the diabetic aorta compared to the untreated diabetic group. Effect of NG can be clearly seen in TEM even after delayed treatment *i.e.* 4 weeks following the confirmation of diabetes.

In conclusion, effect of NG when introduced at 4 weeks post diabetic, for 5 weeks resulted in reduction of oxidative stress evident by the reduce lipid peroxidation activity in diabetic group. It also improved the histomorphological changes of the aortic tissue in chronic diabetes. These findings are comparable to the effects of NG when it was given immediately after the diagnosis of diabetes. However, the effect of NG as antihyperglycemic and antilipidemic when it was introduced after 4 weeks of uncontrolled hyperglycaemia was not evident in this study compared to the earlier study whereby NG is effectively reduced the blood glucose and improved serum lipid profile when introduced at the beginning of the diabetic disease. Administration of NG after 4 weeks diabetes also did not affect the level of NO in the diabetic aortic tissue. Thus detailed research of NG might be needed as to either increased the dose of NG or longer duration of treatment might be considered for NG to be effective in managing diabetes in delayed presentation.

Acknowledgements

This research was fully funded by LESTARI: 600-IRMI/myra5/3/LESTARI (9/2016), Universiti Teknologi MARA (UiTM).

References

- Forouhi NG, Wareham NJ. Epidemiology of diabetes. *Medicine*. 2014; 42:698-702.
- World Health Organization. Diabetes country profiles (Malaysia). <http://www.who.int/diabetes/country-profiles/en/#M>. (accessed on 8th April 2019)
- Forbes JM, Cooper ME. Mechanisms of diabetic complications. *Physiol Rev*. 2013; 93:137-188.
- Giacco F. Oxidative stress and diabetic complications. *Circ Res*. 2011; 107:1058-1070.
- Zhao Y, Vanhoutte PM, Leung SWS. Vascular nitric oxide: Beyond eNOS. *J Pharmacol Sci*. 2015; 129:83-94.
- Pitocco D, Zaccardi F, Di Stasio E, Romitelli F, Santini SA, Zuppi C, Ghirlanda G. Oxidative stress, nitric oxide, and diabetes. *Rev Diabet Stud*. 2010; 7:15-25.
- Tomkin G.H., and Owens D. LDL as a cause of atherosclerosis. *Atheroscler Thromb J Atheroscler Thromb*. 2012; 5:13-21.
- Nezu T, Hosomi N, Aoki S, Matsumoto M. Carotid intima-media thickness for atherosclerosis. *J Atheroscler Thromb*. 2016; 23:18-31.
- Peters N, Jay N, Barraud D, Cravoisy A, Nace L, Bollaert PE, Gibot S. Metformin-associated lactic acidosis in an intensive care unit. *Crit Care*. 2008; 12:R149.
- Bolger AF, Herrington D, Eckel RH, Kaul S, Giugliano RP. Thiazolidinedione drugs and cardiovascular risks. *Circulation*. 2010; 121:1868-1877.
- Deshpande AD, Harris-Hayes M, Schootman M. Epidemiology of diabetes and diabetes-related complications. *Phys Ther*. 2008; 8:1254-1264.
- Priscilla DH, Roy D, Suresh A, Kumar V, Thirumurugan K. Naringenin inhibits α -glucosidase activity: A promising strategy for the regulation of postprandial hyperglycemia in high fat diet fed streptozotocin induced diabetic rats. *Chem Biol*. 2014; 210:77-85.
- Nyane NA, Tlaila TB, Malefane TG, Ndwandwe DE, Owira PMO. Metformin-like antidiabetic, cardio-protective and non-glycemic effects of naringenin: Molecular and pharmacological insights. *Eur J Pharmacol*. 2017; 803:103-111.
- Mulvihill EE, Assini JM, Sutherland BG, Dimattia AS, Khami M, Koppes JB, Sawyez CG, Whitman SC, Huff MW. Naringenin decreases progression of atherosclerosis by improving dyslipidemia in high-fat-fed low-density lipoprotein receptor-null mice. *Arterioscler Thromb Vasc Biol*. 2010; 30:742-748.
- Sharma A, Patar AK, Bhan S. Cytoprotective, antihyperglycemic and antioxidative effect of naringenin on liver and kidneys of Swiss diabetic mice. *Int J Heal Sci Res*. 2016; 6:118-131.
- Ren B, Qin W, Wu F, Wang S, Pan C, Wang L, Zeng B, Ma S, Liang J. Apigenin and naringenin regulate glucose and lipid metabolism, and ameliorate vascular dysfunction in type 2 diabetic rats. *Eur J Pharmacol*. 2016; 773:13-23.
- Wilson RD, Islam S. Fructose-fed streptozotocin-injected rat : An alternative model for type 2 diabetes. *Pharmacol Rep*. 2012; 64:129-139.
- Kim J, Kang M, Choi H, Jeong S, Lee Y, Kim J. Quercetin attenuates fasting and postprandial hyperglycemia in animal models of diabetes mellitus. 2011; 5:107-111.
- Fernandes AAH, Novelli ELB, Junior AF, Galhardi CM. Effect of naringenin on biochemical parameters in the streptozotocin-induced diabetic rats. *Brazilian Arch Biol Technol*. 2009; 52:51-59.
- Al-Rejaie SS, Aleisa AM, Abuhashish HM, Parmar MY, Ola MS, Al-Hosaini AA, Ahmed MM. Naringenin neutralises oxidative stress and nerve growth factor

- discrepancy in experimental diabetic neuropathy. *Neurol Res.* 2015; 37:924-933.
21. Salemi Z, Rafie E, Goodarzi MT, Ghaffari MA. Effect of metformin, acarbose and their combination on the serum visfatin level in nicotinamide/streptozocin-induced type 2 diabetic rats. *Iran Red Crescent Med J.* 2016; 18:e23814.
 22. Abas R, Othman F, Thent ZC. Effect of Momordica charantia fruit extract on vascular complication in type 1 diabetic rats. *EXCLI J.* 2015; 14:179-189.
 23. Al-Dosari DI, Ahmed MM, Al-Rejaie SS, Alhomida AS, Ola MS. Flavonoid naringenin attenuates oxidative stress, apoptosis and improves neurotrophic effects in the diabetic rat retina. *Nutrients.* 2017; 9:pii: E1161.
 24. Rahigude A, Bhutada P, Kaulaskar S, Aswar M, Otari K. Participation of antioxidant and cholinergic system in protective effect of naringenin against type-2 diabetes-induced memory dysfunction in rats. *Neuroscience.* 2012; 226:62-72.
 25. Badalzadeh R, Mohammadi M, Yousefi B, Faranjia S, Najafi M, Mohammadi S. Involvement of glycogen synthase kinase-3 β and oxidation status in the loss of cardioprotection by postconditioning in chronic diabetic male rats. *Adv Pharm Bull.* 2015; 5:321-327.
 26. Davidson EP, Coppey LJ, Shevalye H, Obrosova A, Randy H, Yorek MA. Impaired corneal sensation and nerve loss in a type 2 rat model of chronic diabetes is reversible with combination therapy of menhaden oil, α -lipoic acid and enalapril. *Cornea.* 2017; 36:725-731.
 27. Roghani M, Fallahi F, Moghadami S. Citrus flavonoid naringenin improves aortic reactivity in streptozotocin-diabetic rats. *Indian J Pharmacol.* 2012; 44:382.
 28. Wilson RD, Islam S, Islam MS. Fructose-fed streptozotocin-injected rat: An alternative model for type 2 diabetes. *Pharmacol Rep.* 2012; 64:129-139.
 29. Oršolić N, Gajski G, Garaj-Vrhovac V, Crossed D, Signikić D, Prskalo ZŠ, Sirovina D. DNA-protective effects of quercetin or naringenin in alloxan-induced diabetic mice. *Eur J Pharmacol.* 2011; 656:110-118.
 30. Zografou I, Strachan MWJ, McKnight J. Delay in starting insulin after failure of other treatments in patients with type 2 diabetes mellitus. *Hippokratia.* 2014; 18:306-309.
 31. Kalansooriya A, Whiting PH, Haddad F, Holbrook I, Jennings PE. The relationship between chronic glycaemic control and oxidative stress in type 2 diabetes mellitus. *Br J Biomed Sci.* 2016; 65:71-74.
 32. Nichols GA, Romo-LeTourneau V, Vupputuri S, Thomas SM. Delays in anti-hyperglycaemic therapy initiation and intensification are associated with cardiovascular events, hospitalizations for heart failure and all-cause mortality. *Diabetes Obes Metab.* 2019; 21:1551-1557.
 33. Ramprasath T, Senthamizharasi M, Vasudevan V, Sasikumar S, Yuvaraj S, Selvam GS. Naringenin confers protection against oxidative stress through upregulation of Nrf2 target genes in cardiomyoblast cells. *J Physiol Biochem.* 2014; 70:407-415.
 34. Assini JM, Mulvihill EE, Sutherland BG, Telford DE, Sawyez CG, Felder SL, Chhoker S, Edwards JY, Gros R, Huff MW. Naringenin prevents cholesterol-induced systemic inflammation, metabolic dysregulation, and atherosclerosis in Ldlr^{-/-} mice. *J Lipid Res.* 2013; 54:711-724.
 35. Sandeep MS, Nandini CD. Influence of quercetin, naringenin and berberine on glucose transporters and insulin signalling molecules in brain of streptozotocin-induced diabetic rats. *Biomed Pharmacother.* 2017; 94:605-611.
 36. Leon BM. Diabetes and cardiovascular disease: Epidemiology, biological mechanisms, treatment recommendations and future research. *World J Diabetes.* 2015; 6:1246.
 37. Stout RW. Diabetes and atherosclerosis. *Biomed Pharmacother.* 1993; 47:1-2.
 38. Alam MA, Kauter K, Brown L. Naringin improves diet-induced cardiovascular dysfunction and obesity in high carbohydrate, high fat diet-fed rats. *Nutrients.* 2013; 5:637-650.
 39. Schofield JD, Liu Y, Rao-Balakrishna P, Malik RA, Soran H. Diabetes dyslipidemia. *Diabetes Ther.* 2016; 7:203-219.
 40. Ahmed OM, Hassan MA, Abdel-Twab SM, Abdel Azeem MN. Navel orange peel hydroethanolic extract, naringin and naringenin have anti-diabetic potentials in type 2 diabetic rats. *Biomed Pharmacother.* 2017; 94:197-205.
 41. Yoshikawa T, Naito Y. What is oxidative stress? *Japan Med Assoc J.* 2002; 45:271-276.
 42. Annadurai T, Muralidharan AR, Joseph T, Hsu MJ, Thomas PA, Geraldine P. Antihyperglycemic and antioxidant effects of a flavanone, naringenin, in streptozotocin-nicotinamide-induced experimental diabetic rats. *J Physiol Biochem.* 2012; 68:307-318.
 43. Adela R, Nethi SK, Bagul PK, Barui AK, Mattapally S, Kuncha M, Patra CR, Reddy PN, Banerjee SK. Hyperglycaemia enhances nitric oxide production in diabetes: A study from South Indian patients. *PLoS One.* 2015; 10:1-17.
 44. Qin W, Ren B, Wang S, Liang S, He B, Shi X, Wang L, Liang J, Wu F. Apigenin and naringenin ameliorate PKC β II-associated endothelial dysfunction via regulating ROS/caspase-3 and NO pathway in endothelial cells exposed to high glucose. *Vascul Pharmacol.* 2016; 85:39-49.
 45. Wright E, Scism-Bacon JL, Glass LC. Oxidative stress in type 2 diabetes: The role of fasting and postprandial glycaemia. *Int J Clin Pract.* 2006; 60:308-314.

(Received May 23, 2019; Revised June 30, 2019; Accepted August 20, 2019)

Anti-virulence activities of biflavonoids from *Mesua ferrea* L. flower

Xiaochun Zhang¹, Rongrong Gao¹, Yan Liu¹, Yuhe Cong¹, Dongdong Zhang², Yu Zhang², Xuefei Yang^{2,*}, Chunhua Lu^{1,*}, Yuemao shen¹

¹Key Laboratory of Chemical Biology (Ministry of Education), School of Pharmaceutical Sciences, Shandong University, Jinan, Shandong, China;

²Key Laboratory of Economic Plants and Biotechnology, Kunming Institute of Botany, Chinese Academy of Sciences, Kunming, Yunnan, China.

Summary

Based on the anti-virulence activity on *Salmonella*, the ethyl acetate extract (EAE) of *Mesua ferrea* flower was investigated for its chemical constituents. Ten purified compounds were identified and assayed for their inhibitory activity against Type III secretion system (T3SS) by polyacrylamide gel electrophoresis (SDS-PAGE) and Western blots experiments. We found the biflavonoids, rhusflavanone and mesuaferrone B, exhibited inhibitory effects on the secretion of *Salmonella* pathogenicity island 1 (SPI-1) effector proteins (SipA, B, C and D) without effecting the bacterial growth. In addition, 5, 6, 6'-trihydroxy-[1,1'-biphenyl]-3,3'-dicarboxylic acid (6) is a new natural product from *M. ferrea* flower.

Keywords: *Mesua ferrea* (Roxb.) L., anti-virulence activity, biflavonoids, T3SS

1. Introduction

In the ongoing battle between people and pathogens, natural resources play an important role for saving people's life, therefore, natural medicinal plants used by ancient people are still valuable treasure to seek drugs (1). Bactericides, such as penicillin, can inhibit bacterial growth with high selection pressure and led to rapid increase in antibiotic resistance. Therefore, we need to change the idea to discover new antibiotics. An alternative idea on drug development is to inhibit bacterial virulence (including adhesion, secretion systems, or quorum sensing) (2,3), because virulence blockers inhibit pathogens by disarming the bacteria and preventing normal infection.

As we all know, *Salmonella enterica* is an

important pathogen of humans and live-stocks. The gastroenteritis, dysentery and diarrhea caused by *Salmonella* are serious problems for public health, especially in tropical regions (4). The pathogenicity of *S. enterica* mainly depends on two type three secretion systems (T3SSs), encoded by *Salmonella* pathogenicity island 1 (SPI-1) and SPI-2 (5). During infection, pathogens use the T3SS to inject effector proteins into target host cells, disrupting host defense mechanisms and allowing invasion. Therefore, to reduce virulence or inhibit specialized secretion systems are an obvious aim for us to develop drugs (6,7), and T3ss is a well-studied and attractive anti-virulence target (6).

The whole plant of *M. ferrea* is wildly used as medicinal plant in tropical Asia and India. The dried flowers are used for fever, astringent, anti-inflammation and also used in dysentery and anti-typhoid (8,9). In recent years, many bioactivities of *M. ferrea* were reported including antibacterial (8,10-13), antiarthritic (14), antioxidant and immunomodulatory (15), antispasmodic (16), estrogenic and progestational activity (17) and tyrosinase and elastase inhibitory activity (18). Our screening results on 93 Myanmar medicinal plants suggested that the flower extract of *M. ferrea* exhibited potent antibacterial and anti-T3SS activity (12). Therefore, this study was aiming

[§]These authors contributed equally to this work.

*Address correspondence to:

Dr. Xuefei Yang, Key Laboratory of Economic Plants and Biotechnology, Kunming Institute of Botany, Chinese Academy of Sciences, Kunming 650204, China.

E-mail: xuefei@mail.kib.ac.cn

Dr. Chunhua Lu, School of Pharmaceutical Sciences, Shandong University, Jinan 250012, China.

E-mail: ahua0966@sdu.edu.cn

to explore the anti-virulence active components from *M. ferrea*. The present study investigated the chemical isolation of compounds (**1-10**) from the flowers of *M. ferrea* and identified rhusflavanone (**4**) and mesuaferone B (**5**) as the chemical inhibitors of T3SS of *Salmonella*.

2. Material and Methods

2.1. General experimental procedures

The NMR spectra were obtained on a Bruker Avance DRX-400 NMR spectrometer operating at 400 MHz for ^1H and 100 MHz for ^{13}C in CD_3OD using tetramethylsilane (TMS) as an internal standard. HRESIMS were carried out on an LTQ-Orbitrap XL. Column chromatography (CC) was carried out on medium preparative liquid chromatography (MPLC) (RP-18, 40~63 μm ; Merck KGaA, Germany), Sephadex LH-20 (25-100 μm ; GE Healthcare, Sweden) and normal silica gel (200-300 mesh; Qingdao Haiyang Chemical Co. Ltd., China).

2.2. Bacterial strains and growth condition

The strain used in this study is *Salmonella enterica* serovar Typhimurium UK-1 χ 8956 (*S. Typhimurium*). The bacteria was grown on LB agar media (1% tryptone, 0.5% yeast extract, 1% NaCl, pH 7.4). *S. Typhimurium* was grown in LB broth or on LB agar plates supplemented with 0.2% L-arabinose at 37°C or 25°C with shaking at 220 rpm (19).

2.3. Plant material

The *M. ferrea* flowers were collected from the Hopong Township, Taunggyi Region, Shan State (20o47'27.47"N; 97o10'29.61"E 1115m), Myanmar, in May 2017. It was authenticated by Yu Zhang and the voucher specimen (MB201705TGY016) was deposited in Kunming Institute of Botany, Chinese Academy of Sciences.

2.4. Extraction and isolation

The *M. ferrea* flowers (1.0 kg) were dried and powdered and then extracted three times with 95% ethanol at room temperature. The ethanol extracts were combined and concentrated using a rotary evaporator, under reduced pressure at 40°C to yield a residue. Extractions were dispersed in water and extracted with petroleum ether (PE), ethyl acetate (EA) and n-butanol (Bu) respectively to result in three different crude extracts.

The active screening suggested that EA extract (EAE) and BuE exhibited anti-T3SS activity. In order to identify the anti-virulence components from *M. ferrea*, EAE was subjected to chromatography by MPLC (140

g RP-18) eluted with 30%, 50%, 70% and 100% MeOH (2 L each) to obtain 14 fractions and marked as Fr.1-14.

Fr.3 (467 mg) was further purified by MPLC (40 g RP-18 silica gel) and eluted with 10%, 15%, 20%, 25%, and 30% MeOH, 200 mL each to yield Fr.3A-3G. Fr.3C (22.5 mg) was subjected to CC over silica gel (PE:EA, 5:1, 4:1, 3:1, 2:1 and 1:1) to afford **10** (4.7 mg) and **7** (7.0 mg). Fr.3G (55.6 mg) was subjected to CC over silica gel (PE:EA, 5:1, 4:1, 3:1, 2:1 and 1:1) to afford **8** (4.4 mg). Fr.4 (399 mg) was further purified by MPLC (40g RP-18 silica gel; 10%, 20%, 25%, and 35%MeOH, 200 mL each, respectively) and further normal silica gel CC (PE:EA, 3:1, 2:1 and 1:1) to obtain **6** (7.3 mg). Fr.7 (420 mg) was subjected to MPLC over RP-18 silica gel (40 g) eluted with 40%, 45%, 50% MeOH to obtain Fr.7A-7H. Fr.7D (57.0 mg) was subjected to CC over silica gel (PE:EA, 2:1, 1:1, 1:2 and 1:3) to afford **2** (17.0 mg). Fr.7G (60.3 mg) and further purified by CC over silica gel (PE:EA, 2:1, 1:1 and EA) to afford **1** (16.7 mg). Fr.7H (50.4 mg) was purified by CC over silica gel (PE:EA, 5:1, 4:1, 3:1 and EA) to afford **3** (16.6 mg). Fr.9 (607.8 mg) was subjected to CC over Sephadex LH-20 eluted with MeOH to produce Fr.9A-E. Fr.9C (23.0 mg) was further purified by CC over silica gel (PE:EA, 2:1, 1:1, EA, MeOH) to obtain **4** (12 mg). Fr.9D (35.3 mg) was subjected to CC over silica gel (PE:EA, 10:1, 10:2, 2:1, 1:1 and EA) to afford **5** (6 mg). Fr.9E (20.1 mg) was purified by CC over silica gel (PE:EA, 2:1 and 1:1) to obtain **9** (2.1 mg, from 1:1 eluent).

According to the TLC detection, BuE showed similar behavior with EAE. HPLC detection for fractions EAE and BuE also suggested that compounds **4** and **5** are the main constituents in BuE (Figure S24, <http://www.ddtjournal.com/action/getSupplementalData.php?ID=45>), which can explain the anti-virulence activity of BuE.

2.5. Detection of secreted SPI-1-associated effector proteins

The extracts PEE, EAE and BuE together with the purified 10 compounds (**1-10**) were screened for their inhibitory effects on the secretion of the SPI-1 effector proteins of *S. Typhimurium*. Cytosporone B was used as the positive control (12,20). The 25°C overnight cultures of *S. enterica* were diluted 10 times with LB medium containing 0.2% L-arabinose and cultivated for 4 h at 37°C/220 rpm in the absence or presence of extracts (100 $\mu\text{g}/\text{mL}$) or compounds (100 μM). The supernatant of 1 mL culture was used to obtain secreted proteins. The proteins were precipitated with a final concentration of 10%TCA by repeated at 4°C and centrifuged at 12,000 g for 15 min and washed with 250 μL ice-chilled acetone. The precipitates were dried for 15 min. The pellets were dissolved with loading buffer to an optical density (OD_{600}). The protein samples were

heated to 95°C for 5-10 min to denature the proteins and then analyzed by 10% SDS-PAGE. Protein were visualized either by Coomassie blue or by Western blots.

2.6. Western blots

This procedure was the same as our previous described (12,20). *S. Typhimurium* was cultured and treated as described above. The proteins were separated by 10% SDS-PAGE and blotted onto PVDF membranes. The blotted membrane was washed with 5% w/v BSA (bovine serum albumin) in TBST (Tris-buffered

saline mixed with Tween 20) at room temperature for 1 h. Then, membranes were incubated in 5% BSA containing anti-SipC or anti-FliC monoclonal antibody overnight at 4°C and then washed with TBST (5 min, three times). The membrane was incubated for 1 h in TBST containing the secondary antibody at room temperature with shaking. Then, membranes were washed three times with TBST again. Finally, the membrane was incubated in ECLA reaction buffer (0.1 M Tris-HCl, pH 8.5, 25 mM luminol, 4 mM p-coumaric acid) and ECLB reaction buffer (0.06% v/v H₂O₂ in 0.1 M Tris-HCl, pH 8.5) for 2 min, and proteins were detected by ECL method (Molecular Imager ChemiDoc XRSt; Bio-Rad, Hercules, CA). Relative intensity of protein levels of SipC and FliC were analyzed using Image Lab Software.

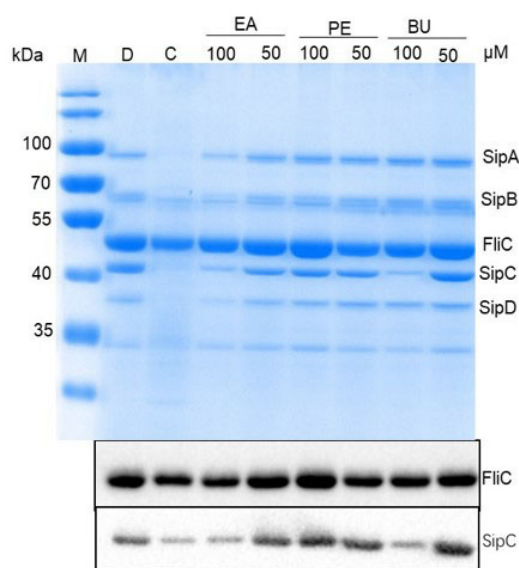


Figure 1. Extracts inhibited secretion of SPI-1 effector proteins. SipA/B/C/D, SPI-1 effector proteins; FliC, flagellar filament protein; M, marker; D, DMSO control; C, CsnB.

3. Results and Discussion

3.1. Structure elucidation of the isolated compounds

The anti-T3SS activity screening and western blot results suggested that the EAE and BuE with 100 μg/mL from *M. ferrea* flower showed evident anti-T3SS effects on the secretion of effector proteins SipA, B, C and D (Figure 1). From EAE, three flavonoids (**1-3**), two biflavonoids (**4** and **5**) and five phenolic compounds (**6-10**) (Figure 2) were obtained and their structures were identified by their ¹H, ¹³C NMR (see supporting information), HSQC, HMBC and ESIMS spectroscopic analyses and further comparing with those reported data. They were identified as kaempferol-3-O-rhamnoside (**1**) (21), quercitrin (**2**) (22), quercetin (**3**) (23,24), rhusflavanone (**4**) (25), mesuaferone B (**5**) (18,26), 5,6,6'-trihydroxy[1.1'-biphenyl]-3,3'-

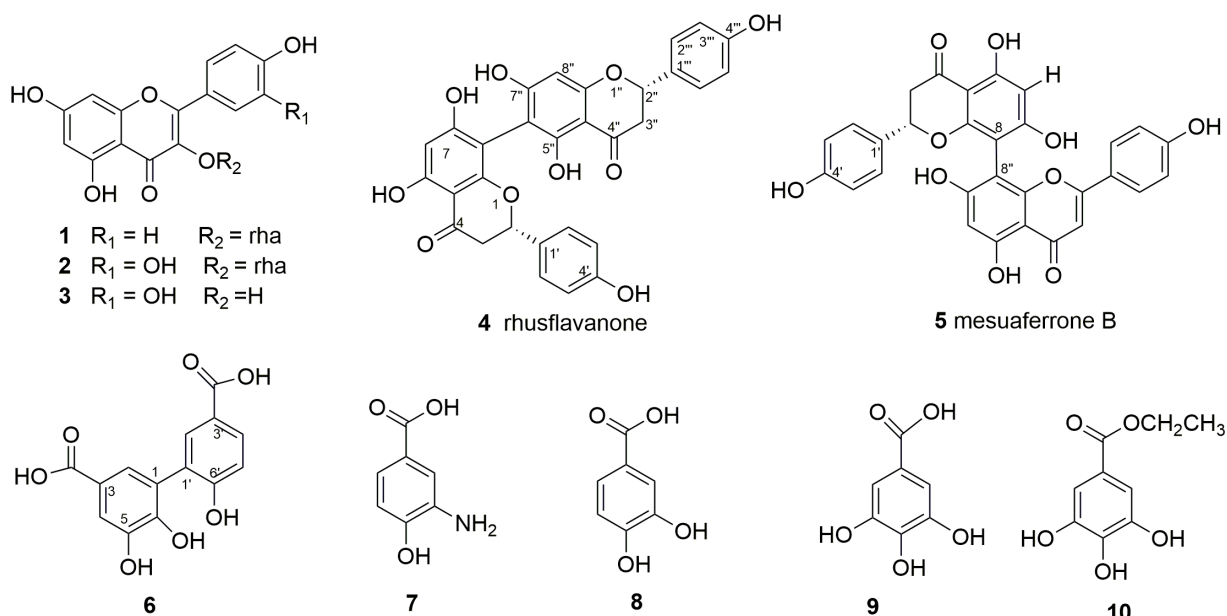


Figure 2. The chemical structures of compounds 1-10.

dicarboxylic acid (**6**), 3-amino-4-hydroxybenzoic acid (**7**) (27,28), procatechuic acid (**8**) (29,30), gallic acid (**9**) (31) and procatechuic acid ethyl ester (**10**) (32,33).

It is emphasized here that **6** was obtained as a colorless powder and it was identified as a new natural product. The molecular formula was determined to be $C_{14}H_{10}O_7$ according to the HRESIMS data of m/z 291.1571 $[M+H]^+$. 1H NMR data (400 MHz in CD_3OD): δ_H 7.51 (d, $J = 1.9$ Hz, H-2), 7.17 (d, $J = 1.8$ Hz, H-4), 7.84 (d, $J = 1.9$ Hz, H-2'), 7.49 (dd, $J = 8.2$, 1.8 Hz, H-4'), 6.87 (d, $J = 8.2$ Hz, H-5'); ^{13}C NMR data (100 MHz in CD_3OD): δ_C : 133.6s (C-1), 112.4d (C-2), 112.1s (C-3), 111.6d (C-4), 146.5s (C-5), 142.1s (C-6), 170.9s (C-7), 133.2s (C-1'), 118.8d (C-2'), 123.4s (C-3'), 124.7d (C-4'), 115.6d (C-5'), 153.4s (C-6'), 170.9s (C-8).

3.2. Rhusflavanone and Mesuaferone B inhibited the secretion of SPI-1 effector proteins

The inhibitory effects on secretion of pathogenicity island-1 (SPI-1)-associated effector proteins on *Salmonella in vitro* were investigated for compounds

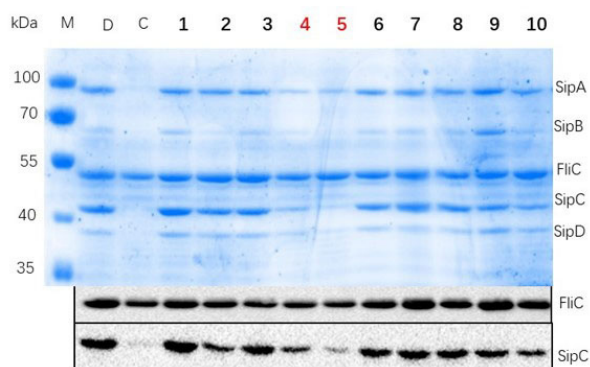


Figure 3. Compounds inhibited secretion of SPI-1 effector proteins. SipA/B/C/D, SPI-1 effector proteins; FliC, flagellar filament protein; M, marker; D, DMSO control; C, CsnB.

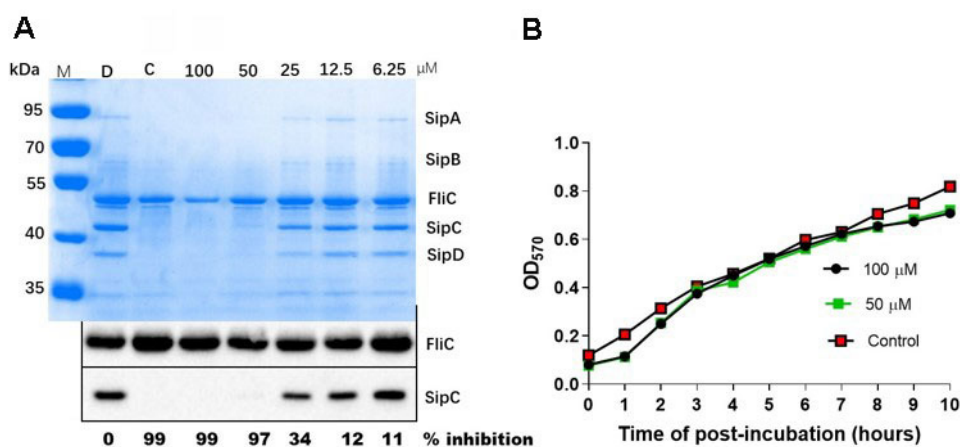


Figure 4. Mesuaferone B (5) inhibited the secretion of SPI-1 effectors in a dose-dependent manner and did not affect growth of *S. Typhimurium*. A) Mesuaferone B inhibited secretion of SPI-1 effector proteins at a range of concentrations from 6.25 to 100 μM detected by SDS-PAGE followed by Coomassie blue staining or Western blotting. M, marker; C, DMSO control. Inhibition percentage was calculated by comparing the SipC blot with that of the DMSO control. B) Mesuaferone B did not inhibit the bacterial growth at a range of concentrations at 50 and 100 μM .

1-10. We found that rhusflavanone (**4**) and mesuaferone B (**5**) exhibited inhibitory effects on the secretion of the T3SS effectors SipA, B, C and D without effecting on FliC (Figure 3). Mesuaferone B can inhibit the secretion of effector proteins in a dose dependent manner (Figure 4a) and no effect on the growth of *Salmonella* (Figure 4b). Therefore, mesuaferone B from *M. ferrea* may be an inhibitor of T3SS of *Salmonella*.

In conclusion, rhusflavanone and mesuaferone B are the anti-virulence components from *M. ferrea* with inhibitory activity on the secretion of effector proteins on *Salmonella*. Although, some researches have reported the diverse activity of biflavonoids (18,25,34,35), no anti-virulence activity has not been reported. Our results provide promising baseline information for the potential use of *M. ferrea* in the treatment of bacterial infections through anti-virulence pathway.

Acknowledgements

This work was supported by the Program for Changjiang Scholars and Innovative Research Team in University (IRT_17R68) and the Southeast Asia Biodiversity Research Institute, Chinese Academy of Sciences (2015CASEABRIRG001). The authors are very grateful to Ms. Yunn Mi Mi Kyaw and Yao Fu, Kunming Institute of Botany, Chinese Academy of Sciences for providing the pictures of *M. ferrea* growing in Myanmar.

References

1. Rasko DA, Sperandio V. Anti-virulence strategies to combat bacteria-mediated disease. *Nat Rev Drug Discov.* 2010; 9:117-128.
2. Heras B, Scanlon MJ, Martin JL. Targeting virulence not

- viability in the search for future antibacterials. *Br J Clin Pharmacol.* 2014; 79:208-215.
3. Duncan MC, Linington RG, Auerbuch V. Chemical inhibitors of the type three secretion system: Disarming bacterial pathogens. *Antimicrob Agents Chemother.* 2012; 56:5433-5441.
 4. Beyrer C, Suwanvanichkij V, Mullany LC, Richards AK, Franck N, Samuels A, Lee TJ. Responding to AIDS, tuberculosis, malaria, and emerging infectious diseases in Burma: Dilemmas of policy and practice. *Plos Med.* 2006; 3:e393.
 5. Lam O, Wheeler J, Tang CM. Thermal control of virulence factors in bacteria: A hot topic. *Virulence.* 2014; 5:852-862.
 6. McShan AC, De Guzman RN. The bacterial type III secretion system as a target for developing new antibiotics. *Chem Biol Drug Des.* 2015; 85:30-42.
 7. Zambelloni R, Connolly JPR, Huerta Uribe A, Burgess K, Marquez R, Roe AJ. Novel compounds targeting the enterohemorrhagic *Escherichia coli* type three secretion system reveal insights into mechanisms of secretion inhibition. *Mol Microbiol.* 2017; 105:606-619.
 8. Mazumder R, Dastidar SG, Basu SP, Mazumder A. Effect of *Mesua ferrea* Linn. flower extract on *Salmonella*. *Indian J Exp Biol.* 2005; 43:566-568.
 9. DeFilipps RA, Krupnick GA. The medicinal plants of Myanmar. *PhytoKeys.* 2018; 102:1-341.
 10. Verotta L, Lovaglio E, Vidari G, Finzi PV, Neri MG, Raimondi A, Parapini S, Taramelli D, Riva A, Bombardelli E. 4-Alkyl- and 4-phenylcoumarins from *Mesua ferrea* as promising multidrug resistant antibacterials. *Phytochemistry.* 2004; 65:2867-2879.
 11. Mazumder R, Dastidar SG, Basu SP, Mazumder A, Singh SK. Antibacterial potentiality of *Mesua ferrea* Linn. flowers. *Phytother Res.* 2004; 18:824-826.
 12. Li T, Zhang D, Oo TN, San MM, Mon AM, Hein PP, Wang Y, Lu C, Yang X. Investigation on the antibacterial and anti-T3SS activity of traditional Myanmar medicinal plants. *Evid Based Complement Alternat Med.* 2018; 2018:2812908.
 13. Mazumder R, Dastidar SG, Basu SP, Mazumder A, Kumar S. Emergence of *Mesua ferrea* Linn. leaf extract as a potent bactericide. *Anc Sci Life.* 2003; 22:160-165.
 14. Jalalpure SS, Mandavkar YD, Khalure PR, Shinde GS, Shelar PA, Shah AS. Antiarthritic activity of various extracts of *Mesua ferrea* Linn. seed. *J Ethnopharmacol.* 2011; 138:700-704.
 15. Chahar MK, Sanjaya Kumar DS, Lokesh T, Manohara KP. *In-vivo* antioxidant and immunomodulatory activity of mesuol isolated from *Mesua ferrea* L. seed oil. *Int Immunopharmacol.* 2012; 13:386-391.
 16. Prasad DN, Basu SP, Srivastava AK. Antispasmodic activity of the crude and purified oil of *Mesua ferrea* seed. *Anc Sci Life.* 1999; 19:74-75.
 17. Meherji PK, Shetye TA, Munshi SR, Vaidya RA, Antarkar DS, Koppikar S, Devi PK. Screening of *Mesua ferrea* (Nagkesar) for estrogenic and progestational activity in human and experimental models. *Indian J Exp Biol.* 1978; 16:932-933.
 18. Zar Wynn Myint K, Kido T, Kusakari K, Prasad Devkota H, Kawahara T, Watanabe T. Rhusflavanone and mesuaferrone B: Tyrosinase and elastase inhibitory biflavonoids extracted from the stamens of *Mesua ferrea* L. *Nat Prod Res.* 2019:1-5.
 19. Curtiss R, 3rd, Wanda SY, Gunn BM, Zhang X, Tinge SA, Ananthnarayan V, Mo H, Wang S, Kong W. *Salmonella enterica* serovar typhimurium strains with regulated delayed attenuation *in vivo*. *Infect Immun.* 2009; 77:1071-1082.
 20. Li J, Lv C, Sun W, Li Z, Han X, Li Y, Shen Y. Cytosporone B, an inhibitor of the type III secretion system of *Salmonella enterica* serovar Typhimurium. *Antimicrob Agents Chemother.* 2013; 57:2191-2198.
 21. Tatsimo NJ, Tane P, Csupor D, Forgo P, Hohmann J. Kaempferol rhamnositides from *Bryophyllum pinnatum*, a medicinal plant used against infectious diseases and as analgesic in Mbouda, Cameroon. *Planta Med.* 2010; 76:1302-1303.
 22. Hasan A, Ahmed I, Jay M, Voirin B. Flavonoid glycosides and an anthraquinone from *Rumex chalepensis*. *Phytochemistry.* 1995; 39:1211-1213.
 23. Olejniczak S, Potrzebowski MJ. Solid state NMR studies and density functional theory (DFT) calculations of conformers of quercetin. *Org Biomol Chem.* 2004; 2:2315-2322.
 24. Wawer I, Zielinska A. ¹³C-CP-MAS-NMR studies of flavonoids. I. Solid-state conformation of quercetin, quercetin 5'-sulphonic acid and some simple polyphenols. *Solid State Nucl Magn Reson.* 1997; 10:33-38.
 25. Lin YM, Chen FC, Lee KH. Hinokiflavone, a cytotoxic principle from *Rhus succedanea* and the cytotoxicity of the related biflavonoids. *Planta Med.* 1989; 55:166-168.
 26. Shrestha S, Park JH, Lee DY, Cho JG, Cho S, Yang HJ, Yong HI, Yoon MS, Han DS, Baek NI. *Rhus parviflora* and its biflavonoid constituent, rhusflavone, induce sleep through the positive allosteric modulation of GABA(A)-benzodiazepine receptors. *J Ethnopharmacol.* 2012; 142:213-220.
 27. Kawaguchi H, Sasaki K, Uematsu K, Tsuge Y, Teramura H, Okai N, Nakamura-Tsuruta S, Katsuyama Y, Sugai Y, Ohnishi Y, Hirano K, Sazuka T, Ogino C, Kondo A. 3-Amino-4-hydroxybenzoic acid production from sweet sorghum juice by recombinant *Corynebacterium glutamicum*. *Bioresour Technol.* 2015; 198:410-417.
 28. Bertasso M, Holzenkämpfer M, Zeeck A, Dall'Antonia F, Fiedler HP. Bagremycin A and B, novel antibiotics from *Streptomyces* sp. Tu 4128. *J Antibiot (Tokyo).* 2001; 54:730-736.
 29. Nguyen DM, Seo DJ, Kim KY, Park RD, Kim DH, Han YS, Kim TH, Jung WJ. Nematicidal activity of 3,4-dihydroxybenzoic acid purified from *Terminalia nigrovenulosa* bark against *Meloidogyne incognita*. *Microb Pathog.* 2013; 59-60:52-59.
 30. Cha JW, Piao MJ, Kim KC, Zheng J, Yao CW, Hyun CL, Kang HK, Yoo ES, Koh YS, Lee NH, Ko MH, Hyun JW. Protective effect of 3,4-dihydroxybenzoic acid isolated from *Cladophora wrightiana* Harvey against ultraviolet B radiation-induced cell damage in human HaCaT keratinocytes. *Appl Biochem Biotechnol.* 2014; 172:2582-2592.
 31. Boyd L, Beveridge EG. Antimicrobial activity of some alkyl esters of gallic acid (3,4,5-trihydroxybenzoic acid) against *Escherichia coli* NCTC 5933 with particular reference to n-propyl gallate. *Microbios.* 1981; 30:73-85.
 32. Tun NL, Hu DB, Xia MY, Zhang DD, Yang J, Oo TN, Wang YH, Yang XF. Chemical constituents from ethanolic extracts of the aerial parts of *Leea aequata* L., a traditional folk medicine of Myanmar. *Nat Prod Bioprospect.* 2019; 9:243-249.
 33. Yang JB, Ji TF, Wang AG, Su YL. Studies on chemical

- constituents from *Davidia involucrata* var. *vilmoriniana*. *Zhongguo Zhong Yao Za Zhi*. 2008; 33:777-779. (in Chinese)
34. Lin YM, Flavin MT, Schure R, Chen FC, Sidwell R, Barnard DL, Huffiman JH, Kern ER. Antiviral activities of biflavonoids. *Planta Med*. 1999; 65:120-125.
35. Lin YM, Anderson H, Flavin MT, Pai YH, Mata-
Greenwood E, Pengsuparp T, Pezzuto JM, Schinazi RF, Hughes SH, Chen FC. *In vitro* anti-HIV activity of biflavonoids isolated from *Rhus succedanea* and *Garcinia multiflora*. *J Nat Prod*. 1997; 60:884-888.
- (Received July 29, 2019; Revised August 13, 2019; Accepted August 21, 2019)

Neurovascular compression syndrome of the brain stem with opsoclonus-myoclonus syndrome combined with vestibular paroxysmia and autonomic symptoms

Yusuke Morinaga*, Kouhei Nii, Kimiya Sakamoto, Ritsurou Inoue, Takafumi Mitsutake, Hayatsura Hanada

Department of Neurosurgery, Fukuoka University Chikushi Hospital, Chikushino-city, Fukuoka, Japan.

Summary

We describe a rare case of neurovascular compression syndrome (NVCS) of the brain stem and opsoclonus-myoclonus syndrome (OMS) complicated with vestibular paroxysmia (VP) and autonomic symptoms. Moreover, we discuss the case with respect to the available information in medical literature. A 36-year-old man with vertigo and nausea had difficulty standing, and was transported by an ambulance to our hospital. He had VP, opsoclonus, cervical myoclonus, anxiety, and restless legs syndrome. Magnetic resonance imaging at hospitalization showed that the dolichoectatic vertebral artery was in contact with the postero-lateral side of the pontomedullary junction. He was diagnosed with NVCS of the brain stem (most likely of the input to the vestibular nucleus) associated with contact with the dolichoectatic vertebral artery. Combination therapy using multiple antiepileptic drugs, such as low-dose carbamazepine, clonazepam, and lacosamide, improved his clinical symptoms. He was finally able to walk and was discharged on day 42 after admission. He is being routinely followed-up since then. Further research is needed to confirm the validity of the combination therapy.

Keywords: Neurovascular compression syndrome, brainstem, opsoclonus myoclonus syndrome, vestibular paroxysmia, autonomic symptoms

1. Introduction

Opsoclonus-myoclonus syndrome (OMS) (1-3) is a rare disease with opsoclonus, cerebellar ataxia, and myoclonus of the trunk, limbs, and neck as the primary symptoms. The probable underlying etiologies eliciting the symptoms include viral encephalitis, malignant tumors, metabolic disorders, and degenerative diseases. Particularly, OMS as paraneoplastic nerve syndrome (PNS), wherein, various neurological symptoms manifest because of the "remote effect" of malignant tumors, is an important etiology. Neuroblastoma is present in about half of the children diagnosed with OMS, and in adults, OMS can be seen as a complication of lung cancer, breast cancer, and ovarian cancer.

While, vestibular paroxysmia (VP) may manifest when arteries in the cerebellar pontine angle cause a segmental, pressure-induced dysfunction of the eighth nerve. There are some case reports of neurovascular compression syndrome (NVCS) presenting with VP (4-7). We encountered a rare case of NVCS of the brainstem complicated with vestibular paroxysmia (VP) and autonomic symptoms combined with OMS. Here, we present the clinical course of the disease and report the findings in light of the existing scientific literature.

2. Case Report

A 36-year-old man with no remarkable medical history and chief complaints of vertigo and nausea, visited an ophthalmologist. Magnetic resonance imaging (MRI) showed no abnormality, and he was prescribed betahistine, kallidinogenase, adenosine triphosphate disodium hydrate granules, and alprazolam for the aforementioned symptoms. A few days later, his vertigo progressed and he was unable to walk, and

*Address correspondence to:

Dr. Yusuke Morinaga, Department of Neurosurgery and Neuroscience, Fukuoka University Chikushi Hospital, 1-1-1 Zokumyoin, Chikushino-shi, Fukuoka Prefecture 818-8502, Japan.

E-mail: yu_the_morio@yahoo.co.jp

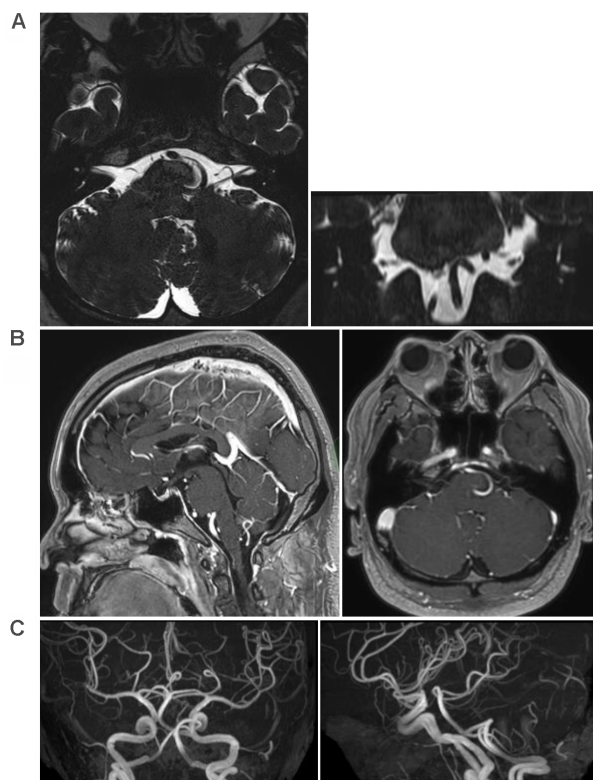


Figure 1. Head magnetic resonance images at hospitalization. A. Magnetic resonance imaging (MRI) - Constructive Interference Steady State at hospitalization shows that the dolichoectatic vertebral artery is in contact with the posterior lateral side of the pontomedullary junction (left, axial view; right, coronal view). B. Gadolinium-T1-weighted MRI at hospitalization shows no tumor and findings similar to Figure 1A. C. MR angiography at hospitalization shows the dolichoectatic vertebral artery.

was transported to our hospital by an ambulance. At hospitalization, he had clear consciousness, blood pressure was 110/62 mmHg, and body temperature was 36.2°C. He had vertigo and nausea, but without facial nerve palsy and tinnitus. He showed no decline in hearing or hearing sensitivity, no sense of ear obstruction, and no difference in hearing ability. Spontaneous nystagmus at rest was noted (horizontal nystagmus was omnidirectional, with biphasic horizontal nystagmus at bilateral lateral gaze, horizontal rotational nystagmus at upward gaze, and swaying omnidirectional saccadic abnormal eye movement during eye-opening in the dark [opsoclonus]). Marked trunk ataxia was found with no quadrupeds. He was unable to sit or stand. He had no other obvious neurological deficits. Momentary involuntary movements of the neck and shoulders (cervical myoclonus) were found. He also had myoclonus, restless leg syndrome, erectile dysfunction. Blood tests showed no abnormal findings (such as tumor markers) other than an LDL level of 182 mg/dL.

There were no remarkable findings in the auditory brainstem response. MRI at hospitalization indicated contact of the left vertebral artery (VA) with the dorso-

lateral area of the ponto-medullary junction (Figures 1A and 1B). A marked bending or meandering of the vertebral artery was observed (Figure 1C). Chest-pelvic computed tomography showed no neoplastic lesion.

Based on the presented symptoms and imaging findings at admission, we suspected OMS and VP associated with NVCS caused by the left VA compressing the brainstem. Based on this initial diagnosis, the patient was administered carbamazepine (CBZ) 400 mg/day from day 1. Although the OMS and VP persisted, the seizure frequency decreased marginally. On day 2, rosuvastatin 5 mg and brotizolam 0.25 mg (oral) were started for managing the dyslipidemia and insomnia, respectively. Etizolam 1.5 mg/day was started on day 10. Lacosamide (LCM) 100 mg/day was started on day 12 which was subsequently increased to 200 mg/day on day 19. When the frequency of the OMS symptoms and VP decreased, clonazepam (CZP) (1.5 mg/day) was introduced to treat the restless leg syndrome. Erectile dysfunction, insomnia, and restless legs syndrome alleviated and the patient was able to walk, and was discharged on day 42. At 12 months post discharge, his OMS occasionally presented as seizures when talking with others. He continued all the previously mentioned prescription drugs except for etizolam and brotizolam because the mental symptoms, such as insomnia and anxiety, disappeared. He has since been in the outpatient follow-up.

Written informed consent was obtained from the patient for the publication of this case report and accompanying images, and the study design was approved by the appropriate ethics review board.

3. Discussion

To the best of our knowledge, although there have been reports of "spino-bulbo-spinal like" reflex because of the pressure of the dolichoectatic VA on the lower brainstem (4), this is the first reported case of OMS with VP and autonomic symptoms combined with NVCS of the brainstem. The main symptoms of VP (5-10) usually lasts for less than one minute and occur more than 30 times a day. Spontaneous or non-rotatable vertigo attacks occur spontaneously and repeatedly over a short period. VP is often caused by direct pulsatile compression of the eighth cranial nerve by an artery at the cerebello-pontine angle.

Neurovascular compression of the eighth cranial nerve is observed in more than 95% of cases presenting VP after MRI. Particularly, the involvement of the anterior inferior cerebellar artery loop is the highest, followed by the posterior inferior cerebellar artery, vertebral artery (VA), or veins. Treatment strategies involve administration of low-dose carbamazepine (200-600 mg/day) or oxcarbazepine (300-900 mg/day), which is equally effective in children. Additionally, lamotrigine, phenytoin, gabapentin, topiramate,

baclofen, and other non-antiepileptic drugs used for trigeminal neuralgia are recommended. However, randomized, placebo-controlled trials are currently in progress, and till date, there is no established treatment. Microvascular decompression of the eighth cranial nerve is especially applicable in cases of intractable drug resistance and non-vascular compression of the eighth cranial nerve due to tumors or cysts. Important differential diagnoses include Meniere's disease, vestibular migraine, benign paroxysmal position vertigo, epileptic vestibular seizures, paroxysmal brainstem attacks (with multiple sclerosis or stroke), nasopharyngeal hiatus, perilymphatic fistula, transient ischemic attack, and panic attack. In our case, 1) The VA was in contact with the dorsolateral surface of the ponto-medullary junction. 2) The patient presented movement disorders such as spontaneous opsoclonus, VP, ataxia, cervical myoclonus, and restless leg syndrome. 3) Moreover, the patient presented autonomic nervous system symptoms and mental symptoms, such as anxiety attack, erectile dysfunction, and insomnia, after the manifestation of the motor symptoms described previously. 4) Antiepileptic drugs targeting the sodium channels (sodium channel blockers), such as low dose CBZ and LCM, were effective. Based on the above characteristics, it is possible that NVCS in the lower brainstem, centering on the vestibular nucleus caused OMS, VP, and autonomic nervous symptoms as output system symptoms involving the vestibular nucleus.

The vestibular nucleus (11) is a nucleus where the primary afferent nerves of the vestibular neurons, derived from the vestibular organ, terminate. In addition to the primary afferent nerve, inputs from the contralateral vestibular nucleus, cerebellar cortex, cerebellar nucleus, hypoglossal nucleus, Cajal stromal nucleus, spinal cord, vestibular area of the cerebral cortex, and brainstem reticular system are also found. The targets include the motor nucleus of the extraocular muscle (artculus nucleus, trochlear nucleus, abduction nucleus) and thalamus. Additionally, nerve fiber connections in the autonomic nervous system nuclei are found. Therefore, the vestibular nucleus is more than a sensory primary relay nucleus, and transmits input from the peripheral vestibule to the center. It also receives various inputs and relays it to various parts of the central nerve and is deeply involved with motor functions, such as eye movement and maintaining the balance of the body, as well as autonomic system functions (Figure 2).

The characteristics of the neural circuit involved in the vestibular nucleus can account for all the clinical symptoms observed in our patient. We considered that the OMS was not associated with PNS because the myoclonus in the OMS was confined to the neck and shoulders, and findings suggestive of a malignant tumor were inconclusive.

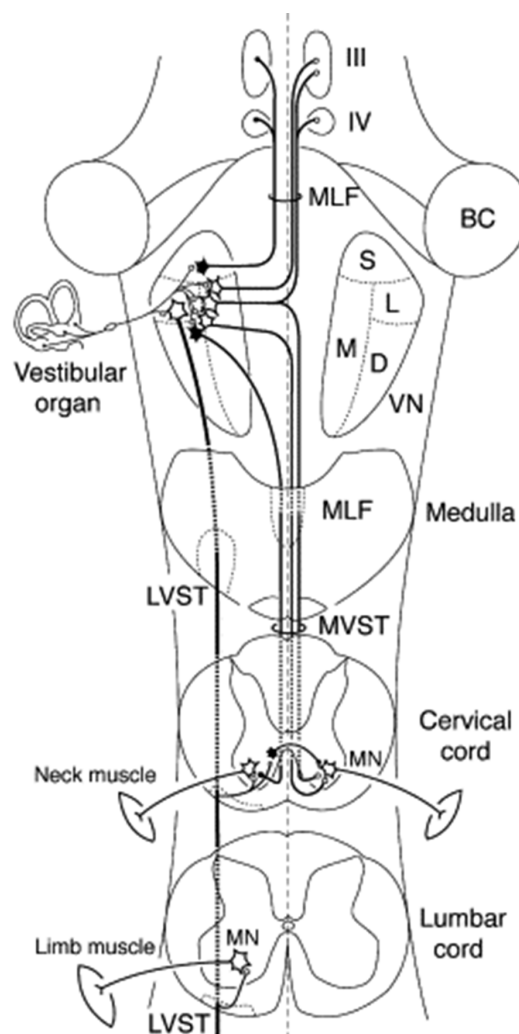


Figure 2. Neural network of the vestibular nucleus. The figure, revised partially from Shinoda *et al.* (11), shows the neural network of the vestibular nucleus.

Therapeutically, low dose CBZ alone did not significantly reduce seizure frequency; therefore, we added LCM, a novel sodium channel blocker, and CZP, a drug for myoclonus, restless legs syndrome, and erectile dysfunction. VP and autonomic symptoms were thought to have improved significantly. Careful follow-up will be continued in the future.

In conclusion, we report a rare case of NVCS of the brainstem (most likely of the input to the vestibular nucleus) with VP and autonomic symptoms combined with OMS. Low dose CBZ, LCM, and CZP combined therapy contributed to the marked decrease of seizure frequency.

Acknowledgements

We would like to thank Editage (www.editage.com) for English language editing. This study did not receive any grants from funding agencies in the public, commercial, or not-for-profit sectors.

References

1. Honnorat J. New findings in adult opsoclonus-myoclonus syndrome. *JAMA Neurol.* 2016; 73:381-382.
2. Hsu SY, Young YH. Opsoclonus-myoclonus syndrome-reply. *JAMA Otolaryngol Head Neck Surg.* 2018; 144:388.
3. Kim DD, Budhram A. Opsoclonus-myoclonus syndrome-additional clinical considerations. *JAMA Otolaryngol Head Neck Surg.* 2018; 144:387-388.
4. Merchant SH, Vial F, Leodori G, Fahn S, Pullman SL, Hallet M. A novel exaggerated "spino-bulbo-spinal like" reflex of lower brainstem origin. *Parkinsonism Relat Disord.* 2018; 18:30435-30438.
5. Brandt T, Dieterich M. Vestibular paroxysmia: Vascular compression of the eighth nerve? *Lancet.* 1994; 343:798-799.
6. Brandt T, Strupp M, Dieterich M. Vestibular paroxysmia: A treatable neurovascular cross-compression syndrome. *J Neurol.* 2016; 263:S90-96.
7. Hufner K, Barresi D, Glaser M, Linn J, Adrion C. Vestibular paroxysmia: Diagnostic features and medical treatment. *Neurology.* 2008; 71:1006-1014.
8. Lawden MC, Bronstein AM, Kennard C. Repetitive paroxysmal nystagmus and vertigo. *Neurology.* 1995; 45:276-280.
9. Strupp M, Lopez-Escamez JA, Kim JS, Straumann D, Jen JC, Carey J, Bisdorff A, Brandt T. Vestibular paroxysmia: Diagnostic criteria. *J Vestib Res.* 2016; 26:409-415.
10. Strupp M, von Stuckrad-Barre S, Brandt T, Tonn JC. Teaching neuroimages: Compression of the eighth cranial nerve causes vestibular paroxysmia. *Neurology.* 2013; 80:77.
11. Shinoda Y, Sugiuchi Y, Izawa Y, Hata Y. Long descending motor tract axons and their control of neck and axial muscles. *Prog Brain Res.* 2006; 151:527-563.

(Received May 30, 2019; Revised August 13, 2019; Accepted August 22, 2019)

A case of drug-induced hypersensitivity syndrome induced by salazosulfapyridine combined with SIADH caused by interstitial pneumonia

Yusuke Morinaga^{1,*}, Ichiro Abe², Tomohiro Minamikawa³, Yusuke Ueda⁴, Kouhei Nii¹, Kimiya Sakamoto¹, Ritsurou Inoue¹, Takafumi Mitsutake¹, Hayatsura Hanada¹, Jun Tsugawa^{5,6}, Kanako Kurihara^{5,6}, Toshio Higashi^{1,6}

¹Department of Neurosurgery, Fukuoka University Chikushi Hospital, Chikushino-city, Fukuoka, Japan;

²Department of Endocrinology and Diabetes Mellitus, Fukuoka University Chikushi Hospital, Chikushino City, Fukuoka, Japan;

³Department of Orthopedics, Fukuoka University Chikushi Hospital, Chikushino City, Fukuoka, Japan;

⁴Department of Respiratory Medicine, Fukuoka University Chikushi Hospital, Chikushino City, Fukuoka, Japan;

⁵Department of Neurology, Fukuoka University Chikushi Hospital, Chikushino-city, Fukuoka, Japan;

⁶Stroke Center, Fukuoka University Chikushi Hospital, Chikushino-city, Fukuoka, Japan.

Summary

We present a case of a patient with drug-induced hypersensitivity syndrome (DIHS) caused by salazosulfapyridine combined with syndrome of inappropriate secretion of antidiuretic hormone (SIADH) caused by interstitial pneumonia (IP). A 67-year-old man with a past history of rheumatism (RA) presented with right hemiparalysis and aphasia as the chief complaints. A diagnosis of left embolic cerebral infarction following trial therapy for RA based on computed tomography findings was made, and external decompression was performed. Salazosulfapyridine was newly started on day 7. Dabigatran was started on day 37. On day 41, the patient developed fever. On day 42, edema and erythema appeared on his face, and erythema and rash appeared on his trunk and extremities, with gradual transition to erythroderma. The drug eruption was initially attributed to the dabigatran. Various symptoms of organ dysfunction (enteritis, myocarditis, interstitial pneumonia, hepatic disorder, stomatitis, and others) then appeared and persisted; hence, a diagnosis of DIHS associated with human herpes virus 6 and cytomegalovirus infection induced by salazosulfapyridine was suggested, and the oral administration of salazosulfapyridine was discontinued on day 53. Hyponatremia was observed in association with exacerbation of IP. Due to low serum osmotic pressure and prompt improvement of the serum sodium level by fluid restriction, the SIADH was attributed to IP. In this case, steroid pulse therapy followed by gradual decrease therapy prevented worsening of the condition.

Keywords: Drug-induced hypersensitivity syndrome, salazosulfapyridine, SIADH, interstitial pneumonia, cytomegalovirus

1. Introduction

Drug-induced hypersensitivity syndrome (DIHS) is an adverse reaction accompanied by fever, rashes, and visceral lesions. DIHS is caused by specific drugs

such as carbamazepine, phenytoin, phenobarbital, zonisamide, allopurinol, salazosulfapyridine, diaphenylsulfone, and mexiletine. The relationship between DIHS and human herpes virus 6 (HHV-6) reactivation is well-known. Symptoms such as fever and hepatitis are closely related to HHV-6 reactivation (1). The combined effect of the immunological response to a drug and the reactivation of HHV-6 can cause severe DIHS (2). If the symptoms of DIHS persist, it is necessary to suspect the involvement of cytomegalovirus reactivation (1). In this report, we

*Address correspondence to:

Dr. Yusuke Morinaga, Department of Neurosurgery, Fukuoka University Chikushi Hospital, 1-1-1 Zokumyoin, Chikushino-city, Fukuoka Prefecture, 818-8502, Japan.

E-mail: yu_the_morio@yahoo.co.jp

present the extremely rare case of a patient with DIHS associated with HHV-6 and cytomegalovirus infection induced by sulfasalazine combined with syndrome of inappropriate secretion of antidiuretic hormone (SIADH) caused by interstitial pneumonia (IP).

2. Case Report

A 67-year-old male patient with a past history of rheumatism (RA), hypertension, and subarachnoid hemorrhage presented to a health facility with right hemiparesis and aphasia as the chief complaints and was subsequently transferred to our hospital. A diagnosis of left embolic cerebral infarction that occurred during a trial for RA was made. His level consciousness as assessed by the Japan Coma Scale was I-3. Blood pressure was 147/88 mmHg and body temperature was 36.0°C. Left upper limb paralysis and left joint deviation were observed at admission.

Laboratory and radiological investigations were conducted, and the results were as follows. Blood count: white blood cells, $6.1 \times 10^3/\mu\text{L}$; red blood cells, $495 \times 10^4/\mu\text{L}$; hemoglobin, 15.6 g/dL; hematocrit, 46.7%; platelets, $25.2 \times 10^4/\mu\text{L}$; biochemistry: Na, 143 mmol/L; K, 4.4 mmol/L; Cl, 104 mmol/L; hemoglobin A1C, 6.0%; low-density lipoprotein, 156 mg/dL; C-reactive protein, 0.02 mg/dL; coagulation: D-dimer less than 0.3 $\mu\text{g/mL}$. The electrocardiography showed a heart rate of 72 beats per min and no abnormal findings. Magnetic resonance imaging of the head at admission (Figures 1A, B) showed extensive embolic cerebral infarction in the vessel-dominated region of the left middle cerebral artery.

On day 1, external decompression was done to relieve cerebral herniation caused by the cerebral infarction. On day 2, we began a course of levetiracetam at a dose of 1,000 mg/day to prevent convulsions. Based on the history of RA, on day 7, salazosulfapyridine was administered at a dose of 500 mg/day and increased

after 7 days (*i.e.*, on day 14) to 1,000 mg/day. The postoperative computed tomography (CT) following cranioplasty showed no increase in hemorrhagic infarction.

On day 37, dabigatran 300 mg/day was started to prevent the recurrence of cerebral infarction. On day 41, the patient developed fever. The following day (day 42), edema and erythema appeared on his face (Figure 2A), and erythema and rash also appeared on his trunk and extremities (Figure 2B). Due to the gradual onset of erythroderma, topical application of diphenhydramine and oral administration of fexofenadine hydrochloride at a dose of 120 mg/day was started.

The CT performed on day 43 showed inflammatory findings in the ileocecal area (Figure 3A) and a mild nodule shadow at the lower right lung (Figure 3B). We suspected that the drug eruption was caused by the dabigatran, and the oral administration of dabigatran was then stopped. On day 45, the patient developed diarrhea and was started on clostridium butyricum at a dose of 6 g/day. On day 50, his respiratory function deteriorated (saturation of percutaneous oxygen, SpO₂ 90%) and oxygen was administered. On day 51, a drug lymphocyte stimulation test was performed for levetiracetam and dabigatran. Both results were negative. Due to further deterioration of his respiratory function on day 53 (saturation of percutaneous oxygen, SpO₂ 80%), the oral administration of salazosulfapyridine was discontinued. A steroid pulse of methylprednisolone at a dose of 1 g/day for a period of 3 days was administered to prevent exacerbation of the IP (Figures 4A and 4B). Following this, the dose of methylprednisolone was reduced to 40 mg/day. Given the possibility of steroidogenic glucose tolerance abnormality, concurrent insulin therapy was administered in combination with methylprednisolone. Cardiac ultrasound examination performed on day 55 showed a pericardial effusion with normal wall motion. The CT performed on day 59 showed that the IP had

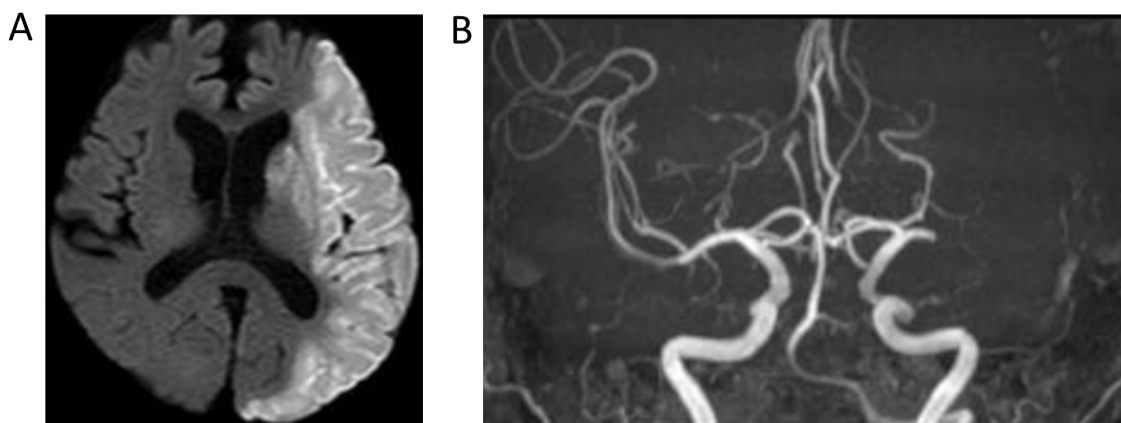


Figure 1. (A) Diffusion weighted image at hospitalization shows acute cerebral infarction consistent with the vessel dominant region of the left middle cerebral artery (left). (B) Magnetic resonance angiography at hospitalization shows the left middle cerebral artery occlusion (right).

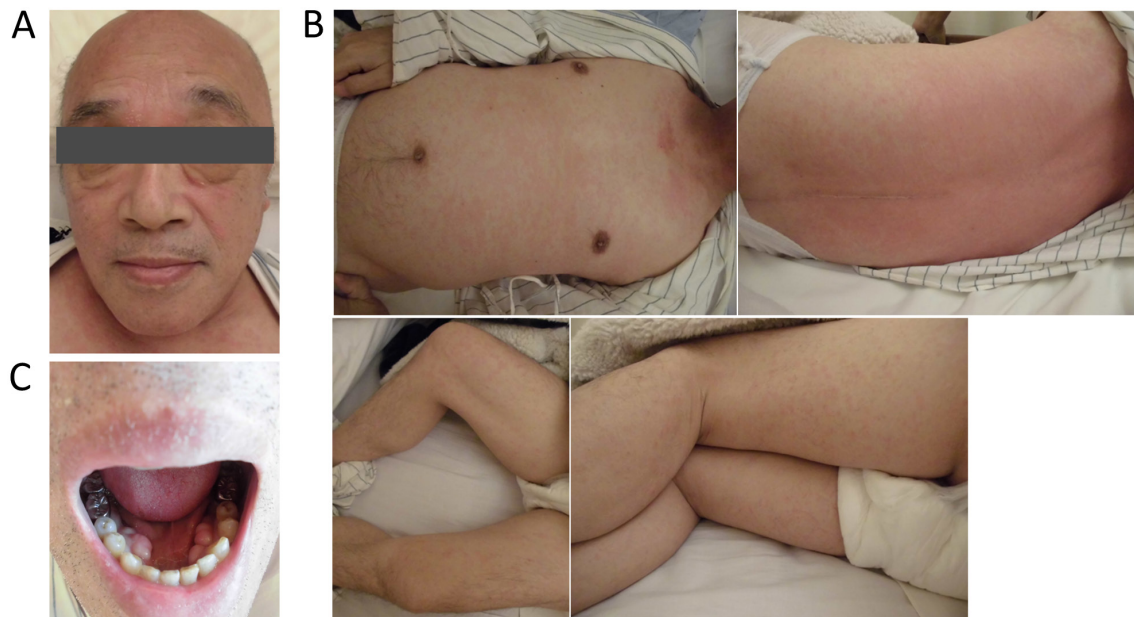


Figure 2. (A) The photograph shows edema and erythema on the patient's face on day 42. (B) The photographs show erythema and rash on the trunk and extremities on day 42. (C)...

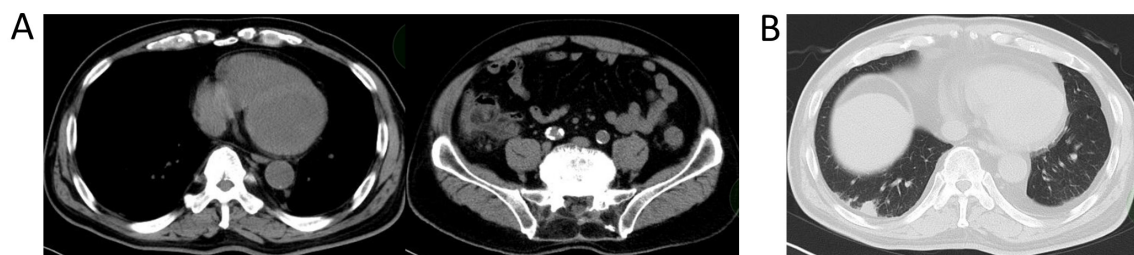


Figure 3. (A) The computed tomography (CT) performed on day 43 shows inflammatory findings in the ileocecal area. (B) The CT performed on day 43 shows mild nodule shadow at the lower right lung.

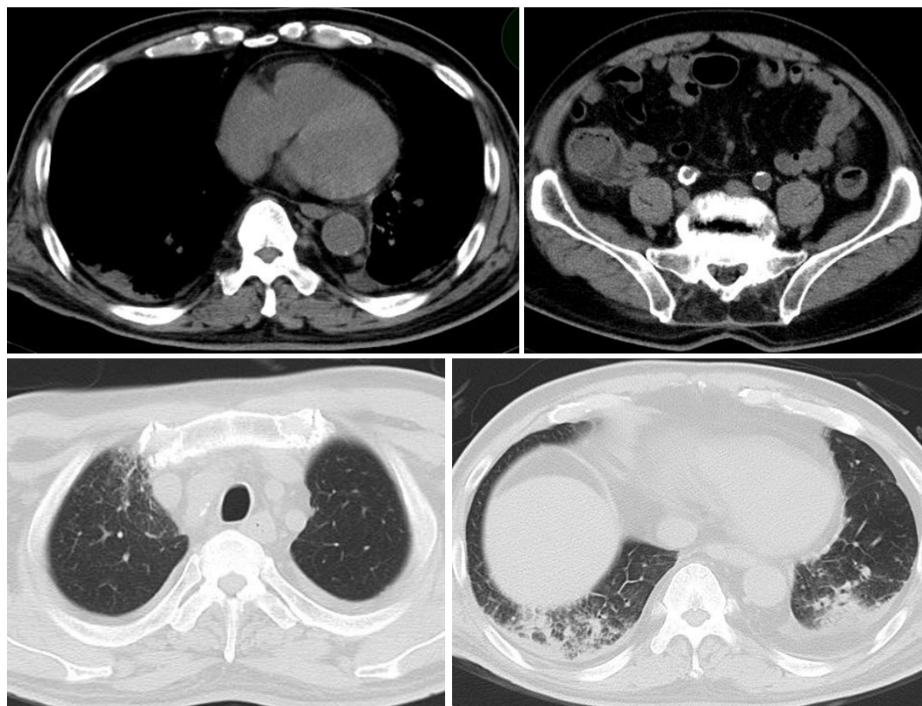


Figure 4. The computed tomography performed on day 43 shows exacerbation of interstitial pneumonia.

worsened and that there was pericardial effusion, while the inflammatory findings in the ileocecal area had decreased (Figures 5A and 5B).

Due to malaise caused by hyponatremia on day 60, fluids were restricted on suspicion of SIADH

caused by the IP. The hyponatremia was then gradually corrected. The patient then developed stomatitis, and a dexamethasone ointment was prescribed. The fever, erythema, and rash recurred on day 66. A CT performed on day 66 (Figures 6A and 6B) showed that

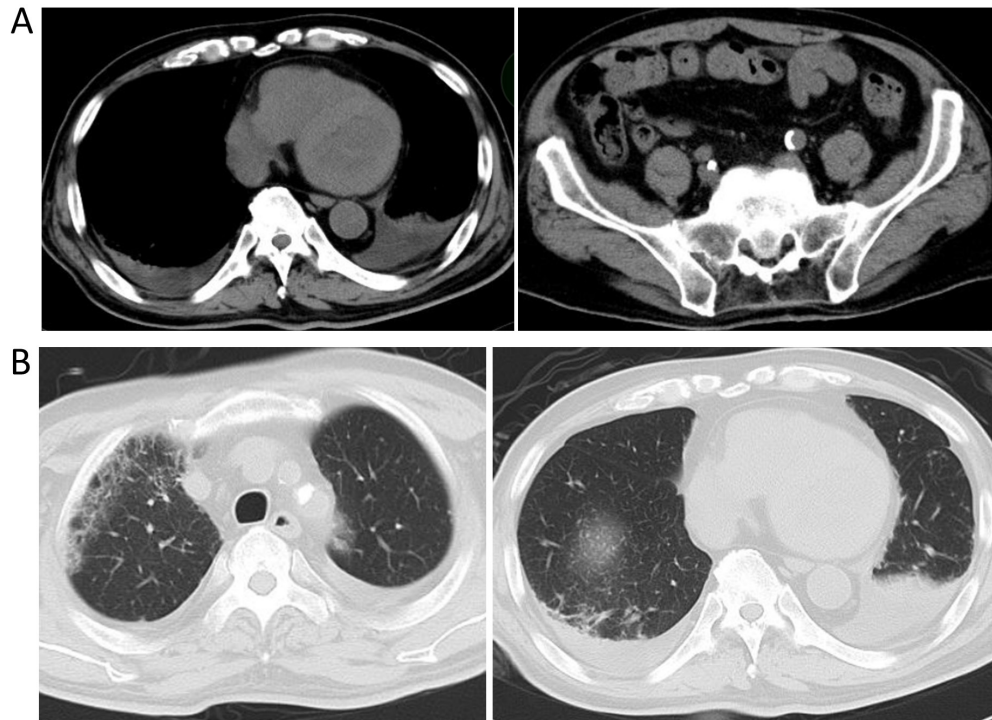


Figure 5. (A) The computed tomography performed on day 59 shows worsened interstitial pneumonia and pericardial effusion, (B) while the inflammatory findings in the ileocecal area appear improved.

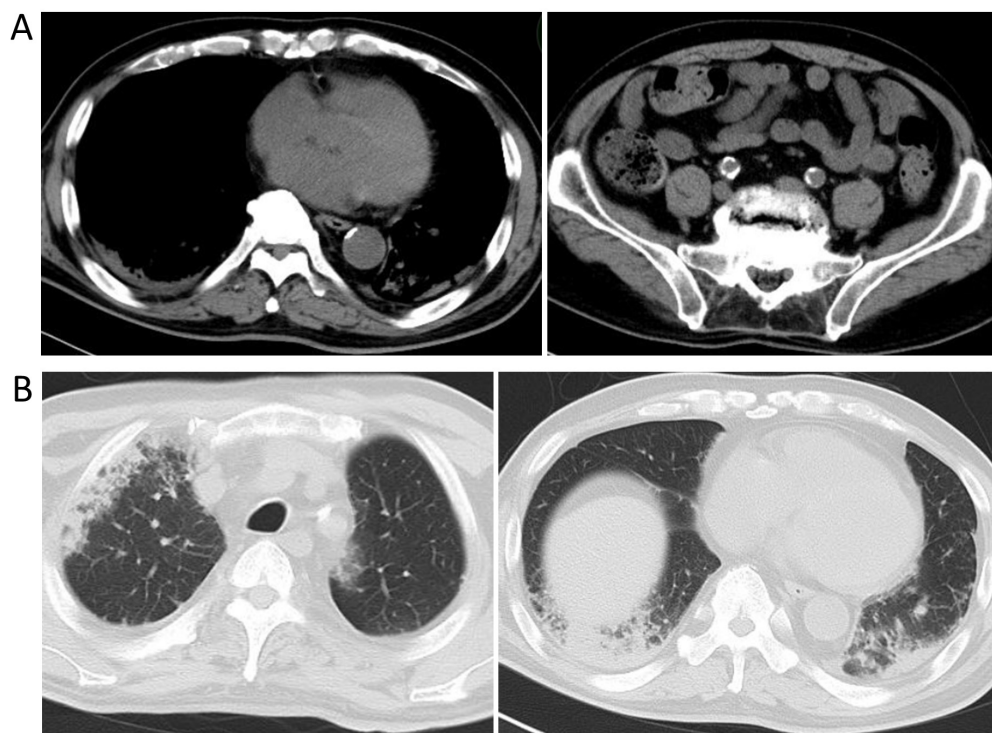


Figure 6. (A) The computed tomography performed on day 66 shows that the pericardial effusion has disappeared, (B) while the interstitial pneumonia has deteriorated.

Table 1. The diagnostic criteria for drug-induced hypersensitivity syndrome (DIHS) based on such clinical symptoms and the reactivation of HHV-6

Diagnostic criteria

- 1 Maculopapular rash developing > 3 weeks after starting a limited number of drugs
- 2 Prolonged clinical symptoms 2 weeks after discontinuing the causative drug
- 3 Fever (> 38°C)
- 4 Elevation of liver enzyme (alanine aminotransferase [ALT] > 100 U/L) or involvement of other organs
- 5 Leukocytosis (> $11 \times 10^3/\mu\text{L}$), atypical lymphocytosis (> 5%) or eosinophilia (> $1.5 \times 10^3/\mu\text{L}$)
- 6 Lymphadenopathy
- 7 Human herpesvirus (HHV)-6 reactivation

Diagnosis of typical DIHS requires the presence of all 7 criteria. Atypical DIHS is diagnosed in patients with 1-5.

the pericardial effusion was no longer present. The IP worsened and prednisolone was increased to a dose of 60 mg/day on day 67.

On day 72, we suspected that the patient had DIHS that had been induced by salazosulfapyridine, and antibody examinations for HHV-6, HHV-7, Epstein-Barr virus (EBV), and cytomegalovirus were performed. The quantification test for HHV-6 DNA was negative (1.4×10^2 copies), and the quantification of HHV-7 DNA was also negative. EB anti-viral capsid antigen (VCA)-immunoglobulin G (IgG) was increased 160-fold and EB anti-VCA-IgM was negative. EB anti-EB nuclear antigen was increased 40-fold, which provided evidence of past EBV infection. As there were positive findings of cytomegalovirus-IgG (enzyme immunoassay) at 15.3 and cytomegalovirus-IgM (enzyme immunoassay) at 1.11, cytomegalovirus reactivation was suspected. Two months following the onset of DIHS, the patient was transferred to a rehabilitation center with a modified Rankin Scale score of 3. After transfer, his skin symptoms recurred intermittently, and psychiatric symptoms were also observed. At 10 months following the onset of DIHS, the patient was still undergoing immunotherapy including prednisolone.

3. Discussion

The period between oral administration of a causative drug and the onset of DIHS (1,2) for many cases is approximately 2 to 6 weeks. Unlike ordinary drug eruptions, DIHS does not occur immediately or within a few days following the oral administration of a drug. There have been reports of DIHS developing after long-term oral administration of a drug or within several weeks of discontinuation of therapy. Systematic symptoms of DIHS include fever, lymphadenopathy, rash (initially mottled papule or erythematous erythematous, often transitioning to erythroderma), hepatic function disorder, renal function disorder, and hematologic abnormalities (leukocytosis, emergence of atypical lymphocytes, and eosinophil multiplication). Incidentally, characteristic erythematous findings such as erythema, edema of the face, red papule of the mouth, pustules, vesicles, and scales, are usually

observed within 1 week of initial drug administration.

The causative drugs are limited. For this reason, DIHS was postulated to be due to an abnormality of metabolic enzymes (3,4). The most frequent causative agent of DIHS in Japan is carbamazepine. The symptoms of DIHS often progress even after stopping the administration of the causative drugs, and complete relief from symptoms often requires longer than 1 month. In typical cases, DIHS is clinically bimodal. This is due to reactivation of HHV-6. In other words, what has been regarded as a very specific course of drug eruption is a complex pathology of drug allergy and virus infection (3,4). Diagnostic criteria for DIHS have been proposed based on such clinical symptoms and the reactivation of HHV-6 (Table 1). Our patient met all seven criteria and was confirmed as a typical case of DIHS induced by salazosulfapyridine.

Reactivation of cytomegalovirus is frequently observed in DIHS (5,6); cytomegalovirus is usually reactivated at the same time or later than HHV-6, suggesting that it could be related to clinical symptoms. Besides fever, mild liver dysfunction, and skin ulcer, severe symptoms such as myocarditis, pneumonia, and gastrointestinal bleeding may occur. If the symptoms of DIHS are prolonged, cytomegalovirus reactivation should be suspected (5,6). Cytomegalovirus infections in DIHS typically: 1) occur among elderly male patients, 2) develop 4 to 5 weeks following the onset of DIHS, 3) develop at the time of reactivation of HHV-6 and are related to HHV-6 DNA loads, and 4) are often prognostic (5). Because cytomegalovirus infection can be treated with appropriate antiviral drugs (ganciclovir), it is important to consider cytomegalovirus reactivation when providing treatment for DIHS. The investigations for cytomegalovirus include IgG antibody titration, measurement of IgM antibody titer, antigenic test, virus DNA, and histopathological examination. Although these methods are the most reliable for the detection of viral DNA, the clinical antigenicity test is also useful (5).

The drug eruption in our patient was suspected to have been induced by dabigatran based on the clinical symptoms that appeared 4 days after its administration. While it is possible that there may have

been cytomegalovirus reactivation, it may have been possible to avoid a severe cytomegalovirus infection such as central nervous system infection (7,8) due to the increased dose of steroids. In addition, due to the early combination of insulin and steroid therapy, there was no transition to fulminant type I diabetic ketoacidosis (9-12). Although diagnosing DIHS was challenging, a severe course of DIHS was avoided by considering the possibility of reactivation of cytomegalovirus.

Hyponatremia was also observed in association with an exacerbation of IP. Due to the serum osmotic pressure, which was as low as 271 mOsm/kgH, and prompt improvement of the serum sodium level by fluid restriction, the SIADH was attributed to IP (13). ADH is neuromodulated by two types of receptors, an osmotic receptor in the hypothalamus and a capacity receptor present in the left atrium, carotid artery, and aorta. Increased plasma osmotic pressure is detected by the osmotic receptor and a reduction in circulating blood volume or blood pressure is detected by the capacity receptor, which both in turn promote ADH secretion (13). Sakuma *et al.* (14) described a patient with phenobarbital-induced hypersensitivity syndrome who had SIADH associated with limbic encephalitis during the course of the disease. However, to the best of our knowledge, there are no reports of DIHS combined with SIADH attributed to IP. In our case, the interstitial capillary blood vessels were impaired following IP in conjunction with reactivation of cytomegalovirus on the background of DIHS. ADH secretion may have been promoted via the capacity receptor due to reduction in the vascular bed in the lung and a decrease in venous return.

In general, steroids (prednisolone 30-50 mg/day) are effective for DIHS treatment, while in severe cases, high-dose steroids and steroid pulse therapy are used. Recently, high-dose intravenous gamma-globulin (IVIG) has been employed, and there are reports of combined use of IVIG with steroid therapy in severe cases (15).

The administration of antiviral drugs is not necessary because HHV-6 reactivation usually occurs on a short-term basis. On the other hand, in the presence of cytomegalovirus infection, with prolongation or severity of symptoms, it is necessary to consider administering ganciclovir (5). In our patient, administration of steroid pulse therapy followed by a gradual decrease in dose prevented severe DIHS. This approach requires further investigation.

In conclusion, we encountered a case of DIHS induced by salazosulfapyridine combined with SIADH attributed to interstitial pneumonia 4 days following the administration of dabigatran that was difficult to diagnose. Timely diagnosis and an increase in the dose of steroids with subsequent tapering prevented worsening of DIHS. In the future, multidrug sensitization, potentially fatal infections, and

convalescent autoimmune diseases may be combined (1,2), and careful follow-up is necessary.

Acknowledgements

We would like to thank Editage (www.editage.com) for English language editing.

References

- Tohyama M, Hashimoto K. Drug-induced hypersensitivity syndrome and HHV-6 reactivation. *Uirusu*. 2009; 59:23-30.
- Tohyama M, Hashimoto K, Yasukawa M, Kimura H, Horikawa T, Nakajima K, Urano Y, Matsumoto K, Iijima M, Shear NH. Association of human herpesvirus 6 reactivation with the flaring and severity of drug-induced hypersensitivity syndrome. *Br J Dermatol*. 2007; 157:934-940.
- Seishima M, Yamanaka S, Fujisawa T, Tohyama M, Hashimoto K. Reactivation of human herpesvirus (HHV) family members other than HHV-6 in drug-induced hypersensitivity syndrome. *Br J Dermatol*. 2006; 155:344-349.
- Kano Y, Hirahara K, Sakuma K, Shiohara T. Several herpesviruses can reactivate in a severe drug-induced multiorgan reaction in the same sequential order as in graft-versus-host disease. *Br J Dermatol*. 2006; 155:301-306.
- Asano Y, Kagawa H, Kano Y, Shiohara T. Cytomegalovirus disease during severe drug eruptions: Report of 2 cases and retrospective study of 18 patients with drug-induced hypersensitivity syndrome. *Arch Dermatol*. 2009; 145:1030-1036.
- Sekiguchi A, Kashiwagi T, Ishida-Yamamoto A, Takahashi H, Hashimoto Y, Kimura H, Tohyama M, Hashimoto K, Iizuka H. Drug-induced hypersensitivity syndrome due to mexiletine associated with human herpes virus 6 and cytomegalovirus reactivation. *J Dermatol*. 2005; 32:278-281.
- Fujino Y, Nakajima M, Inoue H, Kusuha T, Yamada T. Human herpesvirus 6 encephalitis associated with hypersensitivity syndrome. *Ann Neurol*. 2002; 51:771-774.
- Masaki T, Fukunaga A, Tohyama M, Koda Y, Okuda S, Maeda N, Kanda F, Yasukawa M, Hashimoto K, Horikawa T, Ueda M. Human herpes virus 6 encephalitis in allopurinol-induced hypersensitivity syndrome. *Acta Derm Venereol*. 2003; 83:128-131.
- Sekine N, Motokura T, Oki T, Umeda Y, Sasaki N, Hayashi M, Sato H, Fujita T, Kaneko T, Asano Y, Kikuchi K. Rapid loss of insulin secretion in a patient with fulminant type 1 diabetes mellitus and carbamazepine hypersensitivity syndrome. *JAMA*. 2001; 285:1153-1154.
- Seino Y, Yamauchi M, Hirai C, Okumura A, Kondo K, Yamamoto M, Okazaki Y. A case of fulminant type 1 diabetes associated with mexiletine hypersensitivity syndrome. *Diabet Med*. 2004; 21:1156-1157.
- Chiou CC, Chung WH, Hung SI, Yang LC, Hong HS. Fulminant type 1 diabetes mellitus caused by drug hypersensitivity syndrome with human herpesvirus 6 infection. *J Am Acad Dermatol*. 2006; 54:S14-S17.

12. Imagawa A, Hanafusa T, Miyagawa J, Matsuzawa Y. A novel subtype of type 1 diabetes mellitus characterized by a rapid onset and an absence of diabetes-related antibodies. Osaka IDDM Study Group. *N Engl J Med.* 2000; 342:301-307.
13. Sono K, Kawashima T, Maruyama K, Ashizawa M, Kawashima S, Kikkawa K, Nishi Y, Kuroda T, Goto T, Matuzawa Y, Matumura R, Shirai K. A case of interstitial pneumonia accompanying SIADH. *Nihon Kokyuki Gakkai Zasshi.* 2006; 44:178-184.
14. Sakuma K, Kano Y, Fukuhara M, Shiohara T. Syndrome of inappropriate secretion of antidiuretic hormone associated with limbic encephalitis in a patient with drug-induced hypersensitivity syndrome. *Clin Exp Dermatol.* 2008; 33:287-290.
15. Kano Y, Inaoka M, Sakuma K, Shiohara T. Virus reactivation and intravenous immunoglobulin (IVIg) therapy of drug-induced hypersensitivity syndrome. *Toxicology.* 2005; 209:165-167.

(Received June 16, 2019; Revised August 13, 2019; Accepted August 22, 2019)

Focus on diagnosis, treatment, and problems of Barré-Lièou syndrome: Two case reports

Yusuke Morinaga*, Kouhei Nii, Kimiya Sakamoto, Ritsurou Inoue, Takafumi Mitsutake, Hayatsura Hanada

Department of Neurosurgery, Fukuoka University Chikushi Hospital, Chikushino-city, Fukuoka, Japan.

Summary

Barré-Lièou syndrome is a manifestation of various autonomic and secondary symptoms, such as muscle stiffness, tinnitus, dizziness, and pain in the head, neck, eyes, throat, ears, chest, and back. While thought to be caused by hyperactivation of the autonomic nervous system due to trauma, there is currently no firmly established etiology. This, and the nonspecific nature of many of its symptoms, presents a challenge both for clinicians, who must provide a correct diagnosis and patients, who are often misdiagnosed or faced with undue scrutiny from insurance companies. Here, we present two cases of Barré-Lièou syndrome, focusing on the processes leading to diagnosis, treatment, and problems encountered. Case 1 involves a 68-year-old woman whose head computed tomography (CT) scan revealed no abnormalities following a car accident. Approximately 10 months after her initial injury, Barré-Lièou syndrome was suspected because of autonomic symptoms that developed over time. She was prescribed an α -blocker, and 9 months later, her symptoms subsided. Case 2 was a 69-year-old woman who presented with bruising to the right chest and right knee after colliding with a car while riding her bicycle. One month later, Barré-Lièou syndrome was suspected because of her autonomic symptoms. She was prescribed an α -blocker, and 17 months later, her symptoms subsided. Because of the characteristic autonomic and secondary symptoms described above and a positive response to α -blockers, Barré-Lièou syndrome was suspected in both cases. We believe reporting cases will aid in the understanding of this disease and help patients obtain positive outcomes.

Keywords: Autonomic symptoms, Barré-Lièou syndrome, indefinite complaints, traumatic cervical syndrome

1. Introduction

Barré-Lièou syndrome (1) is a condition first reported by a French neurologist, Jean Alexandre Barré, in 1926 and Chinese physician, Yong-Cheon Lièou, in 1928. Various autonomic and secondary symptoms, such as muscle stiffness, tinnitus, and dizziness, are observed in addition to pain in the head, neck, eyes, throat, ears, chest, and back. It is thought that hyperactivation of the autonomic nervous system (mainly the sympathetic nerves) is directly or indirectly stimulated by trauma.

Numerous theories exist, such as the cervical sympathetic hyperactivity theory, theory of disorders of vertebral artery circulation, theory of brainstem disorder, and cervical soft tissue hypertonia theory. However, a solid theory has not yet been established (1,2).

In this paper, we present two cases of Barré-Lièou syndrome and report on literature considerations, focusing on the process leading to diagnosis and treatment, and issues that can occur during this process.

2. Case Report

2.1. Cases 1

In Case 1, a 68-year-old woman, with no history of medical conditions, visited to our hospital after being

*Address correspondence to:

Dr. Yusuke Morinaga, Department of Neurosurgery, Fukuoka University Chikushi Hospital, 1-1-1 Zokumyoin, Chikushino-city, Fukuoka Prefecture, 818-8502, Japan.
E-mail: yu_the_morio@yahoo.co.jp

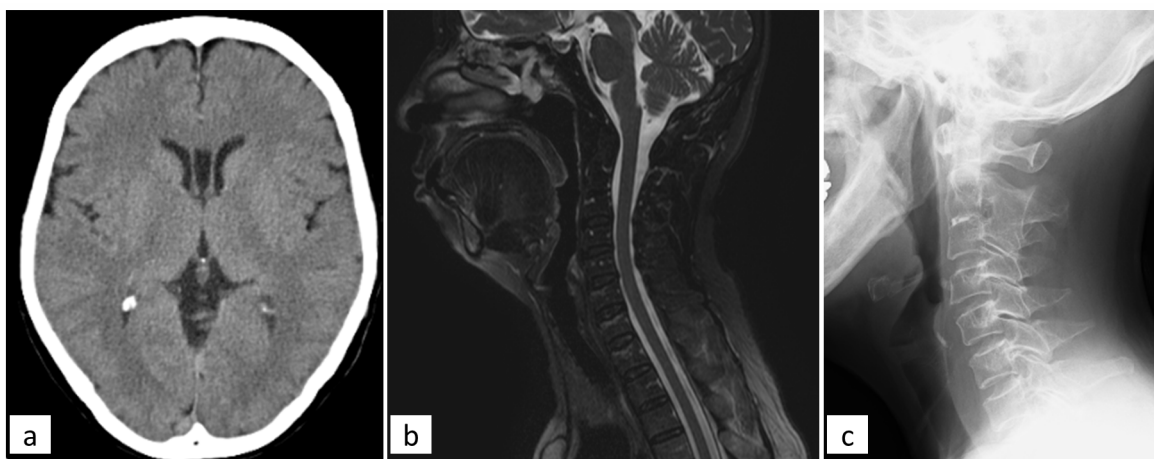


Figure 1. Imaging results for Case Study 1 patient. (a) Head computed tomography (CT) scan. Patient's first visit to our hospital after injury shows no traumatic intracranial hemorrhages or fractures. (b) T2-weighted Magnetic Resonance Image (MRI) after patient presented to our neurosurgery department 10 months after her initial injury. It shows that cervical vertebrae alignment is normal, there is no intramedullary abnormal signal, and C2-3 vertebral-facet joints are fused. The intervertebral discs at C4 / 5, C5 / 6 mildly bulge, but there is no significant excavation into the dural sac. (c) Cervical spine X-ray, 10 months after injury, shows no fractures or deviations.

injured when her car collided with a tree in an attempt to avoid a bicycle. Head computed tomography (CT) scan showed no fractures and she returned home. Approximately one month after the injury, she presented to the ophthalmology department with blurry vision and discomfort and discharge in both eyes. Cervical spine magnetic resonance imaging (MRI) was performed approximately 2 months after her injury and it showed normal. She was admitted to the department of internal medicine with chest and back pain approximately 3 months after injury. The following month, she began experiencing headaches, posterior head and neck pain, dizziness, pharyngeal and laryngeal discomfort, and pain when swallowing. She also developed insomnia and anxiety and began sleeping all day. Approximately 10 months after injury, she presented to our neurosurgery department for the first time due to her persisting symptoms.

At this first visit, the patient presented fully conscious. Physical findings included a blood pressure of 150/92 mm Hg, and a body temperature of 36.2°C. A headache was described as a dull, long-lasting pain (more than 72 h) with a sense of heaviness centered on the back, head, and neck. The nature of her headache was not pulsatile, strangulating, or shocking. She did not have an orthostatic headache, or nystagmus at rest, or while gazing. She had no apparent symptoms of a neurological deficit, no pathological reflexes, and no tinnitus. She had dizziness without cervical rotation, or induction by posture transformation. Hyperemia and discharge were present in both eyes. Additionally, she had constipation after trauma. A variety of subjective symptoms, such as discomfort in both eyes, chest and back pain, headache, dorsal neck pain, dizziness, pharyngeal and laryngeal discomfort, pain when swallowing, insomnia, and anxiety, were also reported

by the patient.

Her blood test revealed no obvious, abnormal findings regarding blood count, biochemistry, or coagulation. A head CT scan at her first visit to our hospital showed no traumatic intracranial hemorrhages or fractures (Figure 1a). We additionally performed a cervical vertebral T2-weighted MRI (Figure 1b). This scan showed normal cervical spine alignment, normal intramedullary signal, and fusion of the vertebral-facet joint of C2-3. In C4/5, C5/6 the intervertebral discs mildly bulged, but there were no significant retractions of the dural sac. Additionally, carotid ultrasonography of the vertebral artery indicated no obvious circulatory insufficiency.

Due to the absence of orthostatic headache and the nature of other accompanying symptoms, intracranial hypotension syndrome was not suspected. At the initial visit to our department, Barré-Lièou syndrome was suspected based on the diverse autonomic symptoms and secondary symptoms after trauma. Trazodone (50 mg/day), an oral sympathetic nervous system and α -receptor blocker, was started. Soon after, the majority of her symptoms disappeared, however, occasionally chest, pharyngeal, and laryngeal pain reemerged. Because she did not reach complete remission, and since her systolic blood pressure remained at a safe level, around 120-130 mm Hg, we continued oral administration of trazodone.

Approximately 13 months after the initial injury, the patient was again injured, this time in a two-car collision, and visited an orthopedist. No obvious fractures or deviations were observed in the cervical spine X-ray image (Figure 1c). However, neck pain, discomfort in the pharynx and larynx, pain when swallowing, and insomnia worsened. We suspected the exacerbation of Barré-Lièou syndrome.

With this second injury triggered, compensation

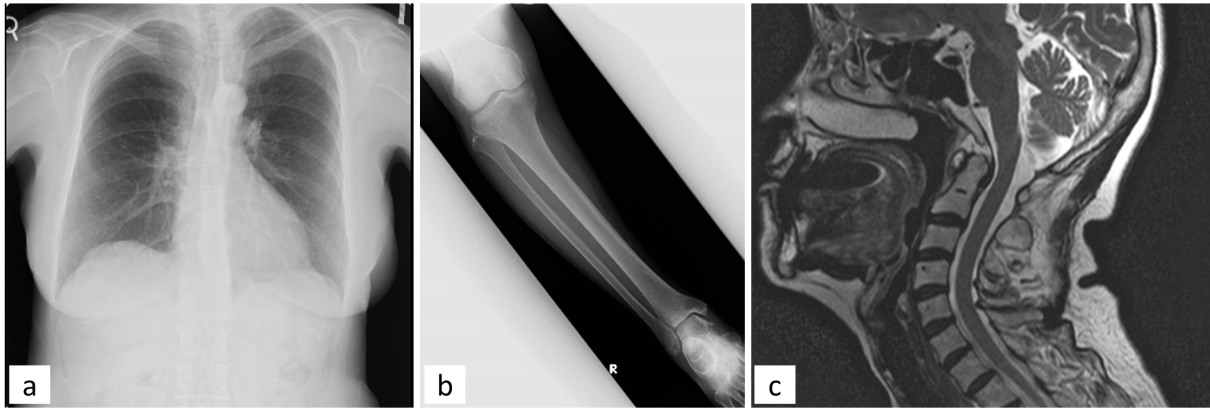


Figure 2. Imaging results for Case Study 2 patient. (a) Chest and (b) right leg X-rays show no fractures or deviations upon initial visit after injury. (c) T2-weighted Magnetic Resonance Image (MRI), taken 1 month after injury, shows normal cervical vertebrae alignment, no intramedullary abnormal signal, and C1-3 vertebral-facet joints are fused. The intervertebral discs at C4 / 5, C5 / 6 mildly bulge, but there is no significant excavation into the dural sac.

from the insurance company, for the initial injury, was canceled. Our department issued a diagnosis document to the insurance company proclaiming, "this patient was diagnosed with, and is being treated for, Barré-Lièou syndrome after her first injury. Her current symptoms are an exacerbation of this disease caused by the second injury." However, the insurance company declined to continue compensation following the second injury. The patient was exhausted from negotiations with the insurance company and was temporarily depressed. She wished to avoid trouble with this company and switched to an individual health insurance plan. She is currently being followed up as an outpatient because, approximately 19 months after her first injury, all her symptoms have disappeared.

2.2. Case 2

Case 2 involves a 69-year-old woman with no history of adverse medical conditions. She collided with a car, while riding her bicycle, and presented to our emergency room outpatient facility. Dizziness, neck pain, chest and back pain, pharyngeal and laryngeal discomfort, and pain when swallowing emerged the day following the injury, and she returned home after being diagnosed with right chest and right knee bruising, supported by X-ray results. Then, without improvement of chest pain and back pain, she visited the emergency room in our hospital again. The cause could not be identified with chest and abdominal contrast CT. Four days after the injury, she visited an orthopedist, but no abnormality was pointed out. She had discomfort in and hyperemia of both eyes, and her insomnia and anxiety symptoms appeared to be caused by exacerbation of autonomic symptoms 10 days after injury. Approximately 1 month after the injury, she visited our neurosurgery department hoping to improve her symptoms.

The patient presented fully conscious at her initial

visit. Physical findings indicated her blood pressure was 130/82 mm Hg and her body temperature was 36.1°C. A headache was described as a dull, long-lasting (more than 72 hours) pain with a sense of heaviness, centered on the back of the head and neck. The nature of her headache was not pulsatile, strangulating, or shocking. She had no orthostatic headache, no nystagmus at rest or while gazing, no apparent neurological deficit symptoms, no pathological reflexes, and no tinnitus. She had dizziness without cervical rotation or induction by posture transformation. Hyperemia of both eyes and eye discharge were found. She also had constipation after trauma.

The patient reported subjective symptoms, including discomfort of both eyes, chest and back pain, headache, dorsal neck pain, dizziness, pharyngeal and laryngeal discomfort, pain when swallowing, insomnia, and anxiety.

The patient's blood test revealed no obvious abnormalities regarding blood count, biochemistry, or coagulation. X-ray of the chest and right lower thigh indicated no apparent fractures or displacements (Figures 2a and 2b). Cervical vertebral T2-weighted MRI showed normal cervical spine alignment, no abnormal intramedullary signal, and fusion of the vertebral-facet joint of C1-3 (Figure 2c). Finally, carotid ultrasonography indicated no obvious circulatory insufficiency in the vertebral artery.

Due to the absence of orthostatic headache and the nature of other accompanying symptoms, a diagnosis of intracranial hypotension syndrome was excluded. During this visit, Barré-Lièou syndrome was suspected based on her diverse autonomic and secondary symptoms after trauma. An oral drug, which is a sympathetic nervous system blocker, trazodone (50 mg/day), was started. Following treatment, her blurriness, discharge, and discomfort in both eyes, headache, dorsal neck pain, dizziness, insomnia, anxiety, and constipation disappeared. However, occasionally back

pain reappeared, therefore, she continued oral trazodone administration.

Six months after the injury, the insurance company became suspicious of her symptoms and, as with our Case 1 patient, proposed canceling compensation. The patient worried about responding to the insurance company and decided to stop oral administration because her symptoms had improved. Her back pain worsened afterwards, and she went to an osteopathic clinic of her own volition, but her symptoms did not improve. After restarting 50 mg/day of trazodone, her symptoms disappeared, and complete remission was obtained approximately 18 months after injury.

Written informed consent was obtained from the patients for the publication of these two case reports and the accompanying images, and the study design was approved by the appropriate ethics review board.

3. Discussion

Barré-Lièou syndrome is a refractory disease that exhibits cervical pain and various autonomic and secondary symptoms (insomnia, anxiety, depression, *etc.*) and is considered a subtype of traumatic cervical syndrome (1). The Quebec classification is well-known for its scoring of traumatic cervical syndrome, classifying severity between grades 0 – IV (3). We recommend an early exit from bed in cases of grade III or lower without fracture, dislocation, or spinal cord injury, and discontinuation of early treatment within 3 months (2). As a subjective and nonspecific complaint, Barré-Lièou syndrome is liable to be an indefinite complaint as it lacks objective neurological findings and biomarkers. The symptoms are as follows: (1) inner ear symptoms: dizziness, tinnitus, and feelings of obstruction of the ear; (2) eye symptoms: blurred vision, fatigue, discomfort, and sight loss (asthenopia); (3) chest and back symptoms: chest pain, back pain, arrhythmia, and respiratory distress; (4) pharyngeal and laryngeal symptoms: hoarseness, discomfort in the throat, and swallowing difficulty; (5) head and neck symptoms: headache, sense of head weight, and back of neck pain; (6) others: upper limb and whole body fatigue, upper limb numbness, distraction, secondary psychiatric symptoms (anxiety, depression, and the like), and insomnia (4).

It is important to note that intracranial hypotension syndrome (5), which exhibits symptoms such as headache, dizziness, and nausea when standing because of a decrease in cerebrospinal fluid volume, has clinical characteristics similar to those of Barré-Lièou syndrome. In these cases, a cisternography should be performed for accurate diagnoses. There are reports that epidural blood patch therapy for intracranial hypotension syndrome is effective treatment (2).

In general, a clear diagnosis is difficult, but some symptoms that can aid diagnosis exist: (1) symptoms

that can be explained as autonomic symptoms (however these are mainly subjective, and objective findings are poor); (2) positive response to sympathetic blockade drugs and sympathetic ganglion blocks (mainly symptomatic improvement may be seen by the stellate ganglion block); (3) abnormal imaging results, such as a fracture or dislocation. (4) circulatory failure of the vertebral artery feeding the brainstem (especially cranial nerves V2, 3 and VIII *etc.*) where the central autonomic network exists (especially C3, 4 vertebral bodies, intervertebral disc trauma, arthritis, *etc.*) caused by temporal changes of the cervical spine. If these symptoms exist, the likelihood of Barré-Lièou syndrome will be even higher (4).

In both our cases, carotid artery echoes were negative in the vertebral arterial circulation in the neck, there were no orthostatic headaches, and considering the existence of other accompanying symptoms, intracranial hypotension syndrome was ruled out. Case 1 and Case 2 satisfy all the above criteria (1-4), and a Quebec grade of X Barré-Lièou syndrome was suspected. Furthermore, the fact that trazodone, an oral sympathetic nervous system blocker, was effective supports the cervical sympathetic hyperactivity theory.

Treatment is basically supposed to follow the treatment protocol for cervical sprains, but a stellate ganglion block (one of the cervical sympathetic ganglia) or an α -blocker (a sympatholytic drug) is recommended. In addition, various treatments such as neck epidural block, intravenous drip infusion of prostaglandin E1 (PGE 1), acupuncture, and the like are performed, but a clear treatment effect is not obtained and there are many refractory cases (2). The mental symptoms, insomnia, and autonomic symptoms in our patients disappeared after administration of trazodone. Trazodone is currently effective in both cases, and the stellate ganglion block was not enforced, but will be examined in the future if symptoms exacerbate.

Physicians and patients do encounter problems with the diagnosis of Barré-Lièou syndrome. Because there are few image diagnostics or neurological objective findings, symptoms are often misunderstood as fraudulent to receive compensation for a traffic injury (3). In both our cases, the insurance companies proposed stopping compensation. In Case 1, after a second traffic accident, the patient did not receive compensation despite our letters to the appropriate insurance companies. In Case 2, since her insurance company repeatedly proposed cancelling compensation, the patient stopped drug treatment and sought alternative therapy from an osteopathic clinic, but she later resumed oral administration due to exacerbation of back pain.

As in our cases, patients suspected of fraud often experience litigation problems, and for the same reasons as above, the question of whether disability is residual or primary frequently arises. Furthermore, because this syndrome presents with autonomic symptoms,

psychiatric symptoms, insomnia, and so on, this syndrome is not only treated as an indefinite complaint, but also many physicians who are unfamiliar with this disease do not establish a confirmed diagnosis (5). As mentioned above, its pathophysiology has not been established, so it has not been recognized internationally as an independent syndrome. In the clinical setting, Barré-Lièou syndrome can be diagnosed as a tension-type headache, cervical arm syndrome, traumatic cervical syndrome, or an autonomic imbalance. These conditions are not fully understood, and in that respect, it may be worth considering this syndrome as well.

In our opinion, irrespective of the disease name, we make our determination based on clinical symptoms, and we suspected Barré-Lièou syndrome in the patients who presented with refractory symptoms in this report. We believe that it is worth trying trazodone for post-traumatic sympathetic hyperactivity. In addition, when empirical treatment is successful, informed consent of patients based on the characteristics and problems of the disease is also important. To solve such problems, it is desirable to disseminate information about the pathology to better recognize and increase understanding of the disease by physicians and society.

In conclusion, we reported two cases of Barré-Lièou syndrome from the viewpoint of diagnosis, treatment, and problems, in the context of current literature. Diagnosis was delayed as both patients complained of psychiatric symptoms and had indefinite complaints in the form of a variety of autonomic symptoms, such as headache, eye pain, vision disorder, otic pain, tinnitus, dizziness, back of head pain, discomfort, constipation,

insomnia, and anxiety. Trazodone, which is an α -blocker for Barré-Lièou syndrome, was effective in relieving our patients' symptoms. Enhanced recognition and understanding of this disease by physicians and society are desired.

Acknowledgements

This research did not receive any specific grant from funding agencies in the public, commercial, or not-for-profit sectors. We would like to thank Editage (www.editage.com) for English language editing.

References

1. Li Y, Peng B. Pathogenesis, diagnosis, and treatment of cervical vertigo. *Pain Physician*. 2015; 18:E583-E595.
2. Ishikawa S, Katayama D, Takahara H, Kojo S, Moriyama E, Hashimoto H. Epidural blood patch as a successful treatment of Barré-Lièou syndrome: report of two cases. *Masui*. 2003; 52:1305-1311.
3. Spitzer WO, Skovron ML, Salmi LR, Cassidy JD, Duranceau J, Suissa S, Zeiss E. Scientific monograph of Quebec task force on whiplash-associated disorder: Redefining "whiplash" and its management. *Spine*. 1995; 20:1S-73S.
4. Pearce JM. Barré-Lièou "syndrome". *J Neurol Neurosurg Psychiatry*. 2004; 75:319.
5. Foster CA, Jabbour P. Barré-Lièou syndrome and the problem of the obsolete eponym. *J Laryngol Otol*. 2007; 121:680-683.

(Received June 19, 2019; Revised August 13, 2019; Accepted August 22, 2019)

Guide for Authors

1. Scope of Articles

Drug Discoveries & Therapeutics welcomes contributions in all fields of pharmaceutical and therapeutic research such as medicinal chemistry, pharmacology, pharmaceutical analysis, pharmaceuticals, pharmaceutical administration, and experimental and clinical studies of effects, mechanisms, or uses of various treatments. Studies in drug-related fields such as biology, biochemistry, physiology, microbiology, and immunology are also within the scope of this journal.

2. Submission Types

Original Articles should be well-documented, novel, and significant to the field as a whole. An Original Article should be arranged into the following sections: Title page, Abstract, Introduction, Materials and Methods, Results, Discussion, Acknowledgments, and References. Original articles should not exceed 5,000 words in length (excluding references) and should be limited to a maximum of 50 references. Articles may contain a maximum of 10 figures and/or tables.

Brief Reports definitively documenting either experimental results or informative clinical observations will be considered for publication in this category. Brief Reports are not intended for publication of incomplete or preliminary findings. Brief Reports should not exceed 3,000 words in length (excluding references) and should be limited to a maximum of 4 figures and/or tables and 30 references. A Brief Report contains the same sections as an Original Article, but the Results and Discussion sections should be combined.

Reviews should present a full and up-to-date account of recent developments within an area of research. Normally, reviews should not exceed 8,000 words in length (excluding references) and should be limited to a maximum of 100 references. Mini reviews are also accepted.

Policy Forum articles discuss research and policy issues in areas related to life science such as public health, the medical care system, and social science and may address governmental issues at district, national, and international levels of discourse. Policy Forum articles should not exceed 2,000 words in length (excluding references).

Case Reports should be detailed reports of the symptoms, signs, diagnosis, treatment, and follow-up of an individual patient. Case reports may contain a demographic profile of the patient but usually describe an unusual or novel occurrence. Unreported or unusual side effects or adverse interactions involving medications will also be considered. Case

Reports should not exceed 3,000 words in length (excluding references).

News articles should report the latest events in health sciences and medical research from around the world. News should not exceed 500 words in length.

Letters should present considered opinions in response to articles published in Drug Discoveries & Therapeutics in the last 6 months or issues of general interest. Letters should not exceed 800 words in length and may contain a maximum of 10 references.

3. Editorial Policies

Ethics: Drug Discoveries & Therapeutics requires that authors of reports of investigations in humans or animals indicate that those studies were formally approved by a relevant ethics committee or review board.

Conflict of Interest: All authors are required to disclose any actual or potential conflict of interest including financial interests or relationships with other people or organizations that might raise questions of bias in the work reported. If no conflict of interest exists for each author, please state "There is no conflict of interest to disclose".

Submission Declaration: When a manuscript is considered for submission to Drug Discoveries & Therapeutics, the authors should confirm that 1) no part of this manuscript is currently under consideration for publication elsewhere; 2) this manuscript does not contain the same information in whole or in part as manuscripts that have been published, accepted, or are under review elsewhere, except in the form of an abstract, a letter to the editor, or part of a published lecture or academic thesis; 3) authorization for publication has been obtained from the authors' employer or institution; and 4) all contributing authors have agreed to submit this manuscript.

Cover Letter: The manuscript must be accompanied by a cover letter signed by the corresponding author on behalf of all authors. The letter should indicate the basic findings of the work and their significance. The letter should also include a statement affirming that all authors concur with the submission and that the material submitted for publication has not been published previously or is not under consideration for publication elsewhere. The cover letter should be submitted in PDF format. For example of Cover Letter, please visit <http://www.ddtjournal.com/downloadcentre.php> (Download Centre).

Copyright: A signed JOURNAL PUBLISHING AGREEMENT (JPA) must be provided by post, fax, or as a scanned file before acceptance of the article. Only forms with a hand-written signature are accepted. This copyright will ensure the widest possible dissemination of information. A form facilitating transfer of copyright can be downloaded by clicking the appropriate link and can be returned to the e-mail address or fax number noted on the form (Please visit

Download Centre). Please note that your manuscript will not proceed to the next step in publication until the JPA form is received. In addition, if excerpts from other copyrighted works are included, the author(s) must obtain written permission from the copyright owners and credit the source(s) in the article.

Suggested Reviewers: A list of up to 3 reviewers who are qualified to assess the scientific merit of the study is welcomed. Reviewer information including names, affiliations, addresses, and e-mail should be provided at the same time the manuscript is submitted online. Please do not suggest reviewers with known conflicts of interest, including participants or anyone with a stake in the proposed research; anyone from the same institution; former students, advisors, or research collaborators (within the last three years); or close personal contacts. Please note that the Editor-in-Chief may accept one or more of the proposed reviewers or may request a review by other qualified persons.

Language Editing: Manuscripts prepared by authors whose native language is not English should have their work proofread by a native English speaker before submission. If not, this might delay the publication of your manuscript in Drug Discoveries & Therapeutics.

The Editing Support Organization can provide English proofreading, Japanese-English translation, and Chinese-English translation services to authors who want to publish in Drug Discoveries & Therapeutics and need assistance before submitting a manuscript. Authors can visit this organization directly at <http://www.iacmhr.com/iac-eso/support.php?lang=en>. IAC-ESO was established to facilitate manuscript preparation by researchers whose native language is not English and to help edit works intended for international academic journals.

4. Manuscript Preparation

Manuscripts should be written in clear, grammatically correct English and submitted as a Microsoft Word file in a single-column format. Manuscripts must be paginated and typed in 12-point Times New Roman font with 24-point line spacing. Please do not embed figures in the text. Abbreviations should be used as little as possible and should be explained at first mention unless the term is a well-known abbreviation (e.g. DNA). Single words should not be abbreviated.

Title page: The title page must include 1) the title of the paper (Please note the title should be short, informative, and contain the major key words); 2) full name(s) and affiliation(s) of the author(s); 3) abbreviated names of the author(s); 4) full name, mailing address, telephone/fax numbers, and e-mail address of the corresponding author; and 5) conflicts of interest (if you have an actual or potential conflict of interest to disclose, it must be included as a footnote on the title page of the manuscript; if no conflict of interest exists for each author, please state "There is no conflict of interest to disclose"). Please visit [Download Centre](#) and refer to the title page of the manuscript sample.

Abstract: The abstract should briefly state the purpose of the study, methods, main findings, and conclusions. For article types including Original Article, Brief Report, Review, Policy Forum, and Case Report, a one-paragraph abstract consisting of no more than 250 words must be included in the manuscript. For News and Letters, a brief summary of main content in 150 words or fewer should be included in the manuscript. Abbreviations must be kept to a minimum and non-standard abbreviations explained in brackets at first mention. References should be avoided in the abstract. Key words or phrases that do not occur in the title should be included in the Abstract page.

Introduction: The introduction should be a concise statement of the basis for the study and its scientific context.

Materials and Methods: The description should be brief but with sufficient detail to enable others to reproduce the experiments. Procedures that have been published previously should not be described in detail but appropriate references should simply be cited. Only new and significant modifications of previously published procedures require complete description. Names of products and manufacturers with their locations (city and state/country) should be given and sources of animals and cell lines should always be indicated. All clinical investigations must have been conducted in accordance with Declaration of Helsinki principles. All human and animal studies must have been approved by the appropriate institutional review board(s) and a specific declaration of approval must be made within this section.

Results: The description of the experimental results should be succinct but in sufficient detail to allow the experiments to be analyzed and interpreted by an independent reader. If necessary, subheadings may be used for an orderly presentation. All figures and tables must be referred to in the text.

Discussion: The data should be interpreted concisely without repeating material already presented in the Results section. Speculation is permissible, but it must be well-founded, and discussion of the wider implications of the findings is encouraged. Conclusions derived from the study should be included in this section.

Acknowledgments: All funding sources should be credited in the Acknowledgments section. In addition, people who contributed to the work but who do not meet the criteria for authors should be listed along with their contributions.

References: References should be numbered in the order in which they appear in the text. Citing of unpublished results, personal communications, conference abstracts, and theses in the reference list is not recommended but these sources may be mentioned in the text. In the reference list, cite the names of all authors when there are fifteen or fewer authors; if there are sixteen or more authors, list the first three followed by *et al.* Names of journals should

be abbreviated in the style used in PubMed. Authors are responsible for the accuracy of the references. Examples are given below:

Example 1 (Sample journal reference):
Nakata M, Tang W. Japan-China Joint Medical Workshop on Drug Discoveries and Therapeutics 2008: The need of Asian pharmaceutical researchers' cooperation. *Drug Discov Ther.* 2008; 2:262-263.

Example 2 (Sample journal reference with more than 15 authors):
Darby S, Hill D, Auvinen A, *et al.* Radon in homes and risk of lung cancer: Collaborative analysis of individual data from 13 European case-control studies. *BMJ.* 2005; 330:223.

Example 3 (Sample book reference):
Shalev AY. Post-traumatic stress disorder: Diagnosis, history and life course. In: *Post-traumatic Stress Disorder, Diagnosis, Management and Treatment* (Nutt DJ, Davidson JR, Zohar J, eds.). Martin Dunitz, London, UK, 2000; pp. 1-15.

Example 4 (Sample web page reference):
World Health Organization. The World Health Report 2008 – primary health care: Now more than ever. http://www.who.int/whr/2008/whr08_en.pdf (accessed September 23, 2010).

Tables: All tables should be prepared in Microsoft Word or Excel and should be arranged at the end of the manuscript after the References section. Please note that tables should not in image format. All tables should have a concise title and should be numbered consecutively with Arabic numerals. If necessary, additional information should be given below the table.

Figure Legend: The figure legend should be typed on a separate page of the main manuscript and should include a short title and explanation. The legend should be concise but comprehensive and should be understood without referring to the text. Symbols used in figures must be explained.

Figure Preparation: All figures should be clear and cited in numerical order in the text. Figures must fit a one- or two-column format on the journal page: 8.3 cm (3.3 in.) wide for a single column, 17.3 cm (6.8 in.) wide for a double column; maximum height: 24.0 cm (9.5 in.). Please make sure that artwork files are in an acceptable format (TIFF or JPEG) at minimum resolution (600 dpi for illustrations, graphs, and annotated artwork, and 300 dpi for micrographs and photographs). Please provide all figures as separate files. Please note that low-resolution images are one of the leading causes of article resubmission and schedule delays. All color figures will be reproduced in full color in the online edition of the journal at no cost to authors.

Units and Symbols: Units and symbols conforming to the International System of Units (SI) should be used for physicochemical quantities. Solidus notation (*e.g.* mg/kg, mg/mL, mol/mm²/min) should be used. Please refer to the SI Guide www.bipm.org/en/si/ for standard units.

Supplemental data: Supplemental data might be useful for supporting and enhancing your scientific research and Drug Discoveries & Therapeutics accepts the submission of these materials which will be only published online alongside the electronic version of your article. Supplemental files (figures, tables, and other text materials) should be prepared according to the above guidelines, numbered in Arabic numerals (*e.g.*, Figure S1, Figure S2, and Table S1, Table S2) and referred to in the text. All figures and tables should have titles and legends. All figure legends, tables and supplemental text materials should be placed at the end of the paper. Please note all of these supplemental data should be provided at the time of initial submission and note that the editors reserve the right to limit the size and length of Supplemental Data.

5. Submission Checklist

The Submission Checklist will be useful during the final checking of a manuscript prior to sending it to Drug Discoveries & Therapeutics for review. Please visit [Download Centre](#) and download the Submission Checklist file.

6. Online submission

Manuscripts should be submitted to Drug Discoveries & Therapeutics online at <http://www.ddtjournal.com>. The manuscript file should be smaller than 5 MB in size. If for any reason you are unable to submit a file online, please contact the Editorial Office by e-mail at office@ddtjournal.com

7. Accepted manuscripts

Proofs: Galley proofs in PDF format will be sent to the corresponding author *via* e-mail. Corrections must be returned to the editor (proof-editing@ddtjournal.com) within 3 working days.

Offprints: Authors will be provided with electronic offprints of their article. Paper offprints can be ordered at prices quoted on the order form that accompanies the proofs.

Page Charge: A page charge of \$140 will be assessed for each printed page of an accepted manuscript. The charge for printing color figures is \$340 for each page. Under exceptional circumstances, the author(s) may apply to the editorial office for a waiver of the publication charges at the time of submission.

(Revised February 2013)

Editorial and Head Office:

Pearl City Koishikawa 603
2-4-5 Kasuga, Bunkyo-ku
Tokyo 112-0003
Japan
Tel: +81-3-5840-9697
Fax: +81-3-5840-9698
E-mail: office@ddtjournal.com

JOURNAL PUBLISHING AGREEMENT (JPA)

Manuscript No.:

Title:

Corresponding author:

The International Advancement Center for Medicine & Health Research Co., Ltd. (IACMHR Co., Ltd.) is pleased to accept the above article for publication in Drug Discoveries & Therapeutics. The International Research and Cooperation Association for Bio & Socio-Sciences Advancement (IRCA-BSSA) reserves all rights to the published article. Your written acceptance of this JOURNAL PUBLISHING AGREEMENT is required before the article can be published. Please read this form carefully and sign it if you agree to its terms. The signed JOURNAL PUBLISHING AGREEMENT should be sent to the Drug Discoveries & Therapeutics office (Pearl City Koishikawa 603, 2-4-5 Kasuga, Bunkyo-ku, Tokyo 112-0003, Japan; E-mail: office@ddtjournal.com; Tel: +81-3-5840-9697; Fax: +81-3-5840-9698).

1. Authorship Criteria

As the corresponding author, I certify on behalf of all of the authors that:

- 1) The article is an original work and does not involve fraud, fabrication, or plagiarism.
- 2) The article has not been published previously and is not currently under consideration for publication elsewhere. If accepted by Drug Discoveries & Therapeutics, the article will not be submitted for publication to any other journal.
- 3) The article contains no libelous or other unlawful statements and does not contain any materials that infringes upon individual privacy or proprietary rights or any statutory copyright.
- 4) I have obtained written permission from copyright owners for any excerpts from copyrighted works that are included and have credited the sources in my article.
- 5) All authors have made significant contributions to the study including the conception and design of this work, the analysis of the data, and the writing of the manuscript.
- 6) All authors have reviewed this manuscript and take responsibility for its content and approve its publication.
- 7) I have informed all of the authors of the terms of this publishing agreement and I am signing on their behalf as their agent.

2. Copyright Transfer Agreement

I hereby assign and transfer to IACMHR Co., Ltd. all exclusive rights of copyright ownership to the above work in the journal Drug Discoveries & Therapeutics, including but not limited to the right 1) to publish, republish, derivate, distribute, transmit, sell, and otherwise use the work and other related material worldwide, in whole or in part, in all languages, in electronic, printed, or any other forms of media now known or hereafter developed and the right 2) to authorize or license third parties to do any of the above.

I understand that these exclusive rights will become the property of IACMHR Co., Ltd., from the date the article is accepted for publication in the journal Drug Discoveries & Therapeutics. I also understand that IACMHR Co., Ltd. as a copyright owner has sole authority to license and permit reproductions of the article.

I understand that except for copyright, other proprietary rights related to the Work (e.g. patent or other rights to any process or procedure) shall be retained by the authors. To reproduce any text, figures, tables, or illustrations from this Work in future works of their own, the authors must obtain written permission from IACMHR Co., Ltd.; such permission cannot be unreasonably withheld by IACMHR Co., Ltd.

3. Conflict of Interest Disclosure

I confirm that all funding sources supporting the work and all institutions or people who contributed to the work but who do not meet the criteria for authors are acknowledged. I also confirm that all commercial affiliations, stock ownership, equity interests, or patent-licensing arrangements that could be considered to pose a financial conflict of interest in connection with the article have been disclosed.

Corresponding Author's Name (Signature):

Date:

